Title	有歪中継ワイヤレス協調通信ネットワークにおけるチャネル変動の伝送特性に与える影響解析
Author(s)	申，騫
Citation	
Issue Date	2017-12
Type	Thesis or Dissertation
Text version	ETD
URL	http://hdl.handle.net/10119/15076
Rights	
Description	Supervisor:松本　正，情報科学研究科，博士

SHEN QIAN

STATISTICAL PERFORMANCE CHARACTERIZATION OF LOSSY-FORWARD BASED COOPERATIVE WIRELESS NETWORKS OVER FADING CHANNELS

Academic dissertation to be presented with the assent of the Doctoral Training Committee of Technology and Natural Science of the University of Oulu for public defence in Collaboration room 7, Asahidai, on 5 October 2017, at 2 p.m.

UNIVERSITY OF OULU
and
JAPAN ADVANCED INSTITUTE OF SCIENCE AND TECHNOLOGY
2017

Supervised by
Professor Tad Matsumoto
Professor Markku Juntti

Reviewed by
Adjunct Professor Antti Tölli
Associate Professor Brian Michael Kurkoski
Professor Francis C.M. LAU
Professor Gerhard Bauch
Professor Mineo Kaneko
Professor Takeo Ohgane

ISBN 978-4-903092-48-5

Qian, Shen, Statistical Performance Characterization of Lossy-Forward based Cooperative Wireless Networks over Fading Channels.

University of Oulu Graduate School; University of Oulu, Faculty of Information Technology and Electrical Engineering; Centre for Wireless Communications-Radio Technologies (CWC-RT); Infotech Oulu.

Japan Advanced Institute of Science and Technology, School of Information Science, Information Theory and Signal Processing Laboratory.

JAIST Press, 1-1, Asahidai, Nomi, Ishikawa 923-1292, Japan.

Abstract

Cooperative wireless communications are investigated from the perspective of exploiting statistical nature of channel property variation. The target of this research is to provide analytical assessments and theoretical bounds of lossy-forward (LF) relaying based cooperative communications in various network topologies and propagation conditions, where the channel variation information is efficiently utilized.

The performance of three-node LF relaying over independent block Nakagami-m fading channels is investigated. Based on the source coding with a helper theorem, the exact outage probability expression with arbitrary values of the shape factor m is derived. Furthermore, the decay of the outage curve, referred to as equivalent diversity order, and coding gain of LF relaying are identified based on a yet accurate high signal-to-noise ratio (SNR) outage probability approximation. It is found that the decay of the outage curve is dominated by the less reliable channel of either the source-relay or the relay-destination link. It is also found that in terms of the outage probability, LF relaying is superior to conventional decode-and-forward (DF) relaying where relay keeps silent if error is detected after decoding. This is because the relay in LF always forwards the decoder output to the destination via re-interleaving and re-encoding of the information sequence. Therefore, the whole system can be regarded as a distributed turbo code. Moreover, with LF relaying, not only the outage probability can be reduced, but also the search area for a relay (helper) can be increased compared to conventional DF relaying while keeping the same or even lower outage probability, resulting in significant coverage expansion of the system.

The outage probabilities of LF, decode-and-forward (DF) and adaptive decode-and-forward (ADF) relaying are analyzed in block Rayleigh fading channels, with the aim of identifying the impact of the spatial and temporal correlations of the fading variations. It is proven that the coding gain with LF is larger than with DF but smaller than with ADF, where the ADF scheme utilizes error-free feedback from the relay to the source. It is found that compared to the independent fading case, in the correlated fading, to achieve the lowest outage probability, the relay should be located closer to the destination, or more transmit power should be allocated to the relay, both for reducing the gain loss caused by the fading correlation.

A comparative study on the outage probabilities of LF relaying with the two distributions, Rician and Nakagami-m, is conducted. Kullback-Leibler divergence (KLD) and Jensen-Shannon divergence (JSD) are used to identify the difference between the distributions. It is found that even with a specific parameter setting yielding the same line-of-sight (LOS) ratio, Rician is not equivalent to Nakagami-m model for representing the shape of the entire portion of the distribution.

Furthermore, we derive an upper bound of the outage probability for a two-way LF relaying system over Rician fading channels with a random K-factor. The K-factor is assumed to follow empirical distributions, normal or logistic distributions, which are derived from measurement data. Compared to the two-way DF transmission, the two-way LF transmission is found to achieve lower outage probability regardless of either logistic or normal distribution is used to represent the variation of K-factor. Because with LF, the relay always broadcast the decoder output regardless of whether error is detected after decoding in the information part or not.

The work is extended to a multi-source multi-relay transmission system, where all the links experience the κ-μ fading variations. It is found that, regardless of whether the LOS component exists in the channel or not, the outage performance of the system with orthogonal transmission with joint-decoding scheme is superior to that with maximum ratio transmission scheme.

Keywords: Outage probability, relay channels, lossy-forward (LF), Nakagami-m fading, Rician fading, κ-μ fading, Kullback-Leibler divergence (KLD), Jensen-Shannon divergence (JSD), line-of-sight (LOS) component, diversity order and coding gain

To my son Chisheng and my daughter Chicheng

Preface

This research has been conducted under the framework of joint supervision of doctoral dissertation and for awarding double doctoral degree between University of Oulu (UOulu), Finland and Japan Advanced Institute Science and Technology (JAIST), Japan. At JAIST, the research was carried out at Information Theory and Signal Processing Laboratory, School of Information Science. At UOulu, the work was conducted at Centre for Wireless Communications (CWC).

First of all, I wish to express my deepest gratitude to my supervisor Professor Tad Matsumoto who also supervised me since my master study time. He is full of enthusiasm in his academic life, has taught me a lot of things about research. I would also like to sincerely thank my principal advisor at UOulu, Professor Markku Juntti, for the valuable advices on my research and the efforts to help me accomplish my double doctoral degree study. Without their guidance and encouragement, this dissertation would not be able to reach the current quality level. I appreciate the assistance and valuable suggestions raised by Associate Professor Brian Michael Kurkoski of JAIST. I also wish to devote my sincere thanks to all the reviewers and examiners, Professor Francis C.M. LAU from Hong Kong Polytechnic University, Professor Gerhard Bauch from TU Hamburg-Harburg, Institut für Nachrichtentechnik, Professor Takeo Ohgane from Hokkaido University, Professor Mineo Kaneko from JAIST, Associate Professor Brian Michael Kurkoski from JAIST, and Adjunct Professor Antti Tölli from UOulu for their valuable comments and suggestions to improve the quality of this dissertation.

I would like to take this opportunity to express my gratitude to my colleagues in JAIST for their great support and help in both daily life and academic research, Dr. Xiaobo Zhou, Dr. Meng Cheng, Dr. Penshun Lu, Dr. Xin He, Ms.c. Weiwei Jiang, Ms.c Kun Wu, Ms.c Fan Zhou, Dr. Khoirul Anwar, Dr. Ricardo Antonio Parrao Hernandez, Dr. Francisco Javier Cuadros Romero, Dr. Muhammad Reza Kahar Aziz, Dr. Yasuhiro Takano, Dr. Ade Irawan, Ms.c Garcia Alvarez, Erick Christian, and Ms.c Yu Yu. My deep gratitude also goes to colleagues in CWC, Dr. Valtteri Tervo, Ms.c Jiguang He, Dr. Iqbal Hussain, Dr. Pedro Henrique Juliano Nardelli, and Ms.c Hamidreza Bagheri for their kind help and friendship. I wish to thank Prof. Jari Iinatti, Adjunct Professor Mehdi Bennis, and Dr. Keigo Hasegawa who have served as my follow-up group members and provided a lot of valuable advices. I was very lucky that I joined a very aggressive

team with many talented and kind members. They are very friendly and brilliant. I also would like to thank the administrative staff in both JAIST and UOulu, Aya Inoue, Kyoko Hoshiba, Tomoko Taniguchi, Dr. Anthony Heape, Dr. Minna Silfverhuth, and Kirsi Ojutkangas, for their efforts to make my double doctoral degree study possible.

In addition, I would like to express my gratitude to Doctor Research Fellow (DRF) program of JAIST, Research Grants for JAIST Students, Koden Electronics Co., Ltd, Japan, NEC C&C Foundation, Japan, The Telecommunications Advancement Foundation, Japan, for providing me with financial support such that I can focus on my research work.

Finally, I would like to express my deepest thanks to my parents Pingyi Qian and Xinping Bi far in my homeland. I wish they can accept my apologies for I cannot fulfill my filial duty at their side. Also I want to thank my beloved wife Jian Li for her continual support and encouragement. Without her love and understanding, I could not have made those achievements shown in this dissertation.

Nomi, October 5 2017 Shen Qian

List of abbreviations

AF	Amplify-and-forward
AWGN	Additive white Gaussian noise
BER	Bit error rate
BPSK	Binary phase shift keying
BSC	Binary symmetric channel
cdf	Cumulative distribution function
CEO	Chief executive officer
CSI	Channel state information
DF	Decode-and-forward
EXIT	Extrinsic information transfer
FP7	7th Framework Program
FER	Frame error rate
HI	Horizontal iteration
ICT	Information and communication technology
i.i.d.	Independently and identically distributed
IoT	Internet of things
JSD	Jensen-Shannon divergence
KKT	Karush-Kuhn-Tucker
KLD	Kullback-Leibler divergence
LF	Lossy-forward
LLR	Log-likelihood ratio
LOS	Line-of-sight
MARC	Multiple access relay channel
MAC	Multiple access channel
MIMO	Multiple-input multiple-output
MUD	Multi-user detection
NLOS	Non-line-of-sight
P2P	Point-to-point
pdf	Probability density function
QPSK	Quadrature phase-shift keying

RESCUE	Links-on-the-fly Technology for Robust, Efficient and Smart Communication in Unpredictable Environments
SINR	Signal-to-interference-plus-noise ratio
SNR	Signal-to-noise ratio
VI	Vertical iteration
VR	Virtual reality
XOR	Exclusive-OR
5G	5th generation

List of Symbols

C	channel capacity
$\mathscr{D}$	distortions
E_s	transmit energy per symbol
E^n	dimensionality of channel input
G	geometric gain
G_c	coding gain
G_d	diversity gain
h	complex channel gain
K	Rician factor
m	Nakagami-m shape factor
n	zero-mean AWGN
N_0	noise variation
p_f	bit flipping probability
P_T	total transmit power
R	source coding rate
R^{c}	channel coding rate
$R(\mathscr{D})$	rate-distortion function
α	path loss exponent
γ	instantaneous SNR
$\overline{\gamma}$	average SNR
ρ	correlation coefficient
ρ_s	spatial correlation coefficient
ρ_t	temporal correlation coefficient
$\mathrm{ACC_S}$	accumulator for the source
$\mathrm{ACC_S^{-1}}$	decoder of the accumulator for the source
$\mathrm{C_S}$	encoder for the source
$\mathrm{D_S}$	decode for the source
$\mathrm{M_S}$	modulator for the source
$\mathrm{M_S^{-1}}$	demodulator for the source
Π_{S}	interleaver for the source

Π_{S}^{-1}	de-interleaver for the source
b_{S}	binary information sequence of the source
$\mathrm{ACC}_{\mathrm{R}}$	accumulator for the relay
$\mathrm{ACC}_{\mathrm{R}}^{-1}$	decoder of the accumulator for the relay
C_{R}	encoder for the relay
D_{R}	decode for the relay
M_{R}	modulator for the relay
$\mathrm{M}_{\mathrm{R}}^{-1}$	demodulator for the relay
Π_{R}	interleaver for the relay
Π_{R}^{-1}	de-interleaver for the relay
b_{R}	binary information sequence of the relay
Π_0	interleaver between the source and the relay
Π_0^{-1}	de-interleaver between the source and the relay

$a * b$	binary convolution, i.e., $a * b = a(1-b) + b(1-a)$
$C(\cdot)$	Shannon channel capacity
$C_{cc}(\cdot)$	constellation constrained channel capacity
$C_{cc}^{-1}(\cdot)$	inverse function of constellation constrained channel capacity
$d(\cdot,\cdot)$	distortion measure function
$E[\cdot]$	expectation of random variable
$\exp(\cdot)$	natural exponential function
$H(\cdot,\cdot)$	joint entropy function
$H(\cdot\vert\cdot)$	conditional entropy function
$H(\cdot)$	binary entropy function
$H^{-1}(\cdot)$	inverse of binary entropy function
$I(\cdot;\cdot)$	mutual information function
$I_0(\cdot)$	zero-th order modified Bessel's function of the first kind
min	minimization
$p(\cdot)$	probability density function
$p(\cdot,\cdot)$	joint probability density function
$p(\cdot\vert\cdot)$	conditional probability density function
$Q_1(\cdot,\cdot)$	Marcum Q function
$\Gamma(\cdot)$	Gamma function
$\gamma(\cdot,\cdot)$	lower incomplete gamma function
$\ln(\cdot)$	natural logarithm

$\log(\cdot)$	logarithm function with base 2
$\lg(\cdot)$	logarithm function with base 10
$\Pr(\cdot)$	probability
$\hat{\cdot}$	estimation
$\oplus$	modulo-2 addition

Contents

1 Introduction

Next generation wireless systems (5G) is considered to be the foundation of information and communication technology (ICT)-based society including virtual reality (VR), autonomous vehicles, and internet of things (IoT). By exploiting underutilized frequency spectrum available in millimeter wave, 5G is designed to handle thousands of times of more data traffic and can provide more than ten times the transmission speed compared to the existing networks. Millimeter wave cannot well travel in the presence of obstacles, e.g., buildings and shadowing objects, and tend to be affected by weather, e.g., absorbed by rain [1]. In cooperative communications, relays overhear the wireless signal and enhance the transmission between the nodes. Consequently, the wireless signal can be forwarded over the obstacles with the aid of relays, which can well solve the aforementioned problems. Cooperative communication in wireless networks is also of great importance as it has great potential for achieving diversity gain, enhancing network throughput, and extending communication coverage. This dissertation focuses on statistical performance characterization of the novel lossy-forward (LF)-based cooperative wireless networks and theoretical analysis of system performance by exploiting the statistical nature of channel variations.

In this chapter, we briefly introduce the basic concept of cooperative wireless communications. The wireless channel models are then described. The background and motivation of the research on exploiting channel variation in LF-based cooperative wireless communications are described, which is followed by the in-depth literature survey on the analyses and their results related to this research. The outline of this dissertation and the contributions of this research are also provided.

1.1 Cooperative Communications

Cooperative communication has been recognized as one of the most important techniques not only in designing the next generation wireless communication networks but also enhancing services and coverage of the existing systems, especially when it is used for the coverage expansion or diversity rather than static link design. It was initially introduced by Van der Meulen [2] in 1970s and the information theoretic analyses for the relay networks were intensively conducted by Cover and Gamal in [3]. Before the cooperative communications emerged, the transmission quality only relies on the condition of the direct link between source and destination. However, with cooperative communications, nearby nodes (i.e., base stations, mobile devices, stationary devices) who overhear the source information can serve as relays for helping in transmission. By forming *virtual antenna array* [4] to cooperate with each other to mitigate the signal attenuation due to the variation of the propagation conditions, without having to impose strict constraints in deployment or excessively high hardware complexity compared with *fixed* multiple-input multiple-output (MIMO) techniques, cooperative communications are able to enhance power and spectrum efficiencies and improve communication reliability [5].

1.1.1 Relay Protocols

The relay protocol specifies the processing performed by the relay upon its received signals. Based on the operations at the relay, relay protocols can be mainly classified into following categories [6–9].

Amplify-and-Forward

In amplify-and-forward (AF) relaying (also called observe-and-forward) [7], the received signal sent via the source-relay link is simply scaled and amplified by a relay, and forwarded to the destination. The destination make decision by properly combining signals sent from the source and relay, and thereby spatial diversity can be achieved by the AF protocol. The major problem of the AF protocol is that the noise at the relay is also amplified and forwarded, which causes performance degradation.

Decode-and-Forward

Among the various relaying protocols, decode-and-forward (DF) relaying has drawn significant attentions, and been widely studied. In DF relaying, if the transmitted information sequence is successfully recovered at the relay, the recovered information sequence is re-encoded and forwarded to the destination. The relay keeps silent if error is detected after decoding at the relay to avoid error propagation. Several analyses on the diversity and multiplexing gains as well as their tradeoff of DF relaying have been conducted for half duplex and full duplex systems [10–12]. Various practical

Table 3. Forwarding Strategies

Type	Approach
Static Relaying	A certain implementation for the cooperation is utilized at the relay.
Adaptive Relaying (Selection)	Transmitting terminals adapt transmission format, e.g., cooperative or non-cooperative, based upon the measured SNR.
Adaptive Relaying (Incremental)	Exploiting limited feedback from destination to decide whether relay forwards what it received from the source or keeps silent.

implementations of DF relaying in single-antenna scenarios have been analyzed in [13, 14], and in multiple-antenna scenarios in [15, 16].

Compress-and-Forward

In compress-and-forward relaying, the relay quantizes and compresses the received information by utilizing the source-relay correlation, then forwards the compressed version to the destination. The destination estimates the received information sequence by utilizing the information sequence transmitted from source as a helper [17, 18].

Compute-and-Forward

In compute-and-forward relaying, the relay decodes linear functions of the received signals by using the linear combinations provided by the channel, and forwards the decoded results to the destination. At the destination, the linear combinations are solved for recovering the original information [9].

Derivative Strategies

Various forwarding strategies have been proposed to achieve the benefits of cooperative communications. Laneman *et al.* outlined a variety of strategies [8, 19] which are categorized in Table 3.

1.2 Wireless Channel Models

In wireless communications, radio signal propagation is subject to reflection, diffraction, and scattering due to the obstacles in the environment. These mechanisms affect the radio propagation in different ways, i.e., path-loss, shadowing, and fading [20]. Path-loss is related to transmission distance and free space loss; shadowing (sometimes called large scale fading) indicates the received signal variation around the path-loss attenuation and its statistics are typically well characterized by the log-normal distribution; the (small scale) fading or short-term signal variation is typically caused by multiple signals received via different propagation paths. Due to the existence of a great variety of fading environments, channel fading can be statistically described by different models [21].

Radio signals arrive at the destinations via multiple propagation paths where there are obstacles. Therefore, each component signal received has different energy[1]. The received signal is a superposition of the component signals, which results in amplitude variation and phase rotation. The Rayleigh fading model is widely used to characterize the variations where the amplitude follows Rayleigh distribution over $[0, \infty)$ and the phase follows uniform distribution over $[0, 2\pi)$. The speed of the variation depends on the velocity of the mobile node. Each component signal suffers from different Doppler $shift$, hence the received composite signal composed of the received signal components suffers from Doppler $spread$.

The Rayleigh fading[2] is commonly used to describe random variations due to multi-path effect having non-line-of-sight (NLOS) components, such as densely populated urban areas having a lot of buildings and other objects, resulting in no direct path between the transmitter and the receiver in the wireless channel.

However, in some scenarios, channels are composed of both line-of-sight (LOS) and NLOS components in wireless communications systems, e.g., terrestrial mobile and satellite mobile communications systems. A mathematical model of the channel having LOS and NLOS components is Rician fading, where the amplitude is characterized by a Rician distribution. The Rician fading model is widely used to characterize the channels that exploit the performance gain due to the LOS conditions. Rician factor K denotes the ratio of the LOS component power-to-NLOS components average power. K

[1] We only assume frequency non-selective fading. The impact of the frequency selectivity in relaying system is left as a future work, as described in Chapter 5

[2] Strictly speaking, the first order statistic of vehicle-to-vehicle communication is described by double Rayleigh distribution, if there are non-line-of-sight (NLOS) components. However, this dissertation assumes the simplest NLOS components model, Rayleigh fading.

factor represents severity of fading variation. With $K = 0$, Rician fading reduces to Rayleigh fading. With $K = \infty$, channel is equivalent to static additive white Gaussian noise (AWGN) channel (Receiver hardware always introduces AWGN to the received signal).

Although the Rician distribution is widely used to represent the statistical behaviors of the channels, it is still not accurate enough as the first-order statistics of the channel variations are compared with the measurement data gathered in the fields. The Nakagami-m distribution is derived empirically based on the measurement data [22]. It is known that the Nakagami-m fading is able to better represent the distribution of the channel behaviours compared to the Rician distribution [23]. Nakagami-m model can model a wider range of channel conditions including severe, moderate, light and no fading. It is well known that both Rayleigh and Rician distributions are connected to the Nakagami-m fading model by adjusting the shape factor m representing the fading severity in Nakagami-m model [20, 24].

Yacoub *et al.* proposed two more generalized fading models, κ-μ and η-μ, which are fully characterized in terms of measurable physical parameters and known to be better matched to measurement data than the other models [25]. The κ-μ distribution includes the Rician, the Nakagami-m, and the Rayleigh distributions as special cases, whereas, the η-μ distribution includes the Nakagami-m, the Rayleigh, and the one-sided Gaussian distributions as special cases. In particular, the κ-μ distribution better fits LOS scenarios. The η-μ distribution is better suited for NLOS applications.

1.3 Background and Research Motivations

1.3.1 Research Background

As stated before, cooperative communications have been recognized as the promising technologies for next generation wireless communication systems. A key to create efficient and flexible technologies for the further generation wireless communication networks is to know how the latest results of network information theory can be best utilized in wireless communication network design. For example, in the DF relaying systems, the information sequences sent from the same source are correlated, which, in the theoretical side, invokes the idea of utilizing the source coding with a helper theorem. In the practical system design side, the correlation knowledge can be utilized in the distributed turbo coding with the idea of log likelihood ratio (LLR) updating corresponding to the errors occurring in the network [26, 27]. The theoretical and practical considerations have created the relaying technique called lossy-forward (LF) [27]. It has been proven that LF relaying can reduce outage probability, compared to conventional DF relaying [28].

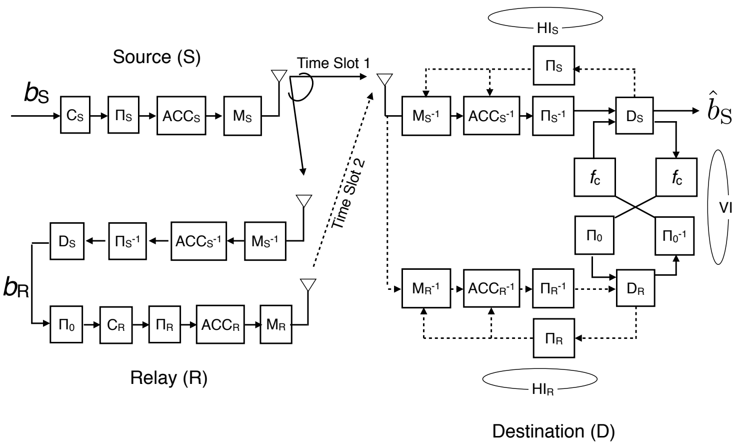

Fig. 1. Coding and decoding structure of the LF relaying system.

In conventional DF relaying [3, 19], the recovered information sequence is discarded at the relay if error is detected after decoding. It has been believed that if the relay re-encodes the information sequence containing error and forwards it to the destination, error propagation will occur, resulting in even worse performance [29]. However, even though error may be detected at the relay, the information sequences transmitted from the source and relay are still correlated. Therefore, the source coding with a helper theorem [30] can be used in this scenario by utilizing the information sequence transmitted from the relay as a helper. In LF relaying, the relay does not aim to perfectly correct the errors occurring in the source-relay link. The decoded information sequence at the relay is re-interleaved, re-encoded, and transmitted to the destination, even though error may be detected in the information sequence after decoding. The probabilities of the errors occurring in the source-relay link can be estimated at the destination [31]. After converting the received signals from the source and the relay to the LLR sequences of the systematic bits, iterative processing for the systematic LLR exchange between the two decoders, one for decoding the signal received via the source-destination link and the other via the relay-destination link, is invoked. The systematic LLR is modified to best utilize the estimate of the error probability of the source-relay link by a LLR modification function [26]. The LLR modification function makes compensation of the systematic LLR values, according to the knowledge of the source-relay link error probability, resulting in decoding performance improvement [27].

The coding/decoding structure of a three-node LF relaying system is shown in Fig. 1. At the source, the binary information sequence b_{S} is first encoded by $\mathrm{C_S}$. Then, the encoded information sequences are interleaved by a random interleaver Π_{S} and doped-accumulated by a $\mathrm{ACC_S}$ (The purpose using $\mathrm{ACC_S}$ is to control the shape of the extrinsic information transfer (EXIT) curve of the demodulator and keep the convergence tunnel open. [40]). Then, the outputs of $\mathrm{ACC_S}$ are mapped onto symbols by a modulator $\mathrm{M_S}$, and broadcasted to both the relay and the destination in the first time slot. The received signal at the relay is first fed to a demodulator $\mathrm{M_S^{-1}}$, followed by the decoder $\mathrm{ACC_S^{-1}}$ of $\mathrm{ACC_S}$. The extrinsic LLR output from $\mathrm{ACC_S^{-1}}$ is fed to the de-interleaver Π_{S}^{-1}, followed by the decoder $\mathrm{D_S}$ of $\mathrm{C_S}$. Instead of performing the fully iterative decoding/detection between $\mathrm{M_S^{-1}}$ and $\mathrm{D_S^{-1}}$, only simple non-iterative decoding is performed. Hard decision is then performed on the output of $\mathrm{D_S^{-1}}$ to obtain the information sequence b_{R} at the relay. With this technique, we can significantly reduce the complexity of the relay compared to conducting iteratively decoding.

Due to the weak decoding at the relay, b_{R} may contain errors. However, b_{R} is again random interleaved by Π_0, channel re-encoded by $\mathrm{C_R}$, re-interleaved by a random interleaver Π_{R} and fed to $\mathrm{ACC_R}$. The purpose of the use of Π_0 is that the interleaved sequence $\Pi_0(b_{\mathrm{R}})$ is made statistically independent of b_{S}. Finally, the information sequence is re-mapped by $\mathrm{M_R}$, and transmitted to the destination in the second time slot.

At the destination, detection process for the signal received in the first and second time slots, respectively, is first performed independently as shown in Fig. 1. At this stage, fully iterative docoding/detection is adopted between $\mathrm{M_S^{-1}}$ and $\mathrm{D_S^{-1}}$, which is referred to as horizontal iteration (HI), as well as between $\mathrm{M_R^{-1}}$ and $\mathrm{D_R^{-1}}$ [27]. After each round of HI, the extrinsic systematic LLRs obtained from the two decoders $\mathrm{D_S}$ and $\mathrm{D_R}$ are further exchanged with each other, which is referred to as vertical iteration (VI). The extrinsic systematic LLR is updated by the function LLR updating function f_c [31]. By utilizing the function f_c, the extrinsic systematic LLRs, forwarded by the relay, help the decoder eliminate the errors in the original information sequence b_{S} by exploiting the correlation knowledge between the source and the relay. Finally, the detection of b_{S} can be completed by making hard decisions of the a posteriori LLRs of the systematic bits outputs from $\mathrm{D_S}$.

The LF technique can be viewed as a distributed joint source-channel coding system with a helper [32–35]. It is shown that with the help of the accumulator, LF can achieve turbo-cliff-like bit error rate (BER) performance over AWGN channels [27, 36].

The LF concept is originated from the idea of Slepian-Wolf cooperation presented in [37]. The coding algorithms are proposed for fading relay channel in [38, 39]. The key concept of the coding technique for LF is introduced in [27], where it assumes that the relay does not need to necessarily recover the information sent from the source perfectly. In [40], a three-node LF relaying over Rayleigh fading channels is studied by identifying the relationship between the DF protocol and Slepian-Wolf coding [41]. However, a drawback of [27, 40] is that the admissible rate region is determined by the Slepian-Wolf theorem which does not perfectly match the problem setup, since only the information of the source needs to be recovered at the destination. Zhou *et al.* [28] eliminate the aforementioned drawback by utilizing the source coding with a helper theorem in the network information theory. Based on [28], the technique is further extended to multiple access relay channel (MARC) [42], where a pair of correlated sources are transmitted to a destination with the aid of one relay. Furthermore, He *et al.*[43] apply the LF technique to the multi-source multi-relay system. A two-relay LF transmission system is proposed and a power allocation scheme for minimizing the outage probability of the two-relay LF system is presented in [44]. The technique is applied to wireless sensor networks, where a simple, yet efficient, power allocation scheme for an arbitrary number of sensors is derived in [45]. The major contributions under the LF relaying framework are summarized in Table 6.

1.3.2 Motivations

The primary goal of this dissertation is to identify the statistical properties performance of the LF-based cooperative wireless networks, and to provide theoretical analysis of system performance by exploiting the statistical characteristics of channel variations. In wireless communications, channels experience variations due to fading. The direct source-destination link and the via-relay link propagations are often found to be in different conditions. Hence, it is quite reasonable to assume that the statistical properties of the fading variations are also different, link by link. A most probably scenario is that since the direct link from source to destination suffers from severe fading, the destination needs the help of a relay via source-relay and relay-destination links which suffer from moderate fading. Hence, we consider the cases that the source-destination link suffers from block Rayleigh fading (or equivalent Rayleigh fading), while the other links (the source-relay and relay-destination links) experience mild fading, e.g., having LOS component. It is, hence, very interesting to identify the impact of the LOS component on system performances.

In practical cooperative networks such as vehicle-to-infrastructure communications, it is often the case that the fading conditions experienced by different links are correlated due to insufficient separation in the space or time domains between the nodes or transmissions [46–48]. Therefore, examining the performance of diversity techniques in correlated fading conditions has been a long lasting problem with great importance [49]. Motivated by this, system performance in correlated fading is also investigated.

Diversity gain shows how fast the outage probability or frame error rate (FER) can decrease by increasing the average SNR $\overline{\gamma}$ [50], by which one can have the insights regarding the factors determining the system performance in fading channels. How many independently varying signal components exist in the propagation medium, and how many of them can be extracted, for example, by using multiple antennas, different and/or time slots determines the diversity order that corresponds to the decay of the outage probability or FER curves as a function of $\overline{\gamma}$. Coding gain appears in the form of the parallel shift of the outage probability/FER curves versus $\overline{\gamma}$. At high SNR, the outage probability P_{out} can be asymptoticly expressed in terms of diversity order and coding gain, as,

$$P_{out} = (G_c \cdot \overline{\gamma})^{-G_d}, \tag{1}$$

where G_d and G_c indicates the diversity order and coding gain, respectively. It should be noted here that in Rayleigh fading environment having NLOS components, the diversity order has only integer values which corresponds to the decay of the outage probability curve. However, in the presence of the LOS component, the decay can take negative real values, depending on the ratio of LOS component to NLOS components. Therefore, we refer the decay of the outage probability curve as to *equivalent diversity order*. This dissertation derives the equivalent diversity order and coding gain for LF relaying over block Nakagami-m fading with arbitrary values of the shape factor m. Also, the account is took of the channel correlations when investigating the diversity order and coding gain for LF, DF, and adaptive decode-and-forward (ADF). Since the capacity-achieving channel codes and infinite frame length are assumed in the theoretical analyses, the obtained theoretical results can be used for evaluating the asymptotic performances of practical systems.

Table 4. Fading channel models.

Channel Type	**Applicable Scenarios**	**Extreme Cases**	**Remarks**
Rayleigh	NLOS conditions	–	–
Rician	NLOS and LOS conditions	Rayleigh fading with Rcian factor $K = 0$; nonfading (AWGN) with $K \to \infty$	–
Nakagami-m	NLOS and LOS conditions	Rayleigh fading with Shape factor $m = 1$; nonfading (AWGN) with $m \to \infty$	empirically derived from measurement data
κ-μ	NLOS and LOS conditions	Nakagami-m fading with $\kappa = 0$; Rician fading with $\mu = 0$	general fading distributions; better fit experimental data

For characterizing the statistical performance under different channel conditions, we consider several fading models, as listed in Table 4. The Rayleigh fading is most widely used propagation model, applicable to the case where there is no signal component along a LOS. The Rician model describes a fading condition where there are both LOS and NLOS paths between the transmitter and the receiver [51]. The Nakagami-m fading is an empirically derived model using field measurement data, and hence is better matched to real propagation scenario compared to the Rician distribution. Therefore, we also consider Nakagami-m model as representing the propagation scenario including LOS and NLOS components. Moreover, a recently proposed general κ-μ model, which better fits experimental data than Rician or Nakagami-m models, is also used to represent the variation of the fading signal in the presence of LOS component.

The Rician and Nakagami-m models are utilized to represent the fading variation having both NLOS and LOS components. They are connected by the Rician factor K and Nakagami-m shape factor m both representing the fading severity. Therefore, the impact difference of the Rician and Nakagami-m fading on outage performance is evaluated. The Kullback-Leibler divergence (KLD) and Jensen-Shannon divergence (JSD) are used to identify the difference between the Rician and Nakagami-m distributions. To further generalize the propagation model with a LOS component, this dissertation applies time-varying K factor scenario, where the K value in the Rician model is assumed to follow empirical distributions, normal or logistic distributions; they were derived from field measurement data [52], and hence recognized as being practical.

Theoretical analysis and performance evaluation of the generic cooperative network model is complicated. Furthermore, if dynamic network topology variation is taken into account, it imposes a lot of challenges. Instead, we decompose the general network into several network models having simple structures that are widely used in cooperative communication research, as summarized in Table 5.

Table 5. System model in each Chapter.

Chapter	**Network Topology**	**Fading Model**
2	Three-Node One-Way Relaying	Nakagami-m Fading, and Correlated Rayleigh Fading
3	Three-Node Two-Way Relaying	Rician Fading with Random K-factor
4	Two-Source Two-Relay Transmission	κ-μ Fading

Although only simple system structures are considered, the information theoretic analysis for these basic network models provides insights into understanding of more generic networks.

1.4 Outline of Dissertation

In Chapter 2, we investigate the performance of a three-node one-way relay system. First of all, the exact outage probability of LF relaying over Nakagami-m fading channels with arbitrary values of the shape factor m is derived. With a yet accurate approximated expressions, the equivalent diversity order and coding gain of LF relaying are identified. Compared with conventional DF relaying, LF relaying can achieve even lower outage probability. We then analyze the impact of the spatial and temporal correlations of the fading variations on the system performance of LF, DF and ADF relaying. The diversity orders with LF, DF, and ADF are derived in the presence of the spatial and temporal fading correlations. Obviously, the larger the correlation, the higher the outage probability. Chapter 2 provides formulas that represents this relationship in a mathematical way. It is found that the optimal relay locations yielding the smallest outage probability move towards to the destination, compared with the case in independent fading. Finally, the differences between the outage performances with LF relaying in Rician and Nakagami-m fading, are also investigated. The Kullback-Leibler divergence (KLD) and Jensen-Shannon divergence (JSD), which represent the difference quantitatively between two probability distributions, are used to verify the performance difference on the outage curves with Rician and Nakagami-m distributions. The analytical results show that, even with the parameter settings yielding the same LOS-to-NLOS power ratio, Rician can not exactly replace the Nakagami-m model to represent the entire shape of distributions.

Chapter 3 propose a two-way LF relaying system utilizing non-orthogonal source-to-relay links transmission, and hence it can achieve significant spectral efficiency gain compared to one-way relaying. Another focus point of Chapter 3 is the impact analysis of time-varying LOS signal energy. We assume the channels suffer from Rician fading with random K factor. The Rician K-factor is assumed to follow empirical distributions derived from measurement data, i.e., logistic and normal distributions. From the analytical results, we found that compared to two-way DF relaying, two-way LF relaying achieves lower outage probability regardless of either logistic or normal distribution is used to represent the variation of K-factor. This is because with LF relaying, the relay always broadcast the decoder output regardless of whether or not error is detected after decoding in the information part, and hence source correlation can be well exploited at the decoder of the destination.

Chapter 4 extends the major results of the previous chapters, and focuses on the problem of transmitting two sources to one destination over a two-relay transmission system. All the links experience κ-μ fading variation, which is more consistent to measurement data than Rician or Nakagami-m model. Two transmission, non-orthogonal maximum ratio transmission and orthogonal transmission with joint-decoding at the destination, are considered as the relay-destination transmission schemes. The theoretical analysis indicates that the outage performance of the two-source two-relay system with orthogonal transmission with joint-decoding scheme outperforms that with maximum ratio transmission scheme.

Chapter 5 summarizes the work and presents insight discussion for the future work.

1.5 Summary of Outcomes

This dissertation is written as a monograph based on two journal papers [53, 54], one letter [55], and two conference papers [56, 57]. The first journal paper [53] has already been published and the other [54] has been accepted. The author has the main responsibility for performing the analysis, generating the numerical results, and writing all the papers [53–57]. The other authors have provided comments and constructive criticisms.

Besides the aforementioned publications, the authors published four other conference papers [58–61] and co-authored several papers in the relevant topic [62–66] during the doctoral study. Furthermore, the author has been involved in creating Technical reports/Deliverables [67–71] under the 7th Framework Program (FP7) Links-on-the-fly Technology for Robust, Efficient and Smart Communication in Unpredictable Environments (RESCUE) project.

Table 6. Summary of major contributions on LF relaying.

Year	Authors	Contributions
2005	Hu and Li [37]	Proposed Slepian-Wolf cooperation, which exploits distributed source coding technologies in wireless cooperative communications.
2007	Woldegebreal and Karl [72]	Considered a network-coding-based MARC in the presence of non-ideal source-relay links, and analyzed the outage performance and coverage.
2007	Sneessens *et al.* [39]	Derived a decoding algorithm which enables the use of turbo-coded DF relaying by taking into account the probability of error between the source and the relay.
2012	Anwar and Matsumoto [27]	Proposed an iterative decoding technique, accumulator-assisted distributed turbo code, where the correlation knowledge between the source and the relay is estimated and exploited.
2013	Cheng *et al.* [40]	Proposed a scheme for exploiting the source-relay correlation in joint-decoding process at the destination, based on the Slepian-Wolf theorem.
2014	Zhou *et al.* [28]	Derived the exact outage probability by utilizing the lossy source-channel separation and source coding with a helper theorems.
2015	Wolf *et al.* [44]	Proposed an optimal power allocation strategy for a two-relay system based on convex optimization to minimize outage probability.
2015	Lu *et al.* [42]	Derived the outage probability for orthogonal MARC for correlated source transmission where erroneous source information estimated at the relay is forwarded.
2016	Wolf *et al.* [45]	Proposed asymptotically optimal power allocation scheme for wireless sensor networks with correlated data from an arbitrary amount of sensors.

2 On the Performance of One-Way Lossy-Forward Relay Wireless Networks

In this chapter, we investigate the performance of three-node LF relaying over independent block Nakagami-m fading channels. Based on the source coding with a helper theorem, the outage probability expression with arbitrary values of the shape factor m is derived. Then, we identify the impact of the spatial and temporal correlations of the fading variations on the outage performances of LF, DF and ADF relaying in correlated Rayleigh fading. Finally, the impact difference of the Rician and Nakagami-m fading on outage performance of the one-way LF relaying system is evaluated.

2.1 Lossy-Forward Transmission over independent Nakagami-m Fading Channels

2.1.1 System Model

We consider a simple three-node relaying system as shown in Fig. 2. The source S communicates with the destination D with the help of a single relay R. The location of R varies in a line parallel to the line connecting S and D between $x = 0$ (nearest to S) and $x = 1$ (nearest to D). Unless otherwise specified, the distant between R and the line connecting S and D is set at $\frac{1}{2}$ of S-D link length. We assume time-division transmission, where the overall transmission is divided into two time slots. In the first time slot, the original uniformly distributed binary information sequence b_{S} is encoded and broadcast from S. The relay R aims to recover the information sequence, and always re-interleaves the information sequence, re-encodes it and forwards the encoder output to D in the second time slot, even though the decoding result may contain error in the original information sequence.

LF Relaying

In conventional DF relaying, R keeps silent if error is detected after decoding in the information sequence sent through the S-R link. With LF relaying, after receiving the signal from S, R attempts to recover b_{S}. Although the decoding result of b_{S} at R,

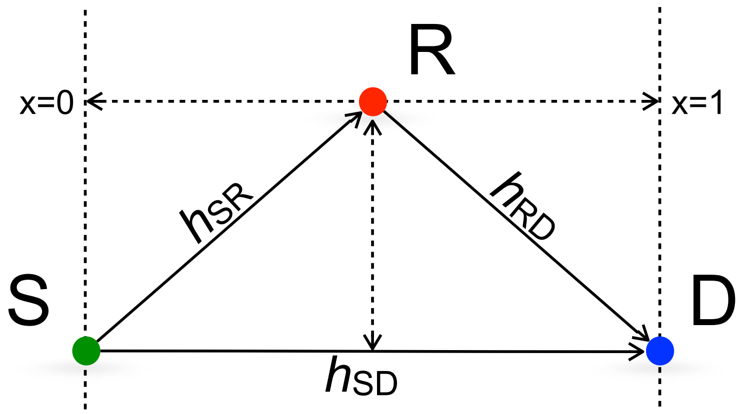

Fig. 2. The schematic of one relay aided communication system, where all the links (the S-R, R-D and S-D links) in Nakagami-m fading.

denoted by b_{R}, may be found to contain error, R re-interleaves the information sequence b_{R}, re-encodes the re-interleaved sequence, and forwards it to D.

The S-R link is virtually modeled by a binary symmetric channel (BSC) model with a crossover probability p_f. More specifically, p_f represents the bit flipping probability between the information sequence obtained after decoding at R and the original information sequence sent from S. Hence, $b_{\mathrm{R}} = b_{\mathrm{S}} \oplus e$, where $\oplus$ denotes the modulo-2 addition and e is a realization of a binary random variable E with $\Pr(E = 1) = p_f$. p_f stays the same within each block while changes block-by-block with its value being determined by the instantaneous SNR.

At D, after receiving the signals from S and R, joint decoding is performed to retrieve the original information b_{S}. Iterative decoding is utilized between two decoders for decoding the information sent from S and R. In the decoding process, the S-R link error probabilities p_f can be estimated at D. The estimated p_f value is used as the correlation knowledge between b_{S} and b_{R} [27]. The LLRs of the systematic bits are exchanged between the two decoders via the interleaver/de-interleaver. Therefore, the system, as a whole, can be viewed as a distributed turbo code.

Channel Model

The signals received at D and R in the first time slot, $y_{\mathrm{D},1}$ and $y_{\mathrm{R},1}$, respectively, and the signal received at D in the second time slot, $y_{\mathrm{D},2}$, are expressed as[3]

$$y_{\mathrm{D},1} = \sqrt{G_{\mathrm{SD}}} h_{\mathrm{SD}} x_1 + n_{\mathrm{D},1}, \tag{2}$$

$$y_{\mathrm{R},1} = \sqrt{G_{\mathrm{SR}}} h_{\mathrm{SR}} x_1 + n_{\mathrm{R},1}, \tag{3}$$

$$y_{\mathrm{D},2} = \sqrt{G_{\mathrm{RD}}} h_{\mathrm{RD}} x_2 + n_{\mathrm{D},2}, \tag{4}$$

respectively, where G_{ij} $(i \in (\mathrm{S},\mathrm{R}), j \in (\mathrm{R},\mathrm{D}), i \neq j)$ are the geometric gains related to the transmit distance of each link. The modulated symbols transmitted from S and R are denoted by x_1 and x_2, respectively. h_{ij} denotes the complex channel gain and $n_{j,1}$ and $n_{j,2}$ are zero-mean AWGN with variance of $N_0/2$ per dimension. It is assumed that $E[|h_{ij}|^2] = 1$ and h_{ij} stays constant over one block duration due to the block fading assumption. We assume that the channel state information (CSI) is only available at the receiver side.

The transmit energy of each symbol is denoted as $E\{|x_1|^2\} = E\{|x_2|^2\} = E_s$. Therefore, the average and instantaneous SNR of each link is expressed as $\overline{\gamma}_{ij} = G_{ij}\frac{E_s}{N_0}$ and $\gamma_{ij} = |h_{ij}|^2 \overline{\gamma}_{ij}$ $(i \in (\mathrm{S},\mathrm{R}), j \in (\mathrm{R},\mathrm{D}), i \neq j)$, respectively. For the sake of simplicity, the variations due to shadowing and the fading frequency selectivity are not taken into account.

We assume that all the links (i.e., the S-R, S-D, and R-D links) suffer from independent block Nakagami-m fading, with the probability density function (pdf) of γ_{ij} given by

$$p(\gamma_{ij}) = \frac{m_{ij}^{m_{ij}} (\gamma_{ij})^{m_{ij}-1}}{\left(\overline{\gamma}_{ij}\right)^{m_{ij}} \Gamma(m_{ij})} \exp\left(-\frac{m_{ij}\gamma_{ij}}{\overline{\gamma}_{ij}}\right), \; m_{ij} > 0.5, \tag{5}$$

where $\Gamma(\cdot)$ is the Gamma function. The shape factor m_{ij} represents the severity of the fading variation of each link.

We consider a scenario that the S-D link suffers from severe fading and the destination needs the help of a relay via S-R and R-D links, which suffer from mild fading, i.e., not as severe as the S-D link. Hence, we set the shape factor of the S-D link $m_{\mathrm{SD}} = 1$, corresponding to Rayleigh fading, while for other links (the S-R and R-D links), we set their m values as parameters $(m_{\mathrm{SR}} > 1, m_{\mathrm{RD}} > 1)$.

[3] The symbol indexes are omitted in (2), (3), and (4) for conciseness.

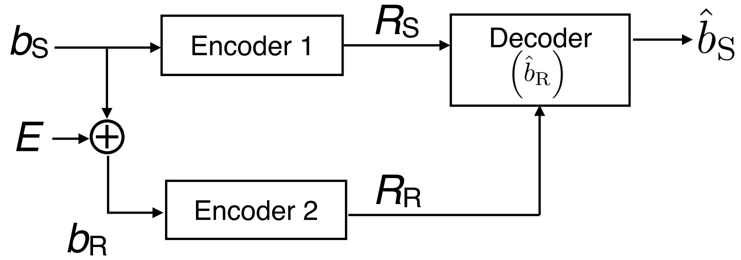

Fig. 3. Block diagram for the coding/decoding of b_S and b_R from the view of source coding with a helper. b_R is the bit-flipped version of b_S and serves as a helper for the decoding of b_S at the decoder .

2.1.2 Outage Probability Analysis

In this section, the definition of admissible rate region and the derivation for outage probability of LF relaying are provided. The outage probability is derived based on both Gaussian codebook capacity and constellation constrained capacity assumptions.

Admissible Rate Region Based on Source Coding with a Helper Theorem

In LF relaying, D aims to recover b_S only and the b_R transmitted from R does not need to be decoded successfully. Therefore, the analysis falls into the problem category of source coding with a helper. In other words, in the LF relay system, b_R servers as a helper for the successful recovery of b_S, as shown in Fig. 3. Assume b_S and b_R are described with rates R_S and R_R, respectively. According to the source coding with a helper theorem [30, Section10.4]

Theorem 1. ***Lossless Source Coding with a Helper*** *b_S can be recovered with an arbitrarily small probability of error if the rate pair (R_S, R_R) satisfies*

$$\begin{cases} R_S & \geq H(b_S|\hat{b}_R), \\ R_R & \geq I(b_R;\hat{b}_R), \end{cases} \tag{6}$$

where $\hat{b}_R$ is the estimate of b_R obtained at the decoder of the destination. $H(\cdot|\cdot)$ and $I(\cdot;\cdot)$ denote the conditional entropy and the mutual information between their arguments, respectively. Eq. (6) indicates that $I(b_R;\hat{b}_R)$ bits per symbol can be used to describe b_R. Then, b_S can be described at the rate of $H(b_S|\hat{b}_R)$ bits per symbol in the presence of a helper $\hat{b}_R$.

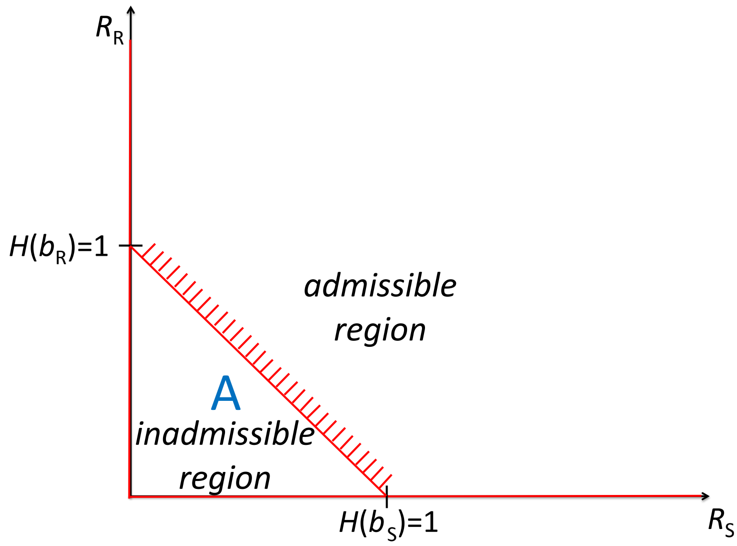

Fig. 4. Rate region for S and R when $p_f = 0$; the red solid line with bars separates the admissible and inadmissible regions.

With the block fading assumption, we also use a BSC model to represent the R-D link, as $\hat{b}_R = b_R \oplus e'$ with $\Pr(E' = 1) = p'_f$, where e' is a realization of a binary random variable E'. Since the source is assumed to be binary, uniform, and independently and identically distributed (i.i.d), (6) can be expressed as [28]

$$\begin{cases} R_S & \geq H(p_f * p'_f), \\ R_R & \geq H(\hat{b}_R) - H(\hat{b}_R|b_R) = 1 - H(p'_f), \end{cases} \tag{7}$$

where $p_f * p'_f = (1-p_f)p'_f + (1-p'_f)p_f$ and $H(\cdot)$ denotes the binary entropy function.

$p_f = 0$ indicates perfect decoding at R, and hence $H(b_S|b_R) = H(b_R|b_S) = 0$. In this case, the inadmissible rate region becomes the triangle area A as shown in Fig. 4. When $0 < p_f \leq 0.5$, the inadmissible region, which can be divided into two areas, B and C, is shown in Fig. 5.

If the relay sends b_R to the destination without error, $\hat{b}_R = b_R$ and $p'_f = 0$, then, the condition is $R_R \geq H(b_R)$ and $R_S \geq H(b_S|b_R)$. In the case $p'_f = 0.5$, which indicates that $\hat{b}_R$ is totally wrong and does not contain any useful information about b_R. Therefore, the condition becomes as $R_S \geq 1$ and $R_R = 0$. In any case of $0 < p'_f < 0.5$, the condition is $R_S \geq H(p_f * p'_f)$ and $R_R \geq 1 - H(p'_f)$.

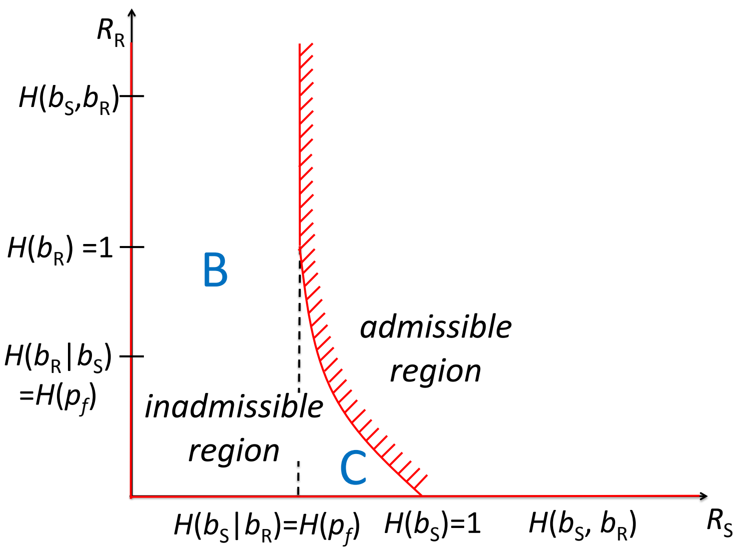

Fig. 5. Rate region for S and R when $p_f \neq 0$; the red solid line with bars separates the admissible and inadmissible regions.

Outage Event of LF relaying

If the rate pair (R_S, R_R) falls into the inadmissible regions in Fig. 4 or Fig. 5, the outage event occurs and D cannot guarantee the reconstruction of b_S with an arbitrarily small error probability. The outage probability of LF relaying can be expressed as

$$P_{out}^{LF} = P_A + P_B + P_C, \tag{8}$$

where P_A, P_B, and P_C denotes the probability that (R_S, R_R) falls into the inadmissible areas A, B, and C, respectively. Taking into account the impact of p_f and p'_f, P_A, P_B, and P_C can further be expressed as

$$P_A = \Pr[p_f = 0, 0 \leq R_S \leq 1, 0 \leq R_R \leq H(p_f * p'_f)], \tag{9}$$

$$P_B = \Pr[0 < p_f \leq 0.5, 0 \leq R_S < H(p_f), R_R \geq 0], \tag{10}$$

$$\begin{aligned} P_C = \Pr[&0 < p_f \leq 0.5, H(p_f) \leq R_S \leq 1, \\ &0 \leq R_R < H(p_f * p'_f)]. \end{aligned} \tag{11}$$

(A) Outage Derivation with Gaussian Codebook Capacity

For calculating the outage probability, first we establish the relationship between γ_{SD} and R_{S}, and the relationship between γ_{RD} and R_{R}. According to the Shannon's lossless source channel separation theorem [73], if the total information transmission rates over the S-D and R-D links satisfy

$$\begin{cases} H(b_{\mathrm{S}}) \cdot R^c_{\mathrm{SD}} \leq R_{\mathrm{S}} \cdot R^c_{\mathrm{SD}} \leq C_{\mathrm{SD}}(\gamma_{\mathrm{SD}}), \\ H(b_{\mathrm{R}}) \cdot R^c_{\mathrm{RD}} \leq R_{\mathrm{R}} \cdot R^c_{\mathrm{RD}} \leq C_{\mathrm{RD}}(\gamma_{\mathrm{RD}}), \end{cases} \tag{12}$$

the error probability can be arbitrarily small at the destination. $C_{i\mathrm{D}}$ and $R^c_{i\mathrm{D}}$, respectively, denote the channel capacity of the i-D link and the normalized spectrum efficiency of the corresponding transmission chain. The normalized spectrum efficiency includes the channel coding and the modulation multiplicity (constellation size). With the assumption that Gaussian codebook is used, the channel capacity $C_{i\mathrm{D}}$ of each link can be expressed as

$$C_{i\mathrm{D}}(\gamma_{i\mathrm{D}}) = \frac{E^n}{2}\log\left(1 + \frac{2\gamma_{i\mathrm{D}}}{E^n}\right),\ (i \in \mathrm{S},\mathrm{R}), \tag{13}$$

where E^n denotes the dimensionality of the channel input, e.g., $E^n = 1$ for binary phase shift keying (BPSK) and $E^n = 2$ for quaternary phase shift keying (QPSK). Hence, the relationship between the instantaneous channel SNR $\gamma_{i\mathrm{D}}$ and its corresponding source coding rate R_i is given by

$$R_i \leq \Theta(\gamma_{i\mathrm{D}}) = \frac{C_{i\mathrm{D}}(\gamma_{i\mathrm{D}})}{R^c_{i\mathrm{D}}} = \frac{E^n}{2R^c_{i\mathrm{D}}}\log\left(1 + \frac{2\gamma_{i\mathrm{D}}}{E^n}\right),\ (i \in \mathrm{S},\mathrm{R}) \tag{14}$$

with its inverse inequality

$$\gamma_{i\mathrm{D}} \geq \Theta^{-1}(R_i) = \frac{E^n}{2}\left(2^{\frac{2R_iR^c_{i\mathrm{D}}}{E^n}} - 1\right). \tag{15}$$

Then, we establish the relationship between γ_{SR} and p_f. Since p_f only depends on the quality of the S-R link, according to Shannon's lossy source channel separation theorem [74], we have

$$R(\mathscr{D}) \cdot R^c_{\mathrm{SR}} \leq C_{\mathrm{SR}}(\gamma_{\mathrm{SR}}), \tag{16}$$

where $R(\mathscr{D})$ denotes the source rate-distortion function with the distortion measure $\mathscr{D}$.

In the case of binary transmission, the Hamming distortion between a source bit x and its estimate $\hat{x}$ given by

$$d(x,\, \hat{x}) = \begin{cases} 0 & \text{if } x = \hat{x}, \\ 1 & \text{if } x \neq \hat{x}, \end{cases} \tag{17}$$

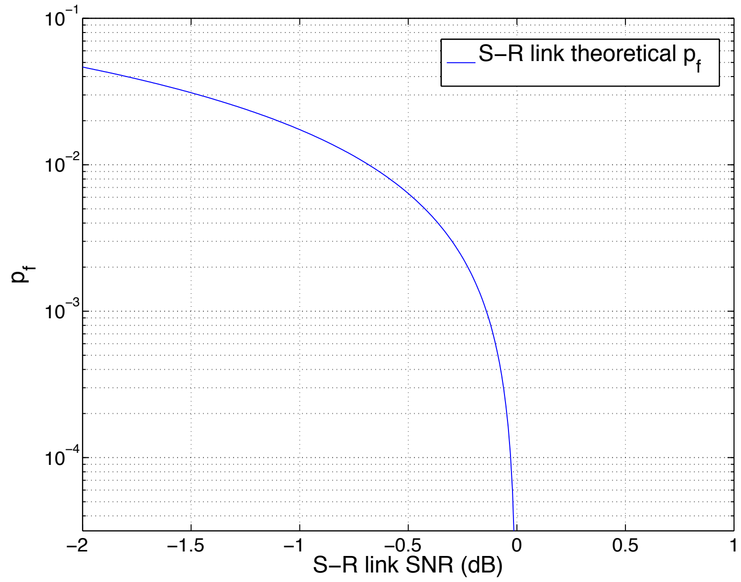

Fig. 6. S-R link Hamming distortion p_f versus SNR, where $E_n = 2$ and $R^c_{\mathrm{SR}} = 1$.

is used as the distortion measure.

With the bit-wise Hamming distortion measure, the sequence-wise distortion measure $\mathscr{D}$ is equivalent to the crossover probability p_f, since both p_f and $\mathscr{D}$ can be regarded as the theoretical BER of the S-R transmission with long enough sequence length. The rate-distortion function is represented as $R(\mathscr{D}) = 1 - H(\mathscr{D})$ for i.i.d binary source [75].

Since we assume that Gaussian codebook is used for the S-R link transmission, the relationship between the required instantaneous channel SNR γ_{SR} and its corresponding source rate $R(\mathscr{D})$ with distortion $\mathscr{D}$ is given by

$$\gamma_{\mathrm{SR}} \geq \frac{E^n}{2}\left(2^{\frac{2R(\mathscr{D})R^c_{\mathrm{SR}}}{E^n}} - 1\right). \tag{18}$$

Then, we can obtain the relationship between p_f and γ_{SR} as

$$p_f = H^{-1}\left(1 - \frac{\frac{E^n}{2}\log\left(1 + \frac{2\gamma_{\mathrm{SR}}}{E^n}\right)}{R^c_{\mathrm{SR}}}\right), \tag{19}$$

with $H^{-1}(\cdot)$ denoting the inverse function of $H(\cdot)$. The relationship between the S-R link SNR and p_f is shown in Fig. 6. It is found from Fig. 6 that the value of error probability p_f decreases as the SNR of the S-R link increases. Note that p_f stays constant within each block duration, but changes block-by-block, because of the block fading assumption.

With the Nakagami-m block fading assumption, the outage probability expressions with LF relaying in (8) can be expressed as

$$\begin{aligned}
P_{\mathrm{A}} =& \Pr[\gamma_{\mathrm{SR}} \geq \Theta^{-1}(1), \Theta^{-1}(0) \leq \gamma_{\mathrm{SD}} \leq \Theta^{-1}(1), \Theta^{-1}(0) \leq \gamma_{\mathrm{RD}} < \Theta^{-1}(1-\Theta(\gamma_{\mathrm{SD}}))] \\
=& \int_{\gamma_{\mathrm{SR}}=\Theta^{-1}(1)}^{\Theta^{-1}(\infty)} \int_{\gamma_{\mathrm{SD}}=\Theta^{-1}(0)}^{\Theta^{-1}(1)} \int_{\gamma_{\mathrm{RD}}=\Theta^{-1}(0)}^{\Theta^{-1}(1-\Theta(\gamma_{\mathrm{SD}}))} p(\gamma_{\mathrm{SR}}) p(\gamma_{\mathrm{SD}}) p(\gamma_{\mathrm{RD}}) d\gamma_{\mathrm{SR}} d\gamma_{\mathrm{SD}} d\gamma_{\mathrm{RD}} \\
=& \frac{1}{\overline{\gamma}_{\mathrm{SD}}} \left(1 - \left[\frac{\gamma\left(m_{\mathrm{SR}}, m_{\mathrm{SR}} \frac{1}{\overline{\gamma}_{\mathrm{SR}}}\right)}{\Gamma(m_{\mathrm{SR}})}\right]\right) \int_{\gamma_{\mathrm{SD}}=\Theta^{-1}(0)}^{\Theta^{-1}(1)} \exp\left(-\frac{\gamma_{\mathrm{SD}}}{\overline{\gamma}_{\mathrm{SD}}}\right) \\
&\cdot \left[\frac{\gamma\left(m_{\mathrm{RD}}, m_{\mathrm{RD}} \frac{\Theta^{-1}(1-\Theta(\gamma_{\mathrm{SD}}))}{\overline{\gamma}_{\mathrm{RD}}}\right)}{\Gamma(m_{\mathrm{RD}})}\right] d\gamma_{\mathrm{SD}},
\end{aligned} \tag{20}$$

$$\begin{aligned}
P_{\mathrm{B}} =& \Pr\left[\Theta^{-1}(0) \leq \gamma_{\mathrm{SR}} \leq \Theta^{-1}(1), \Theta^{-1}(0) \leq \gamma_{\mathrm{SD}} \leq \Theta^{-1}(1-\Theta(\gamma_{\mathrm{SR}})), \gamma_{\mathrm{RD}} \geq \Theta^{-1}(0)\right] \\
=& \int_{\gamma_{\mathrm{SR}}=\Theta^{-1}(0)}^{\Theta^{-1}(1)} \int_{\gamma_{\mathrm{SD}}=\Theta^{-1}(0)}^{\Theta^{-1}(1-\Theta(\gamma_{\mathrm{SR}}))} \int_{\gamma_{\mathrm{RD}}=\Theta^{-1}(0)}^{\Theta^{-1}(\infty)} p(\gamma_{\mathrm{SR}}) p(\gamma_{\mathrm{SD}}) p(\gamma_{\mathrm{RD}}) d\gamma_{\mathrm{SR}} d\gamma_{\mathrm{SD}} d\gamma_{\mathrm{RD}} \\
=& \int_{\gamma_{\mathrm{SR}}=\Theta^{-1}(0)}^{\Theta^{-1}(1)} \frac{m_{\mathrm{SR}}^{m_{\mathrm{SR}}} (\gamma_{\mathrm{SR}})^{m_{\mathrm{SR}}-1}}{(\overline{\gamma}_{\mathrm{SR}})^{m_{\mathrm{SR}}} \Gamma(m_{\mathrm{SR}})} \exp\left(-\frac{m_{\mathrm{SR}}\gamma_{\mathrm{SR}}}{\overline{\gamma}_{\mathrm{SR}}}\right) \left[1 - \exp\left(-\frac{\Theta^{-1}(1-\Theta(\gamma_{\mathrm{SR}}))}{\overline{\gamma}_{\mathrm{SD}}}\right)\right] d\gamma_{\mathrm{SR}}
\end{aligned} \tag{21}$$

and

$$\begin{aligned}
P_{\mathrm{C}} =& \Pr\{\Theta^{-1}(0) \leq \gamma_{\mathrm{SR}} \leq \Theta^{-1}(1), \Theta^{-1}[1-\Theta(\gamma_{\mathrm{SR}})] \\
& \leq \gamma_{\mathrm{SD}} \leq \Theta^{-1}(1), \Theta^{-1}(0) \leq \gamma_{\mathrm{RD}} \leq \Theta^{-1}[\xi(\gamma_{\mathrm{SD}}, \gamma_{\mathrm{SR}})]\} \\
=& \int_{\gamma_{\mathrm{SR}}=\Theta^{-1}(0)}^{\Theta^{-1}(1)} \int_{\gamma_{\mathrm{SD}}=\Theta^{-1}(1-\Theta(\gamma_{\mathrm{SR}}))}^{\Theta^{-1}(1)} \int_{\gamma_{\mathrm{RD}}=\Theta^{-1}(0)}^{\Theta^{-1}[\xi(\gamma_{\mathrm{SD}}, \gamma_{\mathrm{SR}})]} p(\gamma_{\mathrm{SR}}) p(\gamma_{\mathrm{SD}}) p(\gamma_{\mathrm{RD}}) d\gamma_{\mathrm{SR}} d\gamma_{\mathrm{SD}} d\gamma_{\mathrm{RD}} \\
=& \frac{1}{\overline{\gamma}_{\mathrm{SD}}} \int_{\gamma_{\mathrm{SR}}=\Theta^{-1}(0)}^{\Theta^{-1}(1)} \int_{\gamma_{\mathrm{SD}}=\Theta^{-1}(1-\Theta(\gamma_{\mathrm{SR}}))}^{\Theta^{-1}(1)} \exp\left(\frac{-\gamma_{\mathrm{SD}}}{\overline{\gamma}_{\mathrm{SD}}}\right) \frac{m_{\mathrm{SR}}^{m_{\mathrm{SR}}} (\gamma_{\mathrm{SR}})^{m_{\mathrm{SR}}-1}}{(\overline{\gamma}_{\mathrm{SR}})^{m_{\mathrm{SR}}} \Gamma(m_{\mathrm{SR}})} \exp\left(-\frac{m_{\mathrm{SR}}\gamma_{\mathrm{SR}}}{\overline{\gamma}_{\mathrm{SR}}}\right) \\
&\cdot \left[\frac{\gamma\left(m_{\mathrm{RD}}, m_{\mathrm{RD}} \frac{\xi(\gamma_{\mathrm{SD}}, \gamma_{\mathrm{SR}})}{\overline{\gamma}_{\mathrm{RD}}}\right)}{\Gamma(m_{\mathrm{RD}})}\right] d\gamma_{\mathrm{SD}} d\gamma_{\mathrm{SR}},
\end{aligned} \tag{22}$$

where $\xi(\gamma_{\mathrm{SD}}, \gamma_{\mathrm{SR}}) = H\{H^{-1}[1-\Theta(\gamma_{\mathrm{SD}})] * H^{-1}[1-\Theta(\gamma_{\mathrm{SR}})]\}$ and $\gamma(\cdot,\cdot)$ is the lower incomplete gamma function. Since we assume i.i.d. binary sequences, $H(b_{\mathrm{S}}) = H(b_{\mathrm{R}}) = 1$.

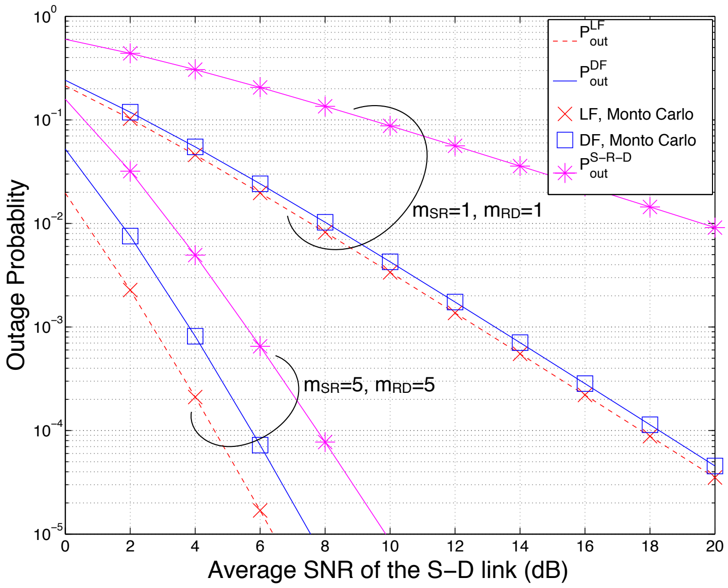

Fig. 7. Outage probability comparison among the LF, DF, and S-R-D transmission with $m_{\mathrm{SD}} = 1$.

Fig. 7 presents the outage probabilities of DF and LF relaying, denoted as $P_{\mathrm{out}}^{\mathrm{DF}}$ and $P_{\mathrm{out}}^{\mathrm{LF}}$. It is found that LF achieves lower outage probability than DF. This is because LF always forwards information sequences from the relay to the destination. The system can be regarded as a distributed turbo code. Note that the theoretical outage probabilities well match their corresponding simulation results obtained by Monte Carlo method. As a reference, the outage probability of a S-R-D transmission without direct S-D link, denoted as $P_{\mathrm{out}}^{\text{S-R-D}}$, is also plotted in the figure. With $m_{\mathrm{SD}} = m_{\mathrm{SR}} = m_{\mathrm{RD}} = 1$, i.e., all the links suffer from Rayleigh fading, $P_{\mathrm{out}}^{\text{S-R-D}}$ only achieves first-order diversity since only one copy of the original information arrive at the destination and hence no diversity gain achieved. With $m_{\mathrm{SR}} = m_{\mathrm{RD}} = 5$, i.e., the S-R and R-D links experience milder fading than the S-D link, $P_{\mathrm{out}}^{\text{S-R-D}}$ can achieve almost the same decay in the outage curve as $P_{\mathrm{out}}^{\mathrm{DF}}$ and $P_{\mathrm{out}}^{\mathrm{LF}}$. This is because with large m_{SR} and m_{RD}, the S-R and R-D links with mild fading dominate the system performance. However, the outage probabilities of relaying with the direct S-D link, i.e., $P_{\mathrm{out}}^{\mathrm{DF}}$ and $P_{\mathrm{out}}^{\mathrm{LF}}$, are always lower than that without the direct S-D link, i.e., $P_{\mathrm{out}}^{\text{S-R-D}}$, due to the spatial diversity gain provided by the S-D link.

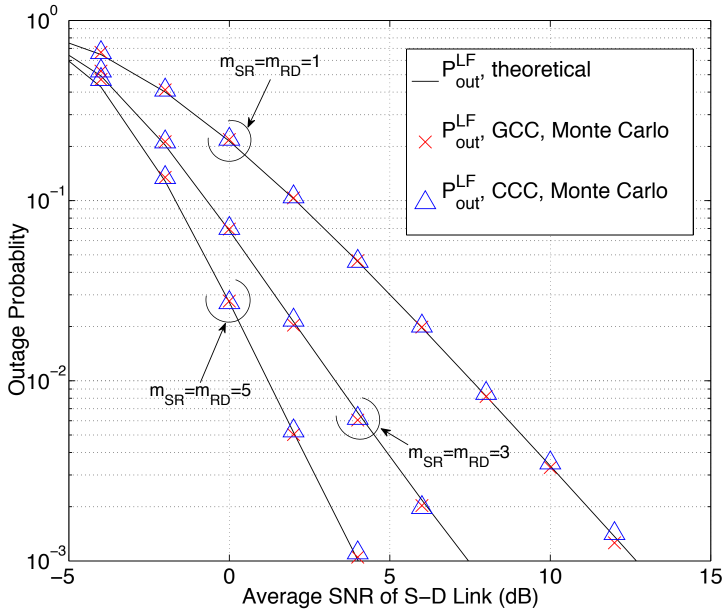

Fig. 8. Comparison of the Gaussian codebook capacity and constellation constrained capacity based outage probability of LF relaying, where $m_{\mathrm{SR}} = m_{\mathrm{RD}}$, $m_{\mathrm{SD}} = 1$, and $G_{\mathrm{SD}} = G_{\mathrm{RD}} = G_{\mathrm{SR}}$.

(B) Outage Derivation with Constellation Constrained Capacity

According to Shannon's source channel separation theorem, if $H(b_i) \cdot R^c_{i\mathrm{D}} \leq R_i \cdot R^c_{i\mathrm{D}} \leq C_{cc}(\gamma_{i\mathrm{D}}), (i \in \mathrm{S}, \mathrm{R})$ is satisfied, the error probability can be made arbitrarily small at the destination, where $C_{cc}(\gamma_{i\mathrm{D}})$ is the channel constellation constrained capacity with the instantaneous SNR $\gamma_{i\mathrm{D}}$ of the i-D link. Since the constellation constrained capacity has no closed-form expression, numerical evaluation yields a relationship between $\gamma_{i\mathrm{D}}$ and R_i as $\gamma_{i\mathrm{D}} \geq C^{-1}_{cc}(R_i \cdot R^c_{i\mathrm{D}})$, where C^{-1}_{cc} represents the inverse function of channel constellation constrained capacity.

Similarly, the relationship between γ_{SR} and p_f is given by $R(\mathscr{D}) \cdot R^c_{\mathrm{SR}} \leq C_{cc}(\gamma_{\mathrm{SR}})$ and $\gamma_{\mathrm{SR}} \geq C^{-1}_{cc}(R(\mathscr{D}) \cdot R^c_{\mathrm{SR}})$, where the distortion $\mathscr{D}$ is equivalent to p_f for a given instantaneous S-R link SNR γ_{SR}. Then, by using the method for calculating the outage probability with Gaussian codebook capacity, the outage probability of LF relaying with constellation constrained capacity can be calculated.

Fig. 8 compares the outage probabilities of LF relaying derived from Gaussian codebook capacity and constellation constrained capacity, denoted as $P^{\mathrm{LF}}_{\mathrm{out}}$, GCC and

$P_{\text{out}}^{\text{LF}}$, CCC, respectively.[4] The Monte Carlo simulation results of the outage probabilities with Gaussian codebook capacity are also presented. We can observe from Fig. 8 that the theoretical outage probabilities with LF relaying, calculated by using numerical integral in (20), (21), and (22), well match their corresponding Monte Carlo simulation results. It is also found that, the difference between $P_{\text{out}}^{\text{LF}}$, GCC and $P_{\text{out}}^{\text{LF}}$, CCC is negligible. This is because in low SNR regime the difference between Gaussian codebook capacity and constellation constrained capacity is very small. On the contrary, in high SNR region, even though the difference between Gaussian codebook capacity and constellation constrained capacity becomes large, p_f approaches zero very quickly, resulting in lossless transmission over the S-R link. Therefore, the difference between Gaussian codebook capacity and constellation constrained capacity based outage probabilities is negligibly small.

2.1.3 Equivalent Diversity Order and Coding Gain

The equivalent diversity order (decay of the outage curve) and coding gain can be obtained by approximating (20), (21), and (22) at high SNR region. Invoking the series representation of incomplete gamma function $\gamma(a,x) = \sum_{n=0}^{\infty} \frac{(-1)^n x^{a+n}}{n!(a+n)}$ [76, equation 8.354.1], together with the approximation $p(\gamma_{ij}) \approx \frac{m_{ij}^{m_{ij}} (\gamma_{ij})^{m_{ij}-1}}{(\overline{\gamma}_{ij})^{m_{ij}} \Gamma(m_{ij})}$ [50], after several steps of mathematical manipulations, the outage probability expression with LF relaying over Nakagami-m fading channels can be approximated as

$$P_{\text{A}} \approx A \cdot A' \cdot \overline{\gamma}_{\text{SD}}^{(-m_{\text{SD}})} \overline{\gamma}_{\text{RD}}^{(-m_{\text{RD}})}, \tag{23}$$

$$P_{\text{B}} \approx B \cdot \overline{\gamma}_{\text{SD}}^{(-m_{\text{SD}})} \overline{\gamma}_{\text{SR}}^{(-m_{\text{SR}})}, \tag{24}$$

$$P_{\text{C}} \approx C \cdot \overline{\gamma}_{\text{SD}}^{(-m_{\text{SD}})} \overline{\gamma}_{\text{RD}}^{(-m_{\text{RD}})} \overline{\gamma}_{\text{SR}}^{(-m_{\text{SR}})}, \tag{25}$$

[4] In the numerical calculation, $E^n = 2$. By assuming a half rate channel code and QPSK modulation for each channel, $R_{ij}^c = 1$ $(i \in (\text{S},\text{R}), j \in (\text{R},\text{D}), i \neq j)$.

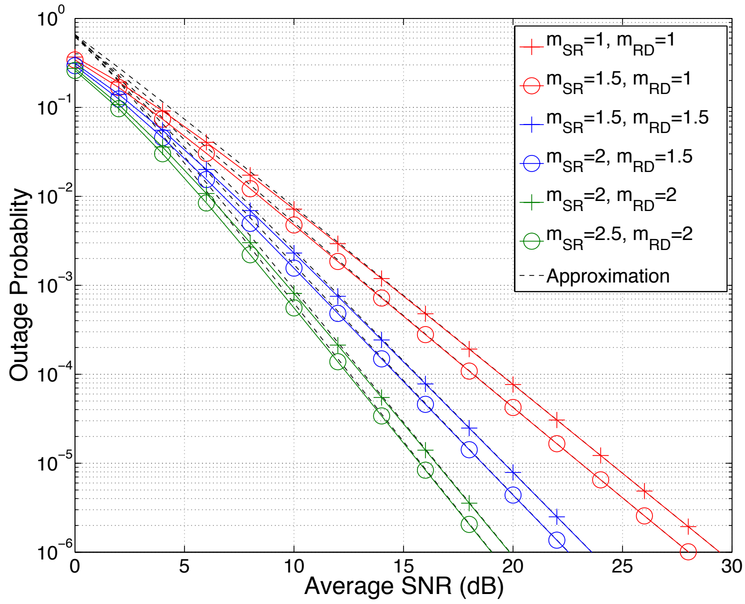

Fig. 9. Comparison of outage curves obtained by using the numerical calculation via (20), (21), and (22) and approximation via (23), (24), and (25), where $m_{\mathrm{SD}} = 1$ and $G_{\mathrm{SD}} = G_{\mathrm{RD}} = G_{\mathrm{SR}}$.

where

$$A = \frac{m_{\mathrm{SD}}^{m_{\mathrm{SD}}} m_{\mathrm{RD}}^{m_{\mathrm{RD}}-1}}{\Gamma(m_{\mathrm{SD}})\Gamma(m_{\mathrm{RD}})} \int_{\gamma_{\mathrm{SD}}=\Theta^{-1}(0)}^{\Theta^{-1}(1)} \frac{\left(\frac{2}{1+\gamma_{\mathrm{SD}}} - 1\right)^{m_{\mathrm{RD}}}}{\gamma_{\mathrm{SD}}^{1-m_{\mathrm{SD}}}} d\gamma_{\mathrm{SD}}, \tag{26}$$

$$B = \frac{m_{\mathrm{SR}}^{m_{\mathrm{SR}}} m_{\mathrm{SD}}^{m_{\mathrm{SD}}-1}}{\Gamma(m_{\mathrm{SD}})\Gamma(m_{\mathrm{SR}})} \int_{\gamma_{\mathrm{SR}}=\Theta^{-1}(0)}^{\Theta^{-1}(1)} \frac{\left(\frac{2}{1+\gamma_{\mathrm{SR}}} - 1\right)^{m_{\mathrm{SD}}}}{\gamma_{\mathrm{SR}}^{m_{\mathrm{SR}}-1}} d\gamma_{\mathrm{SR}}, \tag{27}$$

$$C = \int_{\gamma_{\mathrm{SR}}=\Theta^{-1}(0)}^{\Theta^{-1}(1)} \int_{\gamma_{\mathrm{SD}}=\Theta^{-1}(1-\Theta(\gamma_{\mathrm{SR}}))}^{\Theta^{-1}(1)} \gamma_{\mathrm{SD}}^{m_{\mathrm{SD}}-1} \gamma_{\mathrm{SR}}^{m_{\mathrm{SR}}-1} \frac{m_{\mathrm{SR}}^{m_{\mathrm{SR}}} m_{\mathrm{SD}}^{m_{\mathrm{SD}}} m_{\mathrm{RD}}^{m_{\mathrm{RD}}-1}}{\Gamma(m_{\mathrm{SD}})\Gamma(m_{\mathrm{RD}})\Gamma(m_{\mathrm{SR}})} \xi^{m_{\mathrm{SD}}}(\gamma_{\mathrm{SD}}, \gamma_{\mathrm{SR}}) d\gamma_{\mathrm{SR}} d\gamma_{\mathrm{SD}}. \tag{28}$$

$A' = 1 - \frac{\gamma\left(m_{\mathrm{SR}}, m_{\mathrm{SR}} \frac{1}{\bar{\gamma}_{\mathrm{SR}}}\right)}{\Gamma(m_{\mathrm{SR}})}$ indicates the probability of $p_f = 0$ (i.e., no decoding error at R).

Fig. 9 shows that at high SNR region the approximated outage curves obtained from (23), (24), and (25) well match the numerically calculated curves obtained from (20), (21), and (22). From this observation, it can be concluded that the approximation is sufficiently accurate to calculate the outage probability.

Since the exponent parts in (23), (24), and (25) stay unchanged even if we replace $\overline{\gamma}_{\mathrm{SD}}$, $\overline{\gamma}_{\mathrm{RD}}$, and $\overline{\gamma}_{\mathrm{SR}}$ by a certain representative value $\overline{\gamma}$, we have

$$P_{\mathrm{A}} \approx A \cdot A' \cdot \overline{\gamma}^{(-m_{\mathrm{SD}}-m_{\mathrm{RD}})}, \tag{29}$$

$$P_{\mathrm{B}} \approx B \cdot \overline{\gamma}^{(-m_{\mathrm{SD}}-m_{\mathrm{SR}})}, \tag{30}$$

$$P_{\mathrm{C}} \approx C \cdot \overline{\gamma}^{(-m_{\mathrm{SD}}-m_{\mathrm{RD}}-m_{\mathrm{SR}})}. \tag{31}$$

It is observed from (29), (30), and (31) that, $\overline{\gamma}^{(-m_{\mathrm{SD}}-m_{\mathrm{RD}}-m_{\mathrm{SR}})}$ is upper bounded by $\overline{\gamma}^{(-m_{\mathrm{SD}}-m_{\mathrm{RD}})}$ or $\overline{\gamma}^{(-m_{\mathrm{SD}}-m_{\mathrm{SR}})}$ when $\overline{\gamma}$ increases. Moreover, it is not difficult to find that A' equals one asymptotically at high SNR regime. Therefore, the overall outage probability of LF relaying in Nakagami-m fading can be formulated as

$$P_{\mathrm{out}}^{\mathrm{LF}} = (G_c \cdot \overline{\gamma})^{(-G_d)}, \tag{32}$$

where

$$G_d = m_{\mathrm{SD}} + \min(m_{\mathrm{SR}}, m_{\mathrm{RD}}) \tag{33}$$

and

$$G_c = \begin{cases} \frac{1}{\sqrt[(G_d)]{B}}, & m_{\mathrm{SR}} < m_{\mathrm{RD}} \\ \frac{1}{\sqrt[(G_d)]{A+B}}, & m_{\mathrm{SR}} = m_{\mathrm{RD}} \\ \frac{1}{\sqrt[(G_d)]{A}}, & m_{\mathrm{SR}} > m_{\mathrm{RD}} \end{cases} \tag{34}$$

are the equivalent diversity order[5] and coding gain [50] achieved by LF relaying, respectively. We can see from (33) that, the equivalent diversity order of the LF relaying system is restricted by the less reliable channel of either the S-R or the R-D link.

Since $\overline{\gamma}^{(-m_{\mathrm{SD}}-m_{\mathrm{RD}}-m_{\mathrm{SR}})}$ decreases faster than that of $\overline{\gamma}^{(-m_{\mathrm{SD}}-m_{\mathrm{RD}})}$ and $\overline{\gamma}^{(-m_{\mathrm{SD}}-m_{\mathrm{SR}})}$, as $\overline{\gamma}$ increases, i.e., $\overline{\gamma}^{(-m_{\mathrm{SD}}-m_{\mathrm{RD}}-m_{\mathrm{SR}})}$ approaches zero faster than $\overline{\gamma}^{(-m_{\mathrm{SD}}-m_{\mathrm{RD}})}$ and $\overline{\gamma}^{(-m_{\mathrm{SD}}-m_{\mathrm{SR}})}$ alone, the outage probability is asymptotically equal to

$$P_{\mathrm{out}}^{\mathrm{LF}} \approx \left(\frac{1}{\sqrt[(-m_{\mathrm{SD}}-m_{\mathrm{RD}})]{A}} \cdot \overline{\gamma} \right)^{(-m_{\mathrm{SD}}-m_{\mathrm{RD}})} + \left(\frac{1}{\sqrt[(-m_{\mathrm{SD}}-m_{\mathrm{SR}})]{B}} \cdot \overline{\gamma} \right)^{(-m_{\mathrm{SD}}-m_{\mathrm{SR}})}. \tag{35}$$

If $m_{\mathrm{SR}} < m_{\mathrm{RD}}$, the first term in (35) decreases faster than the second term. Therefore,

$$P_{\mathrm{out}}^{\mathrm{LF}} \approx \left(\frac{1}{\sqrt[(-m_{\mathrm{SD}}-m_{\mathrm{SR}})]{B}} \cdot \overline{\gamma} \right)^{(-m_{\mathrm{SD}}-m_{\mathrm{SR}})} \tag{36}$$

[5] G_d indicates the decay of the outage probability curve versus average SNR $G_{ij}\frac{E_s}{N_0}$ because G_d appears in the exponent part in (32). Therefore, the decay of the outage curve is concerned and it has the equivalent meaning as the diversity order. However, according to the definition, G_d can take arbitrary real number which is related to the shape factor m_{ij}. In this sense, we call the decay of the curve equivalent diversity order, which does not follow the standard definition of the diversity order.

with $G_c = \frac{1}{\sqrt[(-m_{\mathrm{SD}}-m_{\mathrm{SR}})]{B}}$ and $G_d = m_{\mathrm{SD}} + m_{\mathrm{SR}}$. If $m_{\mathrm{SR}} > m_{\mathrm{RD}}$, the second term in (35) decreases faster than the first term. Therefore,

$$P_{\mathrm{out}}^{\mathrm{LF}} \approx \left(\frac{1}{\sqrt[(-m_{\mathrm{SD}}-m_{\mathrm{RD}})]{A}} \cdot \overline{\gamma} \right)^{(-m_{\mathrm{SD}}-m_{\mathrm{RD}})} \tag{37}$$

with $G_c = \frac{1}{\sqrt[(-m_{\mathrm{SD}}-m_{\mathrm{RD}})]{A}}$ and $G_d = m_{\mathrm{SD}} + m_{\mathrm{RD}}$. If $m_{\mathrm{SR}} = m_{\mathrm{RD}} = m_0$, the first term in (35) decreases at the same order as the first term. Therefore,

$$P_{\mathrm{out}}^{\mathrm{LF}} \approx \left(\frac{1}{\sqrt[(-m_{\mathrm{SD}}-m_0)]{A+B}} \cdot \overline{\gamma} \right)^{(-m_{\mathrm{SD}}-m_0)} \tag{38}$$

with $G_c = \frac{1}{\sqrt[(-m_{\mathrm{SD}}-m_0)]{A+B}}$ and $G_d = m_{\mathrm{SD}} + m_0$.

The outage curves shown in Fig. 9 illustrate that the decay in outage curve cannot be obtained by only increasing the m value of either the S-R or R-D link. The outage curves become sharper only when m values of both the S-R and the R-D links increase simultaneously, which is consistent to the conclusion drawn in (33) regarding equivalent diversity order.

2.1.4 Optimal Relay Location

Let d_{SD}, d_{RD}, and d_{SR} denotes the distances between S and D, R and D, and S and R, respectively. With G_{SD} being normalized to the unity, G_{SR} and G_{RD} can be defined as $G_{\mathrm{SR}} = \left(\frac{d_{\mathrm{SD}}}{d_{\mathrm{SR}}}\right)^{\alpha}$ and $G_{\mathrm{RD}} = \left(\frac{d_{\mathrm{SD}}}{d_{\mathrm{RD}}}\right)^{\alpha}$, respectively, where α is the path loss exponent. Then, the average SNRs of the S-R and R-D links can be given as

$$\overline{\gamma}_{\mathrm{SR}} = \overline{\gamma}_{\mathrm{SD}} + 10\lg(G_{\mathrm{SR}})(\mathrm{dB}), \tag{39}$$

$$\overline{\gamma}_{\mathrm{RD}} = \overline{\gamma}_{\mathrm{SD}} + 10\lg(G_{\mathrm{RD}})(\mathrm{dB}). \tag{40}$$

By substituting (39) and (40) into (20), (21), and (22), we can obtain the outage probability expressions with respect to the position of R.

Fig. 10 shows the impact of the relay location on the outage probability, with $\overline{\gamma}_{\mathrm{SR}} = 1$ dB. R is located on the line parallel to the line connecting S and D between $x = 0$ and $x = 1$, as shown in Fig. 2. The distance between the relay and the line connecting S and D is set at $\frac{1}{10}$ of the length of the S-D link[6]. The outage probability of DF relaying is

[6]With longer (or shorter) distant between the relay and the line connecting S and D, outage probabilities increase (or decrease). However the outage probabilities show the same tendencies as those in Fig. 10, Fig. 11, and Fig. 12

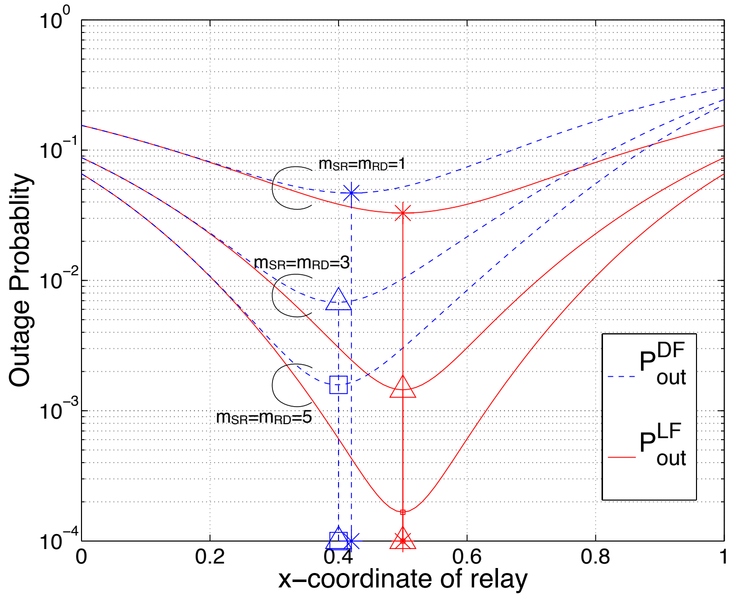

Fig. 10. The optimal relay positions of LF and DF relaying where $m_{\mathrm{SD}} = 1$ and $\alpha = 3.52$. The vertical lines indicate the points where the outage probabilities are minimized.

also depicted as a reference. Joint decoding is considered for both LF and DF at the destination. With DF, the lowest outage probability can be achieved when the relay is located close to the source (left hand side), since the relay has to be located close to the source to guarantee the correct recovery of the information transmitted from the source. It is found that when the relay is close to the source, LF and DF show the same performance. This is because with reliable S-R transmission, the probability that error is detected after decoding at the relay becomes small. In this case, the relay in DF keeps active, which results in DF and LF relaying exhibiting the same outage performance. On the contrary, when the relay moves close to the destination, the probability that error is detected after decoding at the relay increases with the degraded S-R link quality. In the case, the relay in DF keeps silence which results in LF outperforming DF by always forward the decoder output to the destination regardless of whether error is detected after decoding in the information part or not. With LF, the lowest outage probability can be achieved when the relay is located at the midpoint as long as $m_{\mathrm{SR}} = m_{\mathrm{RD}}$. It is observed that the outage curves are symmetric with respect to the midpoint of the line connecting S and D with LF relaying. This is because with LF relaying, the errors due to the S-R link can be corrected at the destination, and therefore, the midpoint ($d_{\mathrm{SR}} = d_{\mathrm{RD}}$)

is the optimal point where the contributions of the S-R and R-D links are balanced. Moreover, while keeping the same or even lower outage probability, LF relaying has a larger range of search area for a relay (helper) than DF relaying.

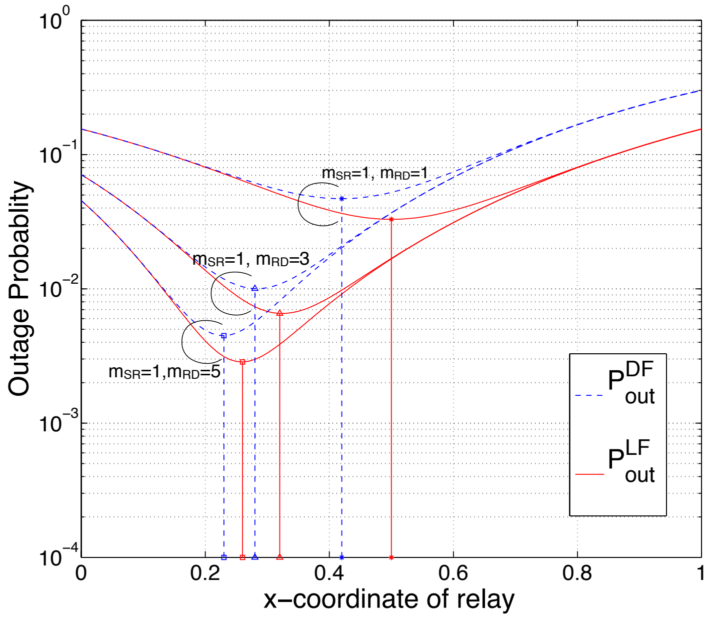

Fig. 11. The optimal relay positions of LF and DF relaying where $m_{SD} = m_{SR} = 1$ and $\alpha = 3.52$. The vertical lines indicate the points where the outage probabilities are minimized.

Figs. 11 and 12 also show the impact of the relay location on the outage probability when either the value of m_{SR} or m_{RD} changes. It can be found that as the m value of either the S-R link or the R-D link becomes large, the optimal relay location shifts close to the destination or the source, respectively. It is also found in Figs. 10, 11 and 12 that when the relay moves close to the source (left hand side), the outage performances of LF and DF with the same m_{SR} and m_{RD} values gradually become identical. This observation indicates that as the length of the S-R link reduces, it becomes less likely the errors happen in the S-R transmission, which results in DF performing the same as LF. Moreover, Fig. 11 shows that, when the relay is located close to the destination (right hand side), the outage probabilities of LF relaying with different m_{RD} values become identical. The same tendency can be found from the outage curves of DF relaying. This indicates that the S-R link with low transmission quality dominates the system outage probability. Note that in Fig. 12 the outage probabilities of LF and DF asymptotically become identical as the relay moves toward to the source regardless of m_{SR} or m_{RD} values. This is because when the distance between the relay and the destination increase, the R-D link quality is degraded. Hence, the R-D link dominates the system outage probability. Note that while keeping the same or ever lower outage probability, the area for searching a relay (helper) can be increased by LF relaying compared to conventional DF relaying. For example, in Fig. 10, for achieving the outage probability not larger than 10^{-2}, the area for the position of the relay indicated by the x-coordinate with LF is larger than that with DF when $m_{SR} = m_{RD} = 3$.

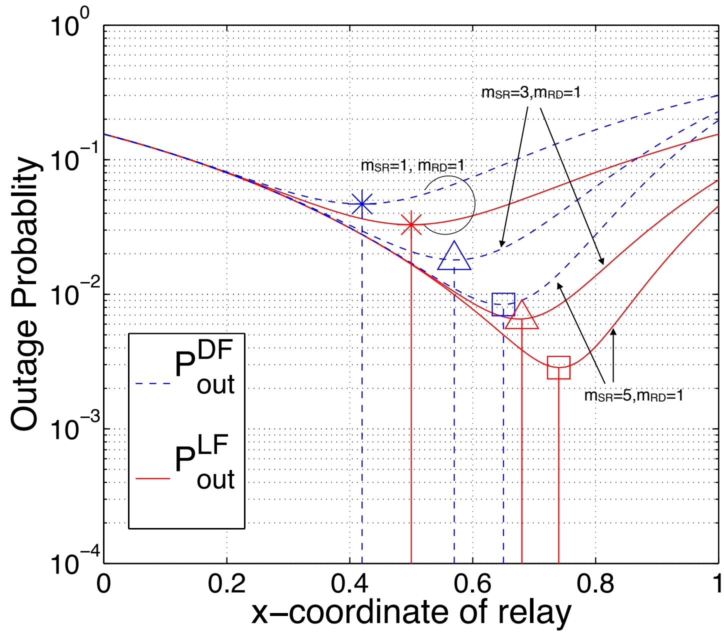

Fig. 12. The optimal relay positions of LF and DF relaying where $m_{SD} = m_{RD} = 1$ and $\alpha = 3.52$. The vertical lines indicate the points where the outage probabilities are minimized.

2.2 Fading Correlations for Wireless Cooperative Communications: Diversity Order and Coding Gain

2.2.1 System and Channels Models

The wireless relay network model used in this section is shown in Fig. 13. A source S communicates with a destination D with the help of a relay R. Each terminal is equipped with a single antenna. Transmission phases are orthogonal and no multiple access channel is involved. The cooperation protocols considered in this section are LF, DF, and ADF relaying.

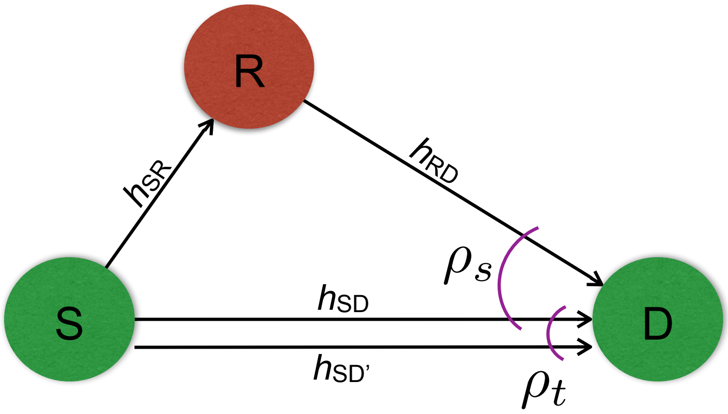

Fig. 13. The schematic scenario of one relay aided communication system.

2.2.2 Relaying

In LF relaying, S broadcasts the coded information sequence to D and R in the first time slot. The information sequence, obtained as the result of decoding at R, is re-interleaved, re-encoded and transmitted to D in the second time slot, even if the decoder detects error.

In conventional DF relaying, S broadcasts the coded information sequence to D and R in the first time slot. R tries to fully recover the received information sequence. If it is successfully recovered, the information sequence is forwarded to D in the second time slot. R keeps silent if error is detected after decoding.

In ADF relaying, S broadcasts the coded information sequence to D and R in the first time slot. If the transmitted information is successfully recovered at R, the recovered information sequence is re-interleaved, re-encoded and transmitted to D in the second time slot. If R detects error in the information part after decoding, R notifies S of the information recovery failure via a feedback link, and S interleaves the information sequence, re-encodes, and retransmits the information sequence to D again.

Correlated Channel Model

The S-D and R-D links are considered to be spatially correlated with the correlation coefficient ρ_s $(0 \leq \rho_s \leq 1)$ representing the spatial correlation between h_{SD} and h_{RD} at the first transmission time slot and the second, respectively. h_{ij} $(i \in \{\mathrm{S,R}\}, j \in \{\mathrm{R,D}\}, i \neq j)$ denotes the complex channel gain of i-j link. The channel gains of the two transmissions over the S-D link are also correlated in time with the correlation coefficient ρ_t $(0 \leq \rho_t \leq 1)$ representing the temporal correlation between h_{SD} and $h_{\mathrm{S'D}}$, where $h_{\mathrm{S'D}}$ denotes the complex channel gain of the S-D link in the second time slot. $\rho_s = 0$ or $\rho_t = 0$ indicate independent fading, and $\rho_s = 1$ or $\rho_t = 1$ for fully correlated case.

In this section, each link is assumed to suffer from frequency non-selective Rayleigh fading. The pdf of instantaneous SNR γ_{ij} is given by

$$p(\gamma_{ij}) = \frac{1}{\bar{\gamma}_{ij}} \exp(-\frac{\gamma_{ij}}{\bar{\gamma}_{ij}}), (i \in \{\mathrm{S,R}\}, j \in \{\mathrm{R,D}\}, i \neq j), \tag{41}$$

2.2.3 Outage Analysis in Independent Fading

Outage Behavior of LF in Independent Fading

Following the same technicals as those used for the outage derivation of LF relaying over Nakagami-m fading channel in the previous section, the outage probability of LF relaying over independent Rayleigh channels can be expressed as

$$
\begin{aligned}
P_{\text{out}}^{\text{LF, Ind}} =& \frac{1}{\overline{\gamma}_{\text{SD}}} \exp\left(-\frac{1}{\overline{\gamma}_{\text{SR}}}\right) \int_{\gamma_{\text{SD}}=\Theta^{-1}(0)}^{\Theta^{-1}(1)} \exp\left(-\frac{\gamma_{\text{SD}}}{\overline{\gamma}_{\text{SD}}}\right) \\
& \left(1-\exp\left(-\frac{\Theta^{-1}(1-\Theta(\gamma_{\text{SD}}))}{\overline{\gamma}_{\text{RD}}}\right)\right) d\gamma_{\text{SD}} \\
& + \frac{1}{\overline{\gamma}_{\text{SR}}} \int_{\gamma_{\text{SR}}=\Theta^{-1}(0)}^{\Theta^{-1}(1)} \left[1-\exp\left(-\frac{\Theta^{-1}(1-\Theta(\gamma_{\text{SR}}))}{\overline{\gamma}_{\text{SD}}}\right)\right] \\
& \cdot \exp\left(-\frac{\gamma_{\text{SR}}}{\overline{\gamma}_{\text{SR}}}\right) d\gamma_{\text{SR}} + \frac{1}{\overline{\gamma}_{\text{SD}}\overline{\gamma}_{\text{SR}}} \int_{\gamma_{\text{SR}}=\Theta^{-1}(0)}^{\Theta^{-1}(1)} \\
& \int_{\gamma_{\text{SD}}=\Theta^{-1}(1-\Theta(\gamma_{\text{SR}}))}^{\Theta^{-1}(1)} \exp\left(-\frac{\gamma_{\text{SD}}}{\overline{\gamma}_{\text{SD}}}\right) \exp\left(-\frac{\gamma_{\text{SR}}}{\overline{\gamma}_{\text{SR}}}\right) \\
& \cdot \left(1-\exp\left(-\frac{\xi(\gamma_{\text{SD}},\gamma_{\text{SR}})}{\overline{\gamma}_{\text{RD}}}\right)\right) d\gamma_{\text{SD}} d\gamma_{\text{SR}}. \qquad (42)
\end{aligned}
$$

Outage Behavior of DF in Independent Fading

In DF relaying, relay keeps silent if error is detected after decoding. When $p_f = 0$, the outage probability of DF is the same as that of LF. When $p_f \neq 0$, the outage probability is equivalent to that of point-to-point S-D transmission. Therefore, the outage probability of DF relaying can be expressed as

$$
\begin{aligned}
P_{\text{out}}^{\text{DF, Ind}} =& \Pr[p_f = 0, 0 \le R_{\text{S}} \le 1, 0 \le R_{\text{R}} \le H(p_f')] + \Pr[0 < p_f \le 0.5, 0 \le R_{\text{S}} \le 1] \\
=& \frac{1}{\overline{\gamma}_{\text{SD}}} \exp\left(-\frac{1}{\overline{\gamma}_{\text{SR}}}\right) \int_{\gamma_{\text{SD}}=\Theta^{-1}(0)}^{\Theta^{-1}(1)} \exp\left(-\frac{\gamma_{\text{SD}}}{\overline{\gamma}_{\text{SD}}}\right) \\
& \left(1-\exp\left(-\frac{\Theta^{-1}(1-\Theta(\gamma_{\text{SD}}))}{\overline{\gamma}_{\text{RD}}}\right)\right) d\gamma_{\text{SD}} \\
& + \left(1-\exp\left(-\frac{\Theta^{-1}(1)}{\overline{\gamma}_{\text{SR}}}\right)\right) \left(1-\exp\left(-\frac{\Theta^{-1}(1)}{\overline{\gamma}_{\text{SD}}}\right)\right). \qquad (43)
\end{aligned}
$$

Outage Behavior of ADF in Independent Fading

With ADF, S retransmits an interleaved and re-encoded version of the information, if it is notified of the decoding failure via a feedback link from R. The outage probability of ADF is the same as that of DF and LF, When $p_f = 0$. When $p_f \neq 0$, the rate region of ADF is shown in Fig. 14. Similarly, the outage probability of ADF when $p_f \neq 0$ is defined as the probability that the source rate pair $(R_{\text{S}}, R_{\text{S}'})$, fall into the inadmissible

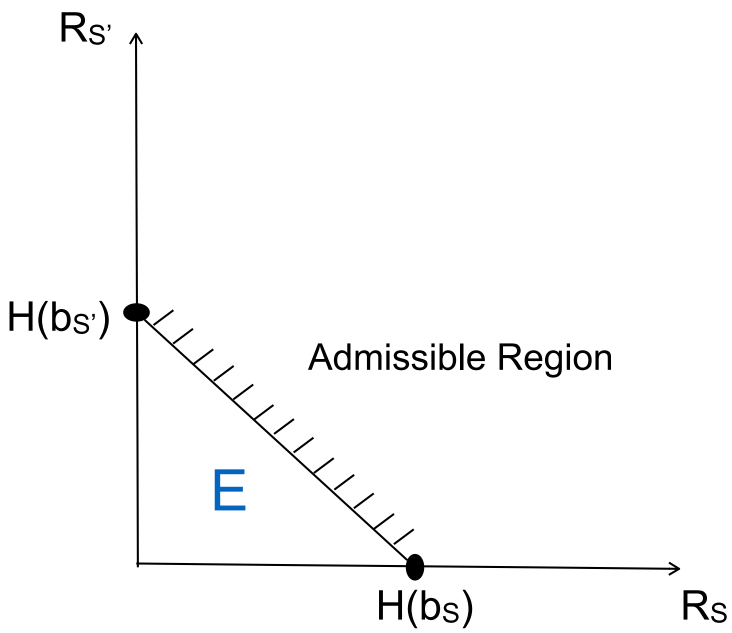

Fig. 14. Rate region for the two transmissions over the S-D link of ADF relaying, when $p_f \neq 0$.

area E shown in Fig. 14. $R_{\text{S'}}$ is the rate of retransmitted information sequence from S. Let P_{E} denotes the probability that $(R_{\text{S}}, R_{\text{S'}})$ fall into the inadmissible area E. The outage probability of ADF relaying is then given by

$$
\begin{aligned}
P_{\text{out}}^{\text{ADF, Ind}} =& P_{\text{A}} + P_{\text{E}} \\
=& \Pr[p_f = 0, 0 \leq R_{\text{S}} \leq 1, 0 \leq R_{\text{R}} \leq H(p_f)] \\
&+ \Pr[0 < p_f \leq 0.5, 0 \leq R_{\text{S}} \leq 1, 0 \leq R_{\text{S'}} \leq H(p_f)] \\
=& \frac{1}{\overline{\gamma}_{\text{SD}}} \exp\left(-\frac{1}{\overline{\gamma}_{\text{SR}}}\right) \int_{\gamma_{\text{SD}}=\Theta^{-1}(0)}^{\Theta^{-1}(1)} \exp\left(-\frac{\gamma_{\text{SD}}}{\overline{\gamma}_{\text{SD}}}\right) \\
&\left(1 - \exp\left(-\frac{\Theta^{-1}(1-\Theta(\gamma_{\text{SD}}))}{\overline{\gamma}_{\text{RD}}}\right)\right) d\gamma_{\text{SD}} \\
&+ \frac{1}{\overline{\gamma}_{\text{S'D}}} \left(1 - \exp\left(-\frac{1}{\overline{\gamma}_{\text{SR}}}\right)\right) \int_{\gamma_{\text{SD}}=\Theta^{-1}(0)}^{\Theta^{-1}(1)} \exp\left(-\frac{\gamma_{\text{SD}}}{\overline{\gamma}_{\text{S'D}}}\right) \\
&\left(1 - \exp\left(-\frac{\Theta^{-1}(1-\Theta(\gamma_{\text{SD}}))}{\overline{\gamma}_{\text{SD}}}\right)\right) d\gamma_{\text{SD}},
\end{aligned}
\tag{44}
$$

where P_{A} is equal to that in (8). The derivations for the explicit expressions of (42), (43), and (44) may not be possible. We use a numerical method [77] to evaluate $P_{\mathrm{out}}^{\mathrm{LF,\ Ind}}$, $P_{\mathrm{out}}^{\mathrm{DF,\ Ind}}$, and $P_{\mathrm{out}}^{\mathrm{ADF,\ Ind}}$.

Approximations

By invoking the property of exponential function $e^{-x} \approx 1 - x$ for small x, corresponding to high SNR regime, the outage probabilities of LF, DF, and ADF relaying, respectively, can be approximated by the closed-form expressions, as,

$$\begin{aligned} P_{\mathrm{out}}^{\mathrm{LF,\ Ind}} \approx & \frac{1}{\overline{\gamma}_{\mathrm{SD}}\overline{\gamma}_{\mathrm{RD}}}\left(1-\frac{1}{\overline{\gamma}_{\mathrm{SR}}}\right)\left(\ln(4)-1+\frac{4\ln(2)-3}{2\overline{\gamma}_{\mathrm{SD}}}\right) \\ & + \frac{1}{\overline{\gamma}_{\mathrm{SD}}\overline{\gamma}_{\mathrm{SR}}}\left(\ln(4)-1+\frac{4\ln(2)-3}{2\overline{\gamma}_{\mathrm{SR}}}\right), \end{aligned} \tag{45}$$

$$\begin{aligned} P_{\mathrm{out}}^{\mathrm{DF,\ Ind}} \approx & \frac{1}{\overline{\gamma}_{\mathrm{SD}}\overline{\gamma}_{\mathrm{RD}}}\left(1-\frac{1}{\overline{\gamma}_{\mathrm{SR}}}\right)\left(\ln(4)-1+\frac{4\ln(2)-3}{2\overline{\gamma}_{\mathrm{SD}}}\right) \\ & + \frac{1}{\overline{\gamma}_{\mathrm{SD}}\overline{\gamma}_{\mathrm{SR}}}, \end{aligned} \tag{46}$$

and

$$\begin{aligned} P_{\mathrm{out}}^{\mathrm{ADF,\ Ind}} \approx & \frac{1}{\overline{\gamma}_{\mathrm{SD}}\overline{\gamma}_{\mathrm{RD}}}\left(1-\frac{1}{\overline{\gamma}_{\mathrm{SR}}}\right)\left(\ln(4)-1+\frac{4\ln(2)-3}{2\overline{\gamma}_{\mathrm{SD}}}\right) \\ & + \frac{1}{\overline{\gamma}_{\mathrm{SD}}^{2}\overline{\gamma}_{\mathrm{SR}}}\left(\ln(4)-1+\frac{4\ln(2)-3}{2\overline{\gamma}_{\mathrm{SD}}}\right). \end{aligned} \tag{47}$$

It is found from Fig. 15 that in spatially or temporary independent fading (i.e., $\rho_s = 0$, and $\rho_t = 0$), the approximated outage curves obtained from (45), (46), and (47) well match the numerically calculated outage curves from (42), (43), and (44). This observation indicates that the approximation is accurate to the exact outage probability.

Diversity Order and Coding Gain

By setting the geometric gain of each link to be identical and replacing $\overline{\gamma}_{ij}$ with a generic $\overline{\gamma}$, corresponding to equilateral triangle node locations (i.e., S, R, and D are located to the vertex of an equilateral triangle), (45), (46), and (47) are reduced to

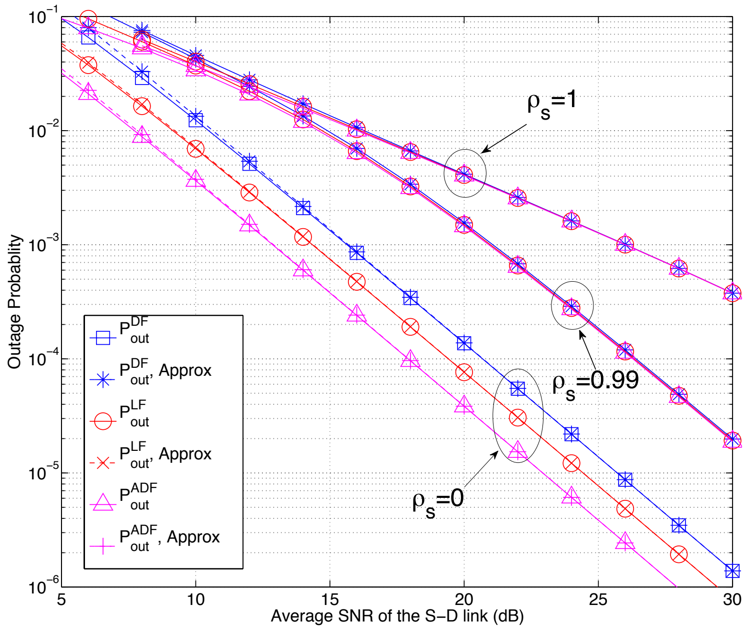

Fig. 15. Comparison between the exact and approximated outage probabilities for LF, DF, and ADF relaying over independent and spatial correlated channels, where the S-R, S-D, and R-D links have equal distances and $\rho_t = 0$.

$$P_{\text{out}}^{\text{LF, Ind}} = \frac{2\ln(4)-2}{(\bar{\gamma})^2} + \frac{8\ln(2)-2\ln(4)-4}{2(\bar{\gamma})^3} - \frac{4\ln(2)-3}{2(\bar{\gamma})^4}, \tag{48}$$

$$P_{\text{out}}^{\text{DF, Ind}} = \frac{\ln(4)}{(\bar{\gamma})^2} + \frac{4\ln(2)-2\ln(4)-2}{2(\bar{\gamma})^3} - \frac{4\ln(2)-3}{2(\bar{\gamma})^4}, \tag{49}$$

and

$$P_{\text{out}}^{\text{ADF, Ind}} = \frac{\ln(4)-1}{(\bar{\gamma})^2} + \frac{4\ln(2)-3}{2(\bar{\gamma})^3}, \tag{50}$$

respectively.

Then, in high average SNR regime, (48), (49), and (50) can further be expressed as

$$P_{\text{out}}^{\text{LF, Ind}} = \left(G_c^{\text{LF}} \cdot \bar{\gamma}\right)^{-G_d^{\text{LF}}}, \tag{51}$$

$$P_{\text{out}}^{\text{DF, Ind}} = \left(G_c^{\text{DF}} \cdot \bar{\gamma}\right)^{-G_d^{\text{DF}}}, \tag{52}$$

and

$$P_{\text{out}}^{\text{ADF, Ind}} = \left(G_c^{\text{ADF}} \cdot \overline{\gamma}\right)^{-G_d^{\text{ADF}}}, \tag{53}$$

where $G_d^{\text{LF}} = G_d^{\text{DF}} = G_d^{\text{ADF}} = 2$ are the diversity orders of LF, DF, and ADF relaying. This is consistent to the decay shown in the outage curves in Fig. 15 (i.e., those with $\rho_s = 0$). $G_c^{\text{LF}} = \frac{1}{\sqrt{2\ln(4)-2}}$, $G_c^{\text{DF}} = \frac{1}{\sqrt{\ln(4)}}$, and $G_c^{\text{ADF}} = \frac{1}{\sqrt{\ln(4)-1}}$ are the coding gains of LF, DF, and ADF relaying, respectively [50]. It is easy to find that $G_c^{\text{ADF}} > G_c^{\text{LF}} > G_c^{\text{DF}}$, which is consistent to the relationship shown in the outage curves in Fig. 15, i.e., with spatially and temporally independent channels ($\rho_s = 0$ and $\rho_t = 0$), $P_{\text{out}}^{\text{DF, Ind}} > P_{\text{out}}^{\text{LF, Ind}} > P_{\text{out}}^{\text{ADF, Ind}}$.

Theorem 2. *The outage probability of LF is smaller than that of DF, i.e., $P_{\text{out}}^{\textit{LF, Ind}} < P_{\text{out}}^{\textit{DF, Ind}}$.*

Proof. The difference between $P_{\text{out}}^{\text{DF, Ind}}$ in (45) and $P_{\text{out}}^{\text{LF, Ind}}$ in (46), is

$$P_{\text{out}}^{\text{LF, Ind}} - P_{\text{out}}^{\text{DF, Ind}} = \frac{1}{\overline{\gamma}_{\text{SD}}\overline{\gamma}_{\text{SR}}}\left(\ln(4) - 2 + \frac{4\ln(2)-3}{2\overline{\gamma}_{\text{SR}}}\right). \tag{54}$$

Let $\Delta = \left(\ln(4) - 2 + \frac{4\ln(2)-3}{2\overline{\gamma}_{\text{SR}}}\right)$. Since

$$\lim_{\overline{\gamma}_{\text{SR}}\to\infty} \Delta = -1.3069 < 0 \tag{55}$$

and

$$\frac{\mathrm{d}\Delta}{\mathrm{d}\overline{\gamma}_{\text{SR}}} = \frac{3-4\ln(2)}{\overline{\gamma}_{\text{SR}}^2} > 0, \tag{56}$$

Δ increases monotonically as $\overline{\gamma}_{\text{SR}}$ increases and limited to -1.3069. Therefore, it proves that (54) always has negative value for any given SNR, which indicates that the $P_{\text{out}}^{\text{LF, Ind}}$ is smaller than $P_{\text{out}}^{\text{DF, Ind}}$. □

Theorem 3. *The outage probability of LF is larger than that of ADF, i.e., $P_{\text{out}}^{\textit{LF, Ind}} > P_{\text{out}}^{\textit{ADF, Ind}}$.*

Proof. The difference between $P_{\text{out}}^{\text{LF, Ind}}$ in (45) and $P_{\text{out}}^{\text{ADF, Ind}}$ in (47) is

$$\begin{aligned} P_{\text{out}}^{\text{LF, Ind}} - P_{\text{out}}^{\text{ADF, Ind}} = &\frac{1}{\overline{\gamma}_{\text{SD}}\overline{\gamma}_{\text{SR}}}\left(\ln(4) - 1 + \frac{4\ln(2)-3}{2\overline{\gamma}_{\text{SR}}}\right) \\ &- \frac{1}{\overline{\gamma}_{\text{SD}}^2\overline{\gamma}_{\text{SR}}}\left(\ln(4) - 1 + \frac{4\ln(2)-3}{2\overline{\gamma}_{\text{SD}}}\right). \end{aligned} \tag{57}$$

We assume $\frac{4\ln(2)-3}{2\overline{\gamma}_{\mathrm{SD}}} \leq \frac{4\ln(2)-3}{2\overline{\gamma}_{\mathrm{SR}}}$ with $\overline{\gamma}_{\mathrm{SD}} > 1$[7]. Since $\left(\ln(4)-1+\frac{4\ln(2)-3}{2\overline{\gamma}_{\mathrm{SD}}}\right) > 0$, we have

$$\begin{aligned}
&\frac{1}{\overline{\gamma}_{\mathrm{SD}}^2\overline{\gamma}_{\mathrm{SR}}}\left(\ln(4)-1+\frac{4\ln(2)-3}{2\overline{\gamma}_{\mathrm{SD}}}\right)\\
&<\frac{1}{\overline{\gamma}_{\mathrm{SD}}\overline{\gamma}_{\mathrm{SR}}}\left(\ln(4)-1+\frac{4\ln(2)-3}{2\overline{\gamma}_{\mathrm{SD}}}\right)\\
&\leq\frac{1}{\overline{\gamma}_{\mathrm{SD}}\overline{\gamma}_{\mathrm{SR}}}\left(\ln(4)-1+\frac{4\ln(2)-3}{2\overline{\gamma}_{\mathrm{SR}}}\right),
\end{aligned} \tag{58}$$

which indicates (57) is greater than 0. This proves $P_{\mathrm{out}}^{\mathrm{LF,\,Ind}} > P_{\mathrm{out}}^{\mathrm{ADF,\,Ind}}$. $\square$

2.2.4 Outage Analysis in Correlated Fading

Let the correlation of two complex channel gains be represented by a correlation coefficient ρ. The joint pdf of two signal amplitudes of correlated Rayleigh fading channels is given by [78]. It is not difficult to convert the amplitude joint pdf into that of two SNRs, γ_1 and γ_2, as

$$p(\gamma_1,\gamma_2)=\frac{1}{\overline{\gamma}_1\overline{\gamma}_2(1-\rho)}I_0\left(\frac{2}{(1-\rho)}\sqrt{\frac{\rho\gamma_1\gamma_2}{\overline{\gamma}_1\overline{\gamma}_2}}\right)\exp\left[-\frac{\frac{\gamma_1}{\overline{\gamma}_1}+\frac{\gamma_2}{\overline{\gamma}_2}}{1-\rho}\right], \tag{59}$$

where $I_0(\cdot)$ is the zero-th order modified Bessel's function of the first kind.

Outage Behavior of LF in Correlated Fading

We follow the same techniques as those used for calculating the outage probability in independent fading in (42). The multiple integral with the constraints (9), (10) and (11) over the joint pdf (59) leads to the outage probability expressions of LF relaying in

[7]Note that the approximated outage expressions (45), (46), and (47) are obtained at high SNR regime. Therefore, it is reasonable to give proof for $\overline{\gamma}_{\mathrm{SD}} > 1$ and $\overline{\gamma}_{\mathrm{SR}} > 1$.

spatially correlated S-D and R-D links, as

$$
\begin{aligned}
P_{\text{out}}^{\text{LF, Cor}} = & \exp\left(-\frac{1}{\overline{\gamma}_{\text{SR}}}\right) \int_{\gamma_{\text{SD}}=\Theta^{-1}(0)}^{\Theta^{-1}(1)} \int_{\gamma_{\text{RD}}=\Theta^{-1}(0)}^{\Theta^{-1}(1-\Theta(\gamma_{\text{SD}}))} \\
& \frac{1}{\overline{\gamma}_{\text{SD}}\overline{\gamma}_{\text{RD}}(1-\rho_s^2)} I_0\left(\frac{2|\rho_s|\gamma_{\text{SD}}\gamma_{\text{RD}}}{\sqrt{\overline{\gamma}_{\text{SD}}\overline{\gamma}_{\text{RD}}}(1-|\rho_s|^2)}\right) \\
& \cdot \exp\left[-\frac{\frac{\gamma_{\text{SD}}}{\overline{\gamma}_{\text{RD}}}+\frac{\gamma_{\text{RD}}}{\overline{\gamma}_{\text{RD}}}}{1-|\rho_s|^2}\right] d\gamma_{\text{SD}} d\gamma_{\text{RD}} \\
& + \int_{\gamma_{\text{SR}}=\Theta^{-1}(0)}^{\Theta^{-1}(1)} \int_{\gamma_{\text{SD}}=\Theta^{-1}(0)}^{\Theta^{-1}(1-\Theta(\gamma_{\text{SR}}))} \int_{\gamma_{\text{RD}}=\Theta^{-1}(0)}^{\Theta^{-1}(\infty)} \\
& \frac{1}{\overline{\gamma}_{\text{SR}}} \exp\left(-\frac{\gamma_{\text{SR}}}{\overline{\gamma}_{\text{SR}}}\right) I_0\left(\frac{2|\rho_s|\gamma_{\text{SD}}\gamma_{\text{RD}}}{\sqrt{\overline{\gamma}_{\text{SD}}\overline{\gamma}_{\text{RD}}}(1-|\rho_s|^2)}\right) \\
& \frac{1}{\overline{\gamma}_{\text{SD}}\overline{\gamma}_{\text{RD}}(1-\rho_s^2)} \exp\left[-\frac{\frac{\gamma_{\text{SD}}}{\overline{\gamma}_{\text{RD}}}+\frac{\gamma_{\text{RD}}}{\overline{\gamma}_{\text{RD}}}}{1-|\rho_s|^2}\right] d\gamma_{\text{SD}} d\gamma_{\text{RD}} d\gamma_{\text{SR}}, \\
& + \int_{\gamma_{\text{SR}}=\Theta^{-1}(0)}^{\Theta^{-1}(1)} \int_{\gamma_{\text{SD}}=\Theta^{-1}(1-\Theta(\gamma_{\text{SR}}))}^{\Theta^{-1}(1)} \int_{\gamma_{\text{RD}}=\Theta^{-1}(0)}^{\Theta^{-1}[\xi(\gamma_{\text{SD}},\gamma_{\text{SR}})]} \\
& \frac{1}{\overline{\gamma}_{\text{SR}}} \exp\left(-\frac{\gamma_{\text{SR}}}{\overline{\gamma}_{\text{SR}}}\right) I_0\left(\frac{2|\rho_s|\gamma_{\text{SD}}\gamma_{\text{RD}}}{\sqrt{\overline{\gamma}_{\text{SD}}\overline{\gamma}_{\text{RD}}}(1-|\rho_s|^2)}\right) \\
& \frac{1}{\overline{\gamma}_{\text{SD}}\overline{\gamma}_{\text{RD}}(1-\rho_s^2)} \exp\left[-\frac{\frac{\gamma_{\text{SD}}}{\overline{\gamma}_{\text{RD}}}+\frac{\gamma_{\text{RD}}}{\overline{\gamma}_{\text{RD}}}}{1-|\rho_s|^2}\right] d\gamma_{\text{SD}} d\gamma_{\text{RD}} d\gamma_{\text{SR}}, \qquad (60)
\end{aligned}
$$

where the pdfs in (42) have been replaced by the joint pdf in (59).

Outage Behavior of DF in Correlated Fading

Similarly, following the techniques for the outage derivation of DF in independent fading in (43), the outage probability expression of DF relaying in the correlated S-D and R-D links can be expressed as,

$$
\begin{aligned}
P_{\text{out}}^{\text{DF, Cor}} = & \exp\left(-\frac{1}{\overline{\gamma}_{\text{SR}}}\right) \int_{\gamma_{\text{SD}}=\Theta^{-1}(0)}^{\Theta^{-1}(1)} \int_{\gamma_{\text{RD}}=\Theta^{-1}(0)}^{\Theta^{-1}(1-\Theta(\gamma_{\text{SD}}))} \\
& \frac{1}{\overline{\gamma}_{\text{SD}}\overline{\gamma}_{\text{RD}}(1-\rho_s^2)} I_0\left(\frac{2|\rho_s|\gamma_{\text{SD}}\gamma_{\text{RD}}}{\sqrt{\overline{\gamma}_{\text{SD}}\overline{\gamma}_{\text{RD}}}(1-|\rho_s|^2)}\right) \\
& \cdot \exp\left[-\frac{\frac{\gamma_{\text{SD}}}{\overline{\gamma}_{\text{RD}}} + \frac{\gamma_{\text{RD}}}{\overline{\gamma}_{\text{RD}}}}{1-|\rho_s|^2}\right] d\gamma_{\text{SD}} d\gamma_{\text{RD}}, \\
& + \left(1-\exp\left(-\frac{\Theta^{-1}(1)}{\overline{\gamma}_{\text{SR}}}\right)\right)\left(1-\exp\left(-\frac{\Theta^{-1}(1)}{\overline{\gamma}_{\text{SD}}}\right)\right), \qquad (61)
\end{aligned}
$$

where the pdfs in (43) have been replaced by the joint pdf in (59).

Outage Behavior of ADF in Correlated Fading

When analyzing the outage probability of ADF, two correlation coefficients ρ_s and ρ_t are taken into account. The outage probability expression of ADF relaying over the links with spatially and temporally correlated fading can be derived by following the techniques for calculating the outage probability in independent fading in (44), as

$$
\begin{aligned}
P_{\text{out}}^{\text{ADF, Cor}} = & \exp\left(-\frac{1}{\overline{\gamma}_{\text{SR}}}\right) \int_{\gamma_{\text{SD}}=\Theta^{-1}(0)}^{\Theta^{-1}(1)} \int_{\gamma_{\text{RD}}=\Theta^{-1}(0)}^{\Theta^{-1}(1-\Theta(\gamma_{\text{SD}}))} \\
& \frac{1}{\overline{\gamma}_{\text{SD}}\overline{\gamma}_{\text{RD}}(1-\rho_s^2)} I_0\left(\frac{2|\rho_s|\gamma_{\text{SD}}\gamma_{\text{RD}}}{\sqrt{\overline{\gamma}_{\text{SD}}\overline{\gamma}_{\text{RD}}}(1-|\rho_s|^2)}\right) \\
& \exp\left[-\frac{\frac{\gamma_{\text{SD}}}{\overline{\gamma}_{\text{RD}}} + \frac{\gamma_{\text{RD}}}{\overline{\gamma}_{\text{RD}}}}{1-|\rho_s|^2}\right] d\gamma_{\text{SD}} d\gamma_{\text{RD}}, \\
& + \left(1-\exp\left(\frac{1}{\overline{\gamma}_{\text{SR}}}\right)\right) \int_{\gamma_{\text{SD}}=\Theta^{-1}(0)}^{\Theta^{-1}(1)} \int_{\gamma_{\text{S'D}}=\Theta^{-1}(0)}^{\Theta^{-1}(1-\Theta(\gamma_{\text{SD}}))} \\
& \frac{1}{\overline{\gamma}_{\text{SD}}\overline{\gamma}_{\text{S'D}}(1-\rho_t^2)} I_0\left(\frac{2|\rho_t|\gamma_{\text{SD}}\gamma_{\text{S'D}}}{\sqrt{\overline{\gamma}_{\text{SD}}\overline{\gamma}_{\text{S'D}}}(1-|\rho_t|^2)}\right) \\
& \exp\left[-\frac{\frac{\gamma_{\text{SD}}}{\overline{\gamma}_{\text{SD}}} + \frac{\gamma_{\text{S'D}}}{\overline{\gamma}_{\text{S'D}}}}{1-|\rho_t|^2}\right] d\gamma_{\text{SD}} d\gamma_{\text{S'D}}, \qquad (62)
\end{aligned}
$$

where the pdfs in (44) have been replaced by the joint pdf in (59). The pdfs of the S-D and R-D links are replaced by the joint pdf having spatial correlation coefficient ρ_s and the pdfs of the two S-D links are replaced by the joint pdf having temporal correlation coefficient ρ_t. Note that, the outage expressions (60), (61), and (62) in correlated fading reduce to those in independent links (42), (43), and (44) when $\rho_s = 0$ and $\rho_t = 0$.

Fig. 15 also plots the outage curves with high spatial correlation ρ_s, where all the S-D, S-R, and R-D links have the same average SNR. It is found from Fig. 15 that with independent S-D and R-D transmission, $\rho_s = 0$, ADF outperforms LF and DF in terms of the outage performance. However, ADF does not show obvious superiority compared to LF and DF with high spatial correlation, $\rho_s = 0.99$, even the two S-D transmissions are independent, $\rho_t = 0$. This is because, since in the high SNR regime, the relay can recover the original information sequence with small probability of error. Hence, R forwards the decoded, re-interleaved, and re-encoded sequence to D, and it less likely uses the S-D link for retransmission in ADF in high S-R link average SNR regime. Therefore, the temporal correlation ρ_t has less impact on the outage performance than the spatial correlation ρ_s. In this case, the value of spatial correlation ρ_s of the complex fading gains h_{SD} and h_{RD} in the first and the second time slot, respectively, dominates the outage probability. On the contrary, in the low SNR regime, ADF can achieve better outage performance than LF and DF but slightly, since the errors may not be well eliminated in every link with low SNR, resulting in that the admissible rate region is not satisfied.

The impact of spatial correlation ρ_s on the outage probabilities of LF, DF and ADF relaying are demonstrated in Fig. 16. As can be seen from the figure, over the entire ρ_s value region, LF exhibits superior outage performance to DF. This is because with LF, the relay system can be seen as a distributed turbo code. It is also found that ADF achieves lower outage probability than LF. This is because the inadmissible rate region with ADF is made smaller than LF by the feedback information, as shown in Fig. 5 and Fig. 14. It is observed that for all the three relaying schemes, the outage probabilities increase as the spatial correlation ρ_s between the channel complex gains with the S-D and R-D links in the two transmission time slots becomes large, since the correlation degrades the outage performances. Intuitively, spatial correlation decreases the statistical independence of fading variations in the S-D and R-D links. It is also found that the gaps among the outage curves with DF, LF, and ADF relaying decrease as the value of ρ_s increases. This is because the larger the spatial correlation, the smaller the contribution provided by the R-D link transmission. Hence, the system performances largely depend on the S-D link, which results in DF, LF, and ADF relaying exhibiting the similar performance.

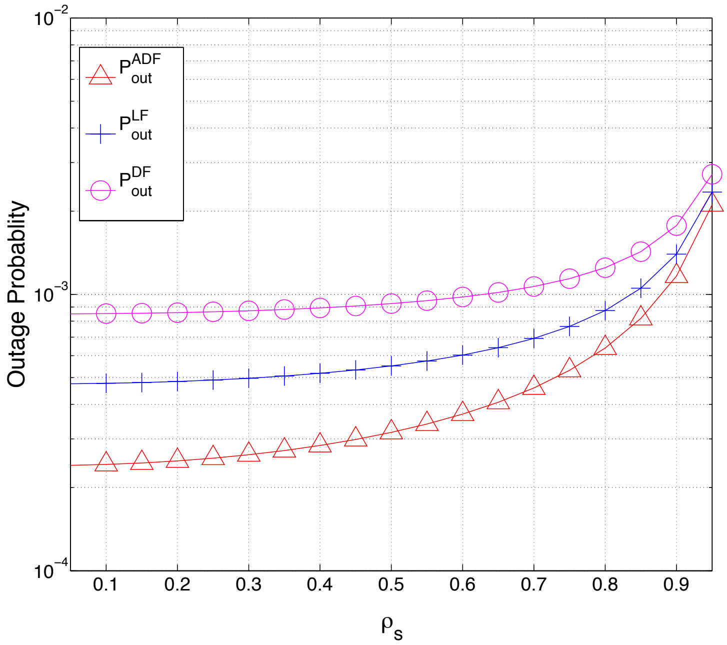

Fig. 16. Outage probability versus the spatial correlation ρ_s, where $\rho_t = 0$ and $\overline{\gamma}_{\mathrm{SD}} = 16$.

Fig. 17 shows the outage performance of ADF relaying with the temporal correlation ρ_t and spatial correlation ρ_s as parameters. As can be seen from the Fig. 17, the higher the ρ_s or ρ_t values, the larger the outage probability. The impact of ρ_s on outage performance is almost the same as that of ρ_t. This is because the average SNR of the S-R link is set at $\overline{\gamma}_{\mathrm{SR}} = 1.6$ dB. With such low average, the probability that the S-R link instantaneous SNR above the outage threshold is equal to that below the outage threshold, which is 50%. It means that the probability of the source retransmit signal equals to the probability of the relay forwards signal, which results in the impact of ρ_s and ρ_t on outage performance being the same.[8]

[8]For showing ρ_t has the same impact as ρ_s, the average SNR of the S-R link is set at $\overline{\gamma}_{\mathrm{SR}} = 1.6$ dB. In such low SNR region, the outage probability varies very slightly with ρ_s and ρ_t. For clearly showing the outage surface in Fig. 17, we use linear scale in Z-coordinate.

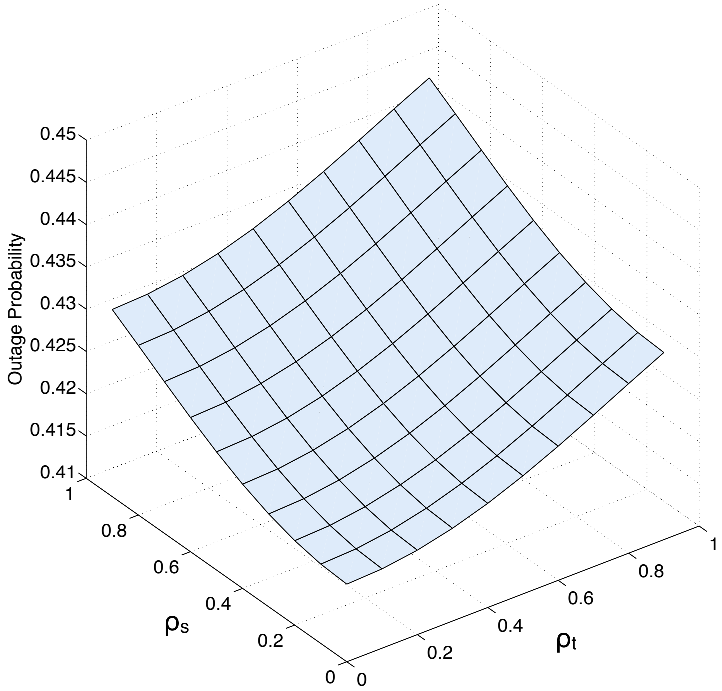

Fig. 17. Impacts of temporal correlation ρ_t and spatial correlation ρ_s on the outage probability of ADF, $\overline{\gamma}_{\mathrm{SR}} = 1.6$.

Approximations

The Bessel function of the first kind can be expressed with its series expansion by Frobenius method [79, 9.1.10], as:

$$I_0(x) = \sum_{m=0}^{\infty} \frac{(-1)^m}{m!\Gamma(m+1)} \left(\frac{x}{2}\right)^{2m}. \tag{63}$$

Then, (60), (61), and (62) can be, respectively, approximated as

$$\begin{aligned} P_{\mathrm{out}}^{\mathrm{LF,\,Cor}} \approx & \left(1 - \frac{1}{\overline{\gamma}_{\mathrm{SR}}}\right) \left(\frac{\ln(4) - 1}{\overline{\gamma}_{\mathrm{SD}} \overline{\gamma}_{\mathrm{RD}} (1 - \rho_s^2)} + \frac{2\ln(2) - 3}{2\overline{\gamma}_{\mathrm{SD}}^2 \overline{\gamma}_{\mathrm{RD}} (1 - \rho_s^2)} \right. \\ & \left. + \frac{\ln(4) - \frac{3}{2}}{\overline{\gamma}_{\mathrm{SD}} \overline{\gamma}_{\mathrm{RD}}^2 (1 - \rho_s^2)} \right) + \frac{2\ln(4) - 3}{2\overline{\gamma}_{\mathrm{SD}} \overline{\gamma}_{\mathrm{SR}}^2} + \frac{2\ln(4) - 3}{2\overline{\gamma}_{\mathrm{SD}}^2 \overline{\gamma}_{\mathrm{SR}}} \\ & + \frac{\ln(4) - 1}{2\overline{\gamma}_{\mathrm{SD}} \overline{\gamma}_{\mathrm{SR}}} + \frac{4\ln(16) - 11}{4\overline{\gamma}_{\mathrm{SD}}^2 \overline{\gamma}_{\mathrm{SR}}^2}, \end{aligned} \tag{64}$$

$$
\begin{aligned}
P_{\text{out}}^{\text{DF, Cor}} \approx & \left(1-\frac{1}{\overline{\gamma}_{\text{SR}}}\right)\left(\frac{\ln(4)-1}{\overline{\gamma}_{\text{SD}}\overline{\gamma}_{\text{RD}}(1-\rho_s^2)}+\frac{2\ln(2)-3}{2\overline{\gamma}_{\text{SD}}^2\overline{\gamma}_{\text{RD}}(1-\rho_s^2)}\right. \\
& \left.+\frac{\ln(4)-\frac{3}{2}}{\overline{\gamma}_{\text{SD}}\overline{\gamma}_{\text{RD}}^2(1-\rho_s^2)}\right)+\frac{1}{\overline{\gamma}_{\text{SD}}\overline{\gamma}_{\text{SR}}},
\end{aligned} \tag{65}
$$

and

$$
\begin{aligned}
P_{\text{out}}^{\text{ADF, Cor}} \approx & \left(1-\frac{1}{\overline{\gamma}_{\text{SR}}}\right)\left(\frac{\ln(4)-1}{\overline{\gamma}_{\text{SD}}\overline{\gamma}_{\text{RD}}(1-\rho_s^2)}+\frac{2\ln(2)-3}{2\overline{\gamma}_{\text{SD}}\overline{\gamma}_{\text{S'D}}\overline{\gamma}_{\text{RD}}(1-\rho_s^2)}\right. \\
& \left.+\frac{\ln(4)-\frac{3}{2}}{\overline{\gamma}_{\text{SD}}\overline{\gamma}_{\text{RD}}^2(1-\rho_s^2)}\right)+\frac{\ln(4)-1}{\overline{\gamma}_{\text{SD}}\overline{\gamma}_{\text{RD}}\overline{\gamma}_{\text{SR}}(1-\rho_t^2)} \\
& +\frac{4\ln(2)-3}{2\overline{\gamma}_{\text{SD}}\overline{\gamma}_{\text{S'D}}\overline{\gamma}_{\text{RD}}\overline{\gamma}_{\text{SR}}(1-\rho_t^2)}+\frac{\ln(4)-\frac{3}{2}}{\overline{\gamma}_{\text{SD}}\overline{\gamma}_{\text{RD}}^2\overline{\gamma}_{\text{SR}}(1-\rho_t^2)}.
\end{aligned} \tag{66}
$$

The accuracy of the approximations is demonstrated in Fig. 18 in section 2.2.5.

Diversity Order

The diversity order d is defined as [21]

$$
d=-\lim_{\overline{\gamma}\to\infty}\frac{\log(P_{\text{out}})}{\log(\overline{\gamma})}. \tag{67}
$$

According to (67), the diversity order of LF, DF, ADF over correlated channels can be expressed as

$$
\begin{aligned}
d_{\text{LF}} &= -\lim_{\overline{\gamma}\to\infty}\frac{\log(P_{\text{out}}^{\text{LF, Cor}})}{\log(\overline{\gamma})} \\
&= -\lim_{\overline{\gamma}\to\infty}\left\{\log\left[\frac{5\ln(4)-7}{2\overline{\gamma}^3}+\frac{4\ln(16)-11}{4\overline{\gamma}^4}+\left(1-\frac{1}{\overline{\gamma}}\right)\right.\right. \\
&\quad \cdot\left.\left.\left(\frac{\ln(4)-1}{\overline{\gamma}^2(1-\rho_s^2)}+\frac{2\ln(2)-2\ln(4)-6}{2\overline{\gamma}^3(1-\rho_s^2)}\right)\right]/\log(\overline{\gamma})\right\}=2,\rho_s\neq 1,
\end{aligned} \tag{68}
$$

$$
\begin{aligned}
d_{\text{DF}} &= -\lim_{\overline{\gamma}\to\infty}\frac{\log(P_{\text{out}}^{\text{DF, Cor}})}{\log(\overline{\gamma})} \\
&= -\lim_{\overline{\gamma}\to\infty}\left\{\log\left[\frac{2\ln(4)-3}{\overline{\gamma}^3}+\frac{\ln(4)-1}{2\overline{\gamma}^2}+\frac{4\ln(16)-11}{4\overline{\gamma}^4}\right.\right. \\
&\quad +\left.\left.\left(1-\frac{1}{\overline{\gamma}}\right)\left(\frac{\ln(4)-1}{\overline{\gamma}^2(1-\rho_s^2)}+\frac{2\ln(2)+2\ln(4)-6}{2\overline{\gamma}^3(1-\rho_s^2)}\right)\right]/\log(\overline{\gamma})\right\}=2,\rho_s\neq 1,
\end{aligned} \tag{69}
$$

and

$$
\begin{aligned}
d_{\mathrm{ADF}} &= -\lim_{\overline{\gamma}\to\infty} \frac{\log(P_{\mathrm{out}}^{\mathrm{ADF,\,Cor}})}{\log(\overline{\gamma})} \\
&= -\lim_{\overline{\gamma}\to\infty} \left\{ \log\left[\frac{\ln(4)-1}{\overline{\gamma}^3(1-\rho_t^2)} + \frac{4\ln(2)+2\ln(4)-6}{2\overline{\gamma}^4(1-\rho_t^2)} \right.\right. \\
&\left.\left. + \left(1-\frac{1}{\overline{\gamma}}\right)\left(\frac{\ln(4)-1}{\overline{\gamma}^2(1-\rho_s^2)} + \frac{2\ln(2)-3}{2\overline{\gamma}^3(1-\rho_s^2)} + \frac{\ln(4)-\frac{3}{2}}{\overline{\gamma}^3(1-\rho_s^2)} \right) \right] / \log(\overline{\gamma}) \right\} = 2, \\
&\rho_s \neq 1, \rho_t \neq 1, \qquad (70)
\end{aligned}
$$

where $\overline{\gamma}_{\mathrm{SD}}$, $\overline{\gamma}_{\mathrm{RD}}$, and $\overline{\gamma}_{\mathrm{SR}}$ are represented by a generic symbol $\overline{\gamma}$ under the equilateral triangle nodes location assumption. It is shown that the full diversity gain can be achieved by LF, DF, and ADF relaying as long as $\rho_s \neq 1$ for LF and DF, and $\rho_s \neq 1$ and $\rho_t \neq 1$ for ADF. When $\rho_s = 1$ and $\rho_t = 1$, i.e., in fully correlated fading, the diversity order reduces to one.

2.2.5 Optimal Relay Locations for Minimizing the Outage Probability

In this subsection, we investigate the optimal relay locations which minimize the outage probabilities of LF, DF, and ADF relaying. The outage expressions can be rewritten so that they are functions of the position of the relay by taking the geometric gain into consideration. It is shown that the optimization for the relay location can be formulated as a convex optimization problem.

Optimal Relay Locations in Independent Fading

Substituting (39) and (40) in section 2.1.4, which represent the relationships between the average SNRs and the geometric gains, into (45), (46), and (47), yields the outage probability expressions of LF, DF, and ADF relaying over the links suffering from independent fading with respect to the position of R as

$$P_{\text{out}}^{\text{LF, Ind}} = \frac{1}{\overline{\gamma}_{\text{SD}}\left(\overline{\gamma}_{\text{SD}} + 10\lg(\frac{1}{1-d})^{\alpha}\right)} \left(1 - \frac{1}{\overline{\gamma}_{\text{SD}} + 10\lg(\frac{1}{d})^{\alpha}}\right) \cdot \left(\ln(4) - 1 + \frac{4\ln(2)-3}{2\overline{\gamma}_{\text{SD}}}\right) + \frac{1}{\overline{\gamma}_{\text{SD}}\left(\overline{\gamma}_{\text{SD}} + 10\lg(\frac{1}{d})^{\alpha}\right)} \cdot \left(\ln(4) - 1 + \frac{4\ln(2)-3}{2\left(\overline{\gamma}_{\text{SD}} + 10\lg(\frac{1}{d})^{\alpha}\right)}\right), \tag{71}$$

$$P_{\text{out}}^{\text{DF, Ind}} = \frac{1}{\overline{\gamma}_{\text{SD}}\left(\overline{\gamma}_{\text{SD}} + 10\lg(\frac{1}{1-d})^{\alpha}\right)} \left(1 - \frac{1}{\overline{\gamma}_{\text{SD}} + 10\lg(\frac{1}{d})^{\alpha}}\right) \cdot \left(\ln(4) - 1 + \frac{4\ln(2)-3}{2\overline{\gamma}_{\text{SD}}}\right) + \frac{1}{\overline{\gamma}_{\text{SD}}\left(\overline{\gamma}_{\text{SD}} + 10\lg(\frac{1}{d})^{\alpha}\right)}, \tag{72}$$

and

$$P_{\text{out}}^{\text{ADF, Ind}} = \frac{1}{\overline{\gamma}_{\text{SD}}\left(\overline{\gamma}_{\text{SD}} + 10\lg(\frac{1}{1-d})^{\alpha}\right)} \left(1 - \frac{1}{\overline{\gamma}_{\text{SD}} + 10\lg(\frac{1}{d})^{\alpha}}\right) \cdot \left(\ln(4) - 1 + \frac{4\ln(2)-3}{2\overline{\gamma}_{\text{SD}}}\right) + \frac{1}{\overline{\gamma}_{\text{SD}}\left(\overline{\gamma}_{\text{SD}}^{2} + 10\lg(\frac{1}{d})^{\alpha}\right)} \cdot \left(\ln(4) - 1 + \frac{4\ln(2)-3}{2\overline{\gamma}_{\text{SD}}^{2}}\right), \tag{73}$$

under the assumption that R moves along the line between S and D, with which $d_{\text{SR}} = d$ and $d_{\text{RD}} = 1 - d$.

The general optimization problem with regard to d can be formulated as

$$\begin{aligned} d^{*} = \arg\min_{d} \quad & P_{\text{out}}(d) \\ \text{subject to:} \quad & d - 1 < 0, \\ & -d < 0. \end{aligned} \tag{74}$$

The Karush-Kuhn-Tucker (KKT) condition for (74) can be written as

$$\begin{aligned} & \tfrac{\partial P_{\text{out}}(d)}{\partial d} + \mu_1 - \mu_2, \\ & \mu_1 > 0, \\ & \mu_2 > 0, \\ & \mu_1(d-1) < 0, \\ & \mu_2(-d) < 0, \\ & d - 1 < 0, \\ & -d < 0, \end{aligned} \tag{75}$$

where μ_1 and μ_2 are the constraint coefficients.

Proposition 4. *Outage probability expressions of LF, DF, and ADF relaying in* (71)*,* (72)*, and* (73)*, are convex with respect to d* $\in$ *(0, 1).*

Proof. See Appendix 1. $\square$

Taking the first-order derivative of $P_{\text{out}}^{\text{LF, Ind}}$, $P_{\text{out}}^{\text{DF, Ind}}$, and $P_{\text{out}}^{\text{ADF, Ind}}$, respectively, in (71), (72), and (73) with respect to d and setting the derivative results to zero, we have

$$\begin{aligned}\frac{\partial P_{\text{out}}^{\text{LF, Ind}}}{\partial d} =& \frac{\partial \frac{1}{\overline{\gamma}_{\text{SD}}\left(\overline{\gamma}_{\text{SD}}+10\lg(\frac{1}{1-d})^{\alpha}\right)}\left(1-\frac{1}{\overline{\gamma}_{\text{SD}}+10\lg(\frac{1}{d})^{\alpha}}\right)\left(\ln(4)-1+\frac{4\ln(2)-3}{2\overline{\gamma}_{\text{SD}}}\right)}{\partial d}\\ &+\frac{\partial \frac{1}{\overline{\gamma}_{\text{SD}}\left(\overline{\gamma}_{\text{SD}}+10\lg(\frac{1}{d})^{\alpha}\right)}\left(\ln(4)-1+\frac{4\ln(2)-3}{2\left(\overline{\gamma}_{\text{SD}}+10\lg(\frac{1}{d})^{\alpha}\right)}\right)}{\partial d}=0, \end{aligned} \tag{76}$$

$$\begin{aligned}\frac{\partial P_{\text{out}}^{\text{DF, Ind}}}{\partial d} =& \frac{\partial \frac{1}{\overline{\gamma}_{\text{SD}}\left(\overline{\gamma}_{\text{SD}}+10\lg(\frac{1}{1-d})^{\alpha}\right)}\left(1-\frac{1}{\overline{\gamma}_{\text{SD}}+10\lg(\frac{1}{d})^{\alpha}}\right)\left(\ln(4)-1+\frac{4\ln(2)-3}{2\overline{\gamma}_{\text{SD}}}\right)}{\partial d}\\ &+\frac{\partial \frac{1}{\overline{\gamma}_{\text{SD}}\left(\overline{\gamma}_{\text{SD}}+10\lg(\frac{1}{d})^{\alpha}\right)}}{\partial d}=0, \end{aligned} \tag{77}$$

and

$$\begin{aligned}\frac{\partial P_{\text{out}}^{\text{ADF, Ind}}}{\partial d} =& \frac{\partial \frac{1}{\overline{\gamma}_{\text{SD}}\left(\overline{\gamma}_{\text{SD}}+10\lg(\frac{1}{1-d})^{\alpha}\right)}\left(1-\frac{1}{\overline{\gamma}_{\text{SD}}+10\lg(\frac{1}{d})^{\alpha}}\right)\left(\ln(4)-1+\frac{4\ln(2)-3}{2\overline{\gamma}_{\text{SD}}}\right)}{\partial d}\\ &+\frac{\partial \frac{1}{\overline{\gamma}_{\text{SD}}\left(\overline{\gamma}_{\text{SD}}^2+10\lg(\frac{1}{d})^{\alpha}\right)}\left(\ln(4)-1+\frac{4\ln(2)-3}{2\overline{\gamma}_{\text{SD}}^2}\right)}{\partial d}=0. \end{aligned} \tag{78}$$

It may be excessively complex to derive the explicit expression for d^* from (76), (77), and (78). Hence, the Newton-Raphson method [80, Chapter 9] is used to numerically calculate the solution of d^*.

Optimal Relay Locations in Correlated Fading

Similar to the independent fading case, the outage probability expressions of LF, DF and ADF relaying in correlated fading with respect to the position of R can be expressed as (79), (80), and (81).

$$
\begin{aligned}
P_{\text{out}}^{\text{LF, Cor}} = &\left(1 - \frac{1}{\left(\overline{\gamma}_{\text{SD}} + 10\lg(\frac{1}{d})^{\alpha}\right)}\right)\left(\frac{\ln(4)-1}{\overline{\gamma}_{\text{SD}}\left(\overline{\gamma}_{\text{SD}} + 10\lg(\frac{1}{1-d})^{\alpha}\right)(1-\rho_s^2)}\right.\\
&\left. + \frac{2\ln(2)-3}{2\overline{\gamma}_{\text{SD}}^2\left(\overline{\gamma}_{\text{SD}} + 10\lg(\frac{1}{1-d})^{\alpha}\right)(1-\rho_s^2)} + \frac{\ln(4)-\frac{3}{2}}{\overline{\gamma}_{\text{SD}}\left(\overline{\gamma}_{\text{SD}} + 10\lg(\frac{1}{1-d})^{\alpha}\right)^2(1-\rho_s^2)}\right)\\
&+ \frac{2\ln(4)-3}{2\overline{\gamma}_{\text{SD}}\left(\overline{\gamma}_{\text{SD}} + 10\lg(\frac{1}{d})^{\alpha}\right)^2} + \frac{2\ln(4)-3}{2\overline{\gamma}_{\text{SD}}^2\left(\overline{\gamma}_{\text{SD}} + 10\lg(\frac{1}{d})^{\alpha}\right)} + \frac{\ln(4)-1}{2\overline{\gamma}_{\text{SD}}\left(\overline{\gamma}_{\text{SD}} + 10\lg(\frac{1}{d})^{\alpha}\right)}\\
&+ \frac{4\ln(16)-11}{4\overline{\gamma}_{\text{SD}}^2\left(\overline{\gamma}_{\text{SD}} + 10\lg(\frac{1}{d})^{\alpha}\right)^2},
\end{aligned}
\tag{79}
$$

$$
\begin{aligned}
P_{\text{out}}^{\text{DF, Cor}} = &\left(1 - \frac{1}{\left(\overline{\gamma}_{\text{SD}} + 10\lg(\frac{1}{d})^{\alpha}\right)}\right)\left(\frac{\ln(4)-1}{\overline{\gamma}_{\text{SD}}\left(\overline{\gamma}_{\text{SD}} + 10\lg(\frac{1}{1-d})^{\alpha}\right)(1-\rho_s^2)}\right.\\
&\left. + \frac{2\ln(2)-3}{2\overline{\gamma}_{\text{SD}}^2\left(\overline{\gamma}_{\text{SD}} + 10\lg(\frac{1}{1-d})^{\alpha}\right)(1-\rho_s^2)} + \frac{\ln(4)-\frac{3}{2}}{\overline{\gamma}_{\text{SD}}\left(\overline{\gamma}_{\text{SD}} + 10\lg(\frac{1}{1-d})^{\alpha}\right)^2(1-\rho_s^2)}\right)\\
&+ \frac{1}{\overline{\gamma}_{\text{SD}}\left(\overline{\gamma}_{\text{SD}} + 10\lg(\frac{1}{d})^{\alpha}\right)},
\end{aligned}
\tag{80}
$$

$$
\begin{aligned}
P_{\text{out}}^{\text{ADF, Cor}} = &\left(1 - \frac{1}{\left(\overline{\gamma}_{\text{SD}} + 10\lg(\frac{1}{d})^{\alpha}\right)}\right)\left(\frac{\ln(4)-1}{\overline{\gamma}_{\text{SD}}\left(\overline{\gamma}_{\text{SD}} + 10\lg(\frac{1}{1-d})^{\alpha}\right)(1-\rho_s^2)}\right.\\
&\left. + \frac{2\ln(2)-3}{2\overline{\gamma}_{\text{SD}}^2\left(\overline{\gamma}_{\text{SD}} + 10\lg(\frac{1}{1-d})^{\alpha}\right)(1-\rho_s^2)} + \frac{\ln(4)-\frac{3}{2}}{\overline{\gamma}_{\text{SD}}\left(\overline{\gamma}_{\text{SD}} + 10\lg(\frac{1}{1-d})^{\alpha}\right)^2(1-\rho_s^2)}\right)\\
&+ \frac{4\ln(2)-3}{2\overline{\gamma}_{\text{SD}}^2\left(\overline{\gamma}_{\text{SD}} + 10\lg(\frac{1}{1-d})^{\alpha}\right)\left(\overline{\gamma}_{\text{SD}} + 10\lg(\frac{1}{d})^{\alpha}\right)(1-\rho_t^2)}\\
&+ \frac{\ln(4)-\frac{3}{2}}{\overline{\gamma}_{\text{SD}}\left(\overline{\gamma}_{\text{SD}} + 10\lg(\frac{1}{1-d})^{\alpha}\right)^2\left(\overline{\gamma}_{\text{SD}} + 10\lg(\frac{1}{d})^{\alpha}\right)(1-\rho_t^2)}.
\end{aligned}
\tag{81}
$$

The optimization problem for the correlated fading channels' case can also be formulated by (74) for LF, DF, and ADF relaying.

Proposition 5. *Outage probability expressions of LF, DF, and ADF relaying, respectively, given by* (79), (80)*, and* (81)*, are convex with respect to $d \in (0,\, 1)$.*

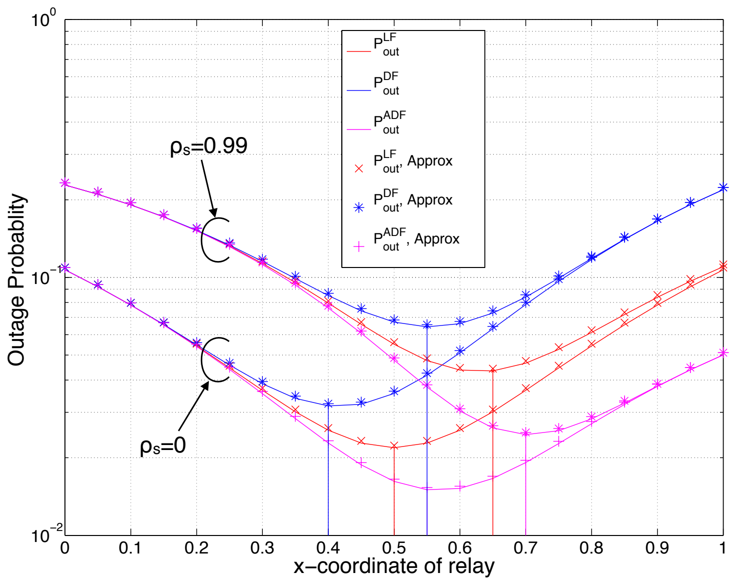

Fig. 18. Outage probabilities versus relay locations for LF, DF, and ADF relaying over spatially independent and correlated channels, where $\rho_t = 0$.

Proof. The convexity of (79), (80), and (81) can be proven by taking second-order partial derivative of $P_{\text{out}}^{\text{LF, Cor}}$, $P_{\text{out}}^{\text{DF, Cor}}$, and $P_{\text{out}}^{\text{ADF, Cor}}$ in (79), (80), and (81) with respect to d, and showing that the derivative results are positive in the range $d \in (0,1)$[9]. □

Take the first-order derivative of $P_{\text{out}}^{\text{LF, Cor}}$, $P_{\text{out}}^{\text{DF, Cor}}$, and $P_{\text{out}}^{\text{ADF, Cor}}$, respectively, in (79), (80), and (81) with respect to d and set the derivative result to zero, $\frac{\partial P_{\text{out}}^{\text{LF, Cor}}}{\partial d} = 0$, $\frac{\partial P_{\text{out}}^{\text{DF, Cor}}}{\partial d} = 0$, and $\frac{\partial P_{\text{out}}^{\text{ADF, Cor}}}{\partial d} = 0$. As in the independent fading case, the optimal relay location d^* for LF, DF, and ADF relaying over correlated fading channels can also be obtained by utilizing an iterative root-finding algorithm [80].

Fig. 18 depicts the impact of the relay location on outage performances of LF, DF and ADF relaying in spatially independent ($\rho_s = 0$) and correlated ($\rho_s = 0.99$) cases. The relay is assumed to move along the line between S ($x = 0$) and D ($x = 1$). Both the numerically calculated outage probabilities and approximated outage probabilities are plotted. It is found from the figure that the approximated and numerically calculated outage probability curves are consistent with each other. This observation indicates the

[9]The details of the proof are straightforward but lengthy, and therefore are omitted here for brevity.

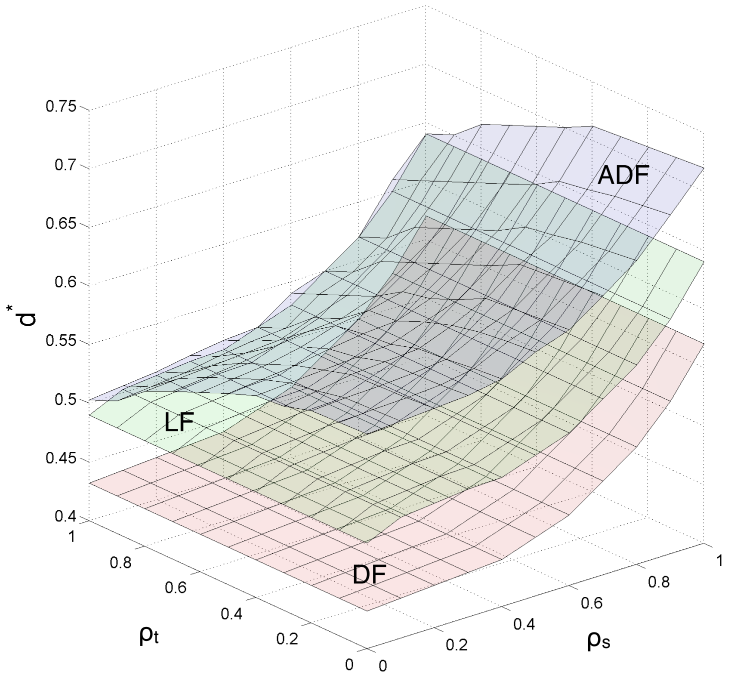

Fig. 19. Impact of temporal correlation ρ_t and spatial correlation ρ_s on optimal relay location d^*, where $\bar{\gamma}_{\mathrm{SD}} = 2$ (dB).

accuracy of the approximations. It is found from Fig. 18 that in spatially and temporally independent fading ($\rho_s = 0,\ \rho_t = 0$) the optimal relay locations for LF, DF, and ADF that achieve the lowest probabilities are $d^* = 0.5$, $d^* < 0.5$ and, $d^* > 0.5$, respectively. In spatially correlated fading ($\rho_s = 0.99$), the optimal relay locations for LF, DF, and ADF relaying shift closer to the destination compared to the case in independent fading. This is because the fading correlation reduces the diversity gain provided by the R-D link transmission, which results in the optimal position of the relay shifting close to the destination to keep the average SNR of the R-D link high.

The impact of the temporal correlation ρ_t and the spatial correlation ρ_s on the optimal relay location d^* of LF, DF, ADF relaying is depicted in Fig. 19. For DF, LF, and ADF relaying, the higher the ρ_s, the larger the d^*, which indicates that the optimal relay locations shift close to the destination as the spatial correlation increases. This is because the average SNR of the R-D link need to be kept high to compensate the loss caused by the fading correlation. Obviously, ρ_t has no impact on d^* in LF and DF relaying. With ADF, it is found that the value of d^* becomes small as ρ_t increases. The time diversity gain achieved by using the S-D link twice is reduced by the temporal correlation, which leads to that the relay should be located close to the source in order to reduce the S-R transmission error. This decreases the probability of retransmission from the source.

2.2.6 Optimal Power Allocation for Minimizing the Outage Probability

In this section, our aim is to minimize the outage probabilities for LF, DF, and ADF relaying by adjusting power allocated to S and R. We consider a transmit power sharing strategy. The source (or the relay) can use the transmit power that is allocated to the system when the power is not used by the relay (or the source). The source and the relay can control its transmit power properly under total transmit power constraint. In this work, we do not consider the practical implementation of the transmit power sharing strategy and only focus on the theoretical analysis. We assume that the CSI is only available at the receiver side. Let the power allocated to S and R be denoted as $P_T k$ and $P_T(1-k)$, respectively, where P_T represents the total transmit power and k $(0 < k < 1)$ is the power allocation ratio. With the noise variance of each link being normalized to the unity, the geometric gain times transmit power is equivalent to their corresponding average SNR. Then the average SNRs of each link can be expressed as functions of k as

$$\overline{\gamma}_{\mathrm{SD}} = P_T k G_{\mathrm{SD}}, \tag{82}$$

$$\overline{\gamma}_{\mathrm{RD}} = P_T (1-k) G_{\mathrm{RD}}, \tag{83}$$

$$\overline{\gamma}_{\mathrm{SR}} = P_T k G_{\mathrm{SR}}. \tag{84}$$

Optimal Power Allocation in Independent Fading

By substituting (82), (83), and (84) into (45), (46), and (47) in section 2.2.3, the outage expressions of LF, DF, and ADF relaying in independent fading with respect to k can be written as

$$\begin{aligned} P_{\mathrm{out}}^{\mathrm{LF,\ Ind}} = &\frac{1}{P_T^2 k(1-k) G_{\mathrm{SD}} G_{\mathrm{RD}}} \left(1 - \frac{1}{P_T k G_{\mathrm{SR}}}\right) \left(\ln(4) - 1 + \frac{4\ln(2)-3}{2P_T k G_{\mathrm{SD}}}\right) \\ &+ \frac{1}{P_T^2 k^2 G_{\mathrm{SD}} G_{\mathrm{SR}}} \left(\ln(4) - 1 + \frac{4\ln(2)-3}{2P_T k G_{\mathrm{SR}}}\right), \end{aligned} \tag{85}$$

$$P_{\text{out}}^{\text{DF, Ind}} = \frac{1}{P_T^2 k(1-k) G_{\text{SD}} G_{\text{RD}}} \left(1 - \frac{1}{P_T k G_{\text{SR}}}\right) \left(\ln(4) - 1 + \frac{4\ln(2) - 3}{2 P_T k G_{\text{SD}}}\right) + \frac{1}{P_T^2 k^2 G_{\text{SD}} G_{\text{SR}}}, \tag{86}$$

and

$$P_{\text{out}}^{\text{ADF, Ind}} = \frac{1}{P_T^2 k(1-k) G_{\text{SD}} G_{\text{RD}}} \left(1 - \frac{1}{P_T k G_{\text{SR}}}\right) \left(\ln(4) - 1 + \frac{4\ln(2) - 3}{2 P_T k G_{\text{SD}}}\right) + \frac{1}{P_T^3 k^3 G_{\text{SR}} G_{\text{SD}}} \left(\ln(4) - 1 + \frac{4\ln(2) - 3}{2 P_T k G_{\text{SD}}}\right), \tag{87}$$

respectively.

The optimization problem with regards to k can be formulated as

$$\begin{aligned} &k^* = \arg\min_k \quad P_{\text{out}}(k) \\ &\text{subject to:} \qquad k - 1 < 0, \quad -k < 0, \quad . \end{aligned} \tag{88}$$

The KKT condition for (88) can be written as

$$\begin{aligned} &\tfrac{\partial P_{\text{out}}(k)}{\partial k} + \mu_3 - \mu_4, \\ &\mu_3 > 0, \\ &\mu_4 > 0, \\ &\mu_3 (k - 1) < 0, \\ &\mu_4 (-k) < 0, \\ &k - 1 < 0, \\ &-k < 0, \end{aligned} \tag{89}$$

where μ_3 and μ_4 are the constraint coefficients.

Proposition 6. *Outage probability expressions of LF, DF, and ADF relaying, respectively, in* (85)*,* (86)*, and* (87)*, are convex with respect to* $k \in (0, 1)$*.*

Proof. See Appendix 2. □

Taking the first-order derivative of $P_{\text{out}}^{\text{LF, Ind}}$, $P_{\text{out}}^{\text{DF, Ind}}$, and $P_{\text{out}}^{\text{ADF, Ind}}$, respectively in (85), (86), and (87) with respect to k and setting the derivative results to zero, we have,

$$\frac{\partial P_{\text{out}}^{\text{LF, Ind}}}{\partial d} = \frac{\partial \frac{1}{P_T^2 k(1-k) G_{\text{SD}} G_{\text{RD}}} \left(1 - \frac{1}{P_T k G_{\text{SR}}}\right) \left(\ln(4) - 1 + \frac{4\ln(2) - 3}{2 P_T k G_{\text{SD}}}\right)}{\partial k} + \frac{\partial \frac{1}{P_T^2 k^2 G_{\text{SD}} G_{\text{SR}}} \left(\ln(4) - 1 + \frac{4\ln(2) - 3}{2 P_T k G_{\text{SR}}}\right)}{\partial k} = 0, \tag{90}$$

$$P_{\text{out}}^{\text{LF, Cor}} = \left(1 - \frac{1}{P_T k G_{\text{SD}}}\right)\left(\frac{\ln(4)-1}{P_T k G_{\text{SD}} P_T (1-k) G_{\text{RD}} (1-\rho_s^2)} + \frac{2\ln(2)-3}{2 P_T k G_{\text{SD}}^2 P_T (1-k) G_{\text{RD}} (1-\rho_s^2)} + \frac{\ln(4)-\frac{3}{2}}{P_T k G_{\text{SD}} P_T (1-k) G_{\text{RD}}^2 (1-\rho_s^2)}\right) + \frac{2\ln(4)-3}{2 P_T k G_{\text{SD}} P_T^2 k^2 G_{\text{SR}}^2} + \frac{2\ln(4)-3}{2 P_T^2 k^2 G_{\text{SD}}^2 P_T k G_{\text{SD}}} + \frac{\ln(4)-1}{2 P_T k G_{\text{SD}} P_T k G_{\text{SD}}} + \frac{4\ln(16)-11}{4 P_T^2 k^2 G_{\text{SD}}^2 P_T^2 k^2 G_{\text{SR}}^2}, \tag{93}$$

$$P_{\text{out}}^{\text{DF, Cor}} = \left(1 - \frac{1}{P_T k G_{\text{SD}}}\right)\left(\frac{\ln(4)-1}{P_T k G_{\text{SD}} P_T (1-k) G_{\text{RD}} (1-\rho_s^2)} + \frac{2\ln(2)-3}{2 P_T k G_{\text{SD}}^2 P_T (1-k) G_{\text{RD}} (1-\rho_s^2)} + \frac{\ln(4)-\frac{3}{2}}{P_T k G_{\text{SD}} P_T (1-k) G_{\text{RD}}^2 (1-\rho_s^2)}\right) + \frac{1}{P_T k G_{\text{SD}} P_T k G_{\text{SD}}}, \tag{94}$$

$$\frac{\partial P_{\text{out}}^{\text{DF, Ind}}}{\partial d} = \frac{\partial \frac{1}{P_T^2 k (1-k) G_{\text{SD}} G_{\text{RD}}} \left(1 - \frac{1}{P_T k G_{\text{SR}}}\right)\left(\ln(4) - 1 + \frac{4\ln(2)-3}{2 P_T k G_{\text{SD}}}\right)}{\partial k} + \frac{\partial \frac{1}{P_T^2 k^2 G_{\text{SD}} G_{\text{SR}}}}{\partial k} = 0, \tag{91}$$

and

$$\frac{\partial P_{\text{out}}^{\text{ADF, Ind}}}{\partial d} = \frac{\partial \frac{1}{P_T^2 k (1-k) G_{\text{SD}} G_{\text{RD}}} \left(1 - \frac{1}{P_T k G_{\text{SR}}}\right)\left(\ln(4) - 1 + \frac{4\ln(2)-3}{2 P_T k G_{\text{SD}}}\right)}{\partial k} + \frac{\partial \frac{1}{P_T^3 k^3 G_{\text{SR}} G_{\text{SD}}} \left(\ln(4) - 1 + \frac{4\ln(2)-3}{2 P_T k G_{\text{SD}}}\right)}{\partial k} = 0. \tag{92}$$

The optimal power allocation ratio k^* can be obtained by numerically solving (90), (91), and (92).

Optimal Power Allocation in Correlated Fading

The outage expressions of LF, DF, and ADF in correlated fading can be written as (93), (94), and (95), respectively. The optimization problem in correlated fading can also be formulated by (88) for LF, DF, and ADF relaying.

Proposition 7. *Outage probability expressions of LF, DF, and ADF relaying, respectively, in* (93)*,* (94)*, and* (95)*, are convex with respect to $k \in (0, 1)$.*

$$
\begin{aligned}
P_{\text{out}}^{\text{ADF, Cor}} = &\left(1 - \frac{1}{P_T k G_{\text{SD}}}\right)\left(\frac{\ln(4)-1}{P_T k G_{\text{SD}} P_T (1-k) G_{\text{RD}} (1-\rho_s^2)} + \frac{2\ln(2)-3}{2 P_T k G_{\text{SD}}^2 P_T (1-k) G_{\text{RD}} (1-\rho_s^2)}\right. \\
&\left. + \frac{\ln(4)-\frac{3}{2}}{P_T k G_{\text{SD}} P_T (1-k) G_{\text{RD}}^2 (1-\rho_s^2)}\right) + \frac{\ln(4)-1}{P_T k G_{\text{SD}} P_T (1-k) G_{\text{RD}} P_T k G_{\text{SD}} (1-\rho_t^2)} \\
&+ \frac{4\ln(2)-3}{2 P_T^2 k^2 G_{\text{SD}}^2 P_T (1-k) G_{\text{RD}} P_T k G_{\text{SD}} (1-\rho_t^2)} + \frac{\ln(4)-\frac{3}{2}}{P_T k G_{\text{SD}} P_T^2 (1-k)^2 G_{\text{RD}}^2 P_T k G_{\text{SD}} (1-\rho_t^2)}.
\end{aligned}
\tag{95}
$$

Proof. The convexity of (93), (94), and (95) can be proven by taking second-order partial derivative of $P_{\text{out}}^{\text{LF, Cor}}$, $P_{\text{out}}^{\text{DF, Cor}}$, and $P_{\text{out}}^{\text{ADF, Cor}}$ in (93), (94), and (95) with respect to k, and showing that the derivative results are positive in the range $k \in (0,1)$[10]. □

By taking the first-order derivative of $P_{\text{out}}^{\text{LF, Cor}}$, $P_{\text{out}}^{\text{DF, Cor}}$, and $P_{\text{out}}^{\text{ADF, Cor}}$, respectively, in (93), (94), and (95) with respect to k and setting the derivative results to zero, $\frac{\partial P_{\text{out}}^{\text{LF, Cor}}}{\partial k} = 0$, $\frac{\partial P_{\text{out}}^{\text{DF, Cor}}}{\partial k} = 0$, and $\frac{\partial P_{\text{out}}^{\text{ADF, Cor}}}{\partial k} = 0$. Similar to the independent fading case, the optimal power allocation ratio k^* of LF, DF, and ADF relaying over correlated fading channels can be numerically obtained.

Fig. 20 presents the impact of the power allocation ratio to S and R on outage probability. We normalize the geometric gain of the S-D link to the unity under the assumption that the relay is located at the midpoint of the S-D link. The total transmit power is set at 2 (dB). It can be observed from Fig. 20 that, the optimal power ratio k^* of LF is larger than that of ADF, and smaller than that of DF, which indicates that LF needs more power for the source than ADF, and needs less power than DF. This is because in DF relaying, the source needs more power to keep the quality of the S-D links for reducing the error probability. With ADF relaying, even though error occurs in the S-R link due to the deep fade of the channel, the source still can retransmit the information sequence to the destination, yielding the time diversity gain. It is also found that when more transmit power is allocated to the source (larger k), the outage curves of DF, LF, and ADF relaying with the same spatial correlation ρ_s asymptotically merge. This indicates that with more transmit power for S, the probability of error occurring in the S-R link reduces, resulting in that R always forwards the received information sequence. Therefore, the outage curves with DF, LF, and ADF become almost the same. Moreover, the larger the spatial correlation ρ_s, the higher the outage

[10]The details of the proof are straightforward but lengthy, and therefore are omitted here for brevity.

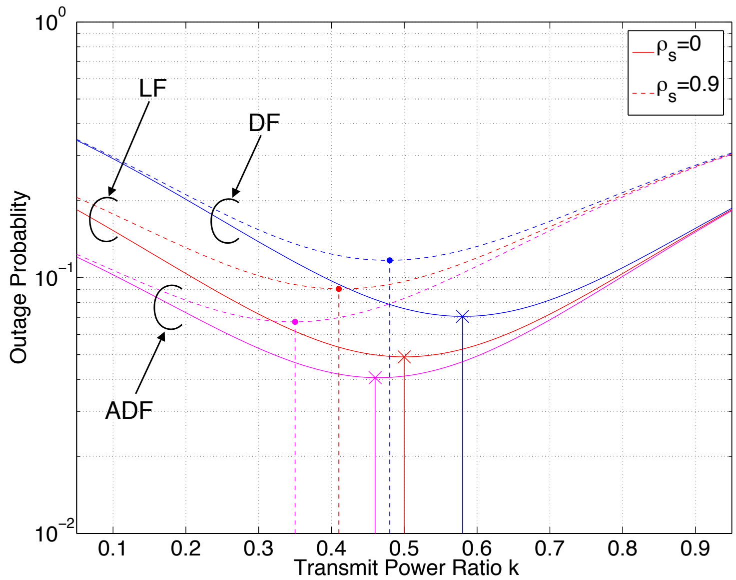

Fig. 20. Outage probabilities versus power allocations for LF, DF, and, ADF relying over independent and correlated channels, where $P_T = 2$ (dB) and $\rho_t = 0$.

probability with the LF, DF, and ADF relaying schemes, however, more transmit power needs to be allocated to R (smaller k) for achieving the lower outage probabilities. This is because correlations reduce the diversity gain provided by the R-D link and R needs more transmit power to maintain the quality of the R-D link. In practice, to keep a certain outage, one can allocate larger range of the transmit power with LF than DF under a total power constraint.

Fig. 21 shows the impact of ρ_t and ρ_s on optimal power allocation ratio k^* for LF, DF, ADF relaying, where the total transmit power for S and R is set at $P_T = 2$ (dB). It can be seen from Fig. 21 that the larger the spatial correlation ρ_s, the larger the optimal k^* value with DF, LF, and ADF. Since the spatial correlation reduce the diversity gain provided by the R-D link, more power needs to be allocated to the source to increase the quality of the S-D transmission. It is also found that, as the temporal correlation ρ_t in ADF increases, the value of optimal k^* decreases, in order to achieve the smallest outage probability. This is because the higher the temporal correlation, the lower the diversity gain provided by the S-D retransmission, which results in that more power should be allocated to the relay to increase the quality of the R-D transmission.

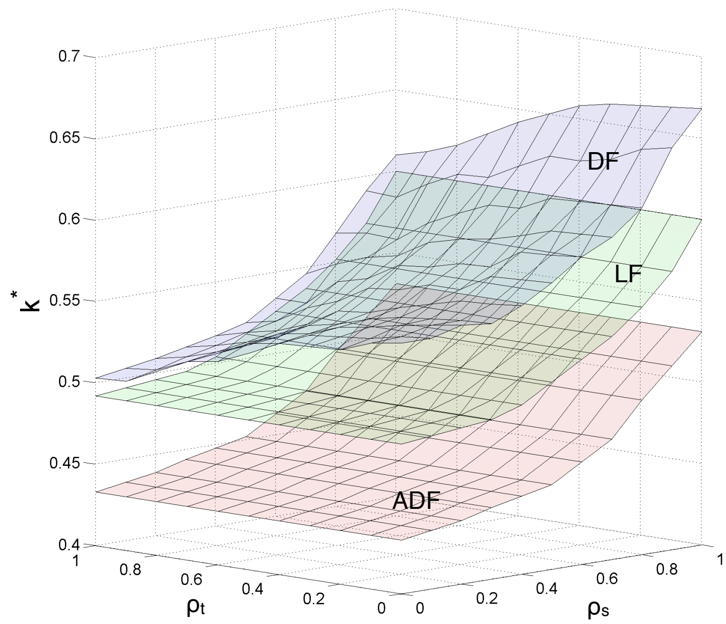

Fig. 21. Impact of temporal correlation ρ_t and spatial correlation ρ_s on optimal power allocation ratio k^*, where $P_T = 2$ (dB).

2.3 Impact Analysis of Line-of-Sight Components in Lossy-Forward Relaying over Fading Channels Having Different Statistical Properties

2.3.1 Channel Model

The S-D link is assumed to experience frequency non-selective block Rayleigh fading which only has NLOS components. Both the S-R and R-D links are assumed to suffer from block fading variation having LOS component, following either Rician or Nakagami-m distribution. The pdf of the instantaneous SNR γ_{ij} $(ij \in (\mathrm{SR}, \mathrm{RD}))$ following Rician distribution is

$$p^{Rici}(\gamma_{ij}) = \left(\frac{(1+K_{ij})\, e^{-K_{ij}}}{\overline{\gamma}_{ij}}\right) \exp\left(-\frac{(1+K_{ij})\gamma_{ij}}{\overline{\gamma}_{ij}}\right) I_0\left(2\sqrt{\frac{K_{ij}\,(1+K_{ij})\,\gamma_{ij}}{\overline{\gamma}_{ij}}}\right), \quad (96)$$

where K_{ij} denotes the ratio of the LOS component power-to-NLOS components average power of the corresponding link.

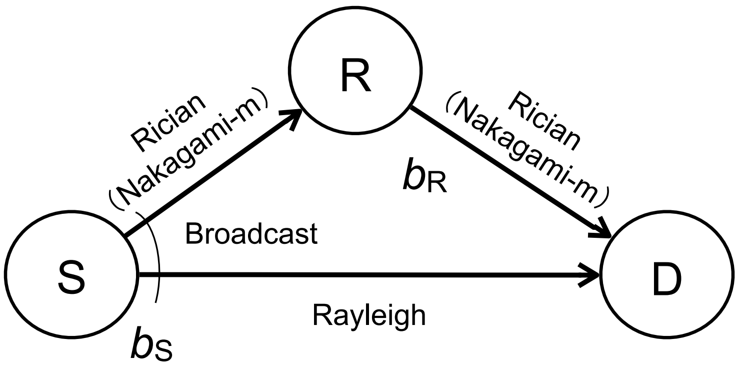

Fig. 22. Single relay LF relaying network. The S-R and R-D links experiences either Rician or Nakagami-m fading.

The Nakagami-m fading with factor m is approximated by Rician fading with factor K [20], [81], as

$$m = \frac{(K+1)^2}{2K+1}. \quad (97)$$

2.3.2 Outage Probability Derivation

Solving (9), (10) and (11) in section 2.1.2 with the pdf (96), given above, of the instantaneous SNR, the outage probability of LF relaying with the fading variations of the S-R and R-D links following Rician distribution can be expressed as

$$\begin{aligned}
P_{\mathrm{A}}^{Rici} =& \int_{\gamma_{\mathrm{SR}}=\Theta^{-1}(1)}^{\Theta^{-1}(\infty)} \int_{\gamma_{\mathrm{SD}}=\Theta^{-1}(0)}^{\Theta^{-1}(1)} \int_{\gamma_{\mathrm{RD}}=\Theta^{-1}(0)}^{\Theta^{-1}(1-\Theta(\gamma_{\mathrm{SD}}))} p^{Rici}(\gamma_{\mathrm{SR}}) p(\gamma_{\mathrm{SD}}) p^{Rici}(\gamma_{\mathrm{RD}}) d\gamma_{\mathrm{SR}} d\gamma_{\mathrm{SD}} d\gamma_{\mathrm{RD}} \\
=& \frac{1}{\overline{\gamma}_{\mathrm{SD}}} Q_1\left(\sqrt{2K_{\mathrm{SR}}}, \sqrt{\frac{2(1+K_{\mathrm{SR}})}{\overline{\gamma}_{\mathrm{SR}}}}\right) \int_{\gamma_{\mathrm{SD}}=\Theta^{-1}(0)}^{\Theta^{-1}(1)} \exp\left(-\frac{\gamma_{\mathrm{SD}}}{\overline{\gamma}_{\mathrm{SD}}}\right) \\
& \cdot \left[1 - Q_1\left(\sqrt{2K_{\mathrm{RD}}}, \sqrt{2\left(1+K_{\mathrm{RD}}\right) \frac{\Theta^{-1}(1-\Theta(\gamma_{\mathrm{SD}}))}{\overline{\gamma}_{\mathrm{RD}}}}\right)\right] d\gamma_{\mathrm{SD}}, \qquad (98)
\end{aligned}$$

$$\begin{aligned}
P_{\mathrm{B}}^{Rici} =& \int_{\gamma_{\mathrm{SR}}=\Theta^{-1}(0)}^{\Theta^{-1}(1)} \int_{\gamma_{\mathrm{SD}}=\Theta^{-1}(0)}^{\Theta^{-1}(1-\Theta(\gamma_{\mathrm{SR}}))} \int_{\gamma_{\mathrm{RD}}=\Theta^{-1}(0)}^{\Theta^{-1}(\infty)} p^{Rici}(\gamma_{\mathrm{SR}}) p(\gamma_{\mathrm{SD}}) p^{Rici}(\gamma_{\mathrm{RD}}) d\gamma_{\mathrm{SR}} d\gamma_{\mathrm{SD}} d\gamma_{\mathrm{RD}} \\
=& \int_{\gamma_{\mathrm{SR}}=\Theta^{-1}(0)}^{\Theta^{-1}(1)} \exp\left(-\frac{(1+K_{\mathrm{SR}})\gamma_{\mathrm{SR}}}{\overline{\gamma}_{\mathrm{SR}}}\right) \left(\frac{(1+K_{\mathrm{SR}})\, e^{-K_{\mathrm{SR}}}}{\overline{\gamma}_{\mathrm{SR}}}\right) \\
& \cdot I_0\left(2\sqrt{\frac{K_{\mathrm{SR}}\left(1+K_{\mathrm{SR}}\right)\gamma_{\mathrm{SR}}}{\overline{\gamma}_{\mathrm{SR}}}}\right) \left[1 - \exp\left(-\frac{\Theta^{-1}(1-\Theta(\gamma_{\mathrm{SR}}))}{\overline{\gamma}_{\mathrm{SD}}}\right)\right] d\gamma_{\mathrm{SR}} \qquad (99)
\end{aligned}$$

and

$$\begin{aligned}
P_{\mathrm{C}}^{Rici} =& \int_{\gamma_{\mathrm{SR}}=\Theta^{-1}(0)}^{\Theta^{-1}(1)} \int_{\gamma_{\mathrm{SD}}=\Theta^{-1}(1-\Theta(\gamma_{\mathrm{SR}}))}^{\Theta^{-1}(1)} \int_{\gamma_{\mathrm{RD}}=\Theta^{-1}(0)}^{\Theta^{-1}[\xi(\gamma_{\mathrm{SD}},\gamma_{\mathrm{SR}})]} p^{Rici}(\gamma_{\mathrm{SR}}) p(\gamma_{\mathrm{SD}}) p^{Rici}(\gamma_{\mathrm{RD}}) \\
& d\gamma_{\mathrm{SR}} d\gamma_{\mathrm{SD}} d\gamma_{\mathrm{RD}} \\
=& \frac{1}{\overline{\gamma}_{\mathrm{SD}}} \left(\frac{(1+K_{\mathrm{SR}})\, e^{-K_{\mathrm{SR}}}}{\overline{\gamma}_{\mathrm{SR}}}\right) \int_{\gamma_{\mathrm{SD}}=\Theta^{-1}(1-\Theta(\gamma_{\mathrm{SR}}))}^{\Theta^{-1}(1)} \int_{\gamma_{\mathrm{SR}}=\Theta^{-1}(0)}^{\Theta^{-1}(1)} \exp\left(\frac{-\gamma_{\mathrm{SD}}}{\overline{\gamma}_{\mathrm{SD}}}\right) \\
& \cdot \exp\left(-\frac{(1+K_{SR})\gamma_{\mathrm{SR}}}{\overline{\gamma}_{\mathrm{SR}}}\right) I_0\left(2\sqrt{\frac{K_{\mathrm{SR}}\left(1+K_{\mathrm{SR}}\right)\gamma_{\mathrm{SR}}}{\overline{\gamma}_{\mathrm{SR}}}}\right) \\
& \cdot \left[1 - Q_1\left(\sqrt{2K_{\mathrm{RD}}}, \sqrt{2\left(1+K_{\mathrm{RD}}\right) \frac{\Theta^{-1}[\xi(\gamma_{\mathrm{SD}},\gamma_{\mathrm{SR}})]}{\overline{\gamma}_{\mathrm{RD}}}}\right)\right] d\gamma_{\mathrm{SD}} d\gamma_{\mathrm{SR}}, \qquad (100)
\end{aligned}$$

where $Q_1(\cdot,\cdot)$ is the Marcum Q function.

The outage probability of LF relaying with the S-R and R-D links suffering from Nakagami-m fading can be derived with the pdf of the instantaneous SNR following Nakagami-m distribution, given in (5) in section 2.1.1, as

$$\begin{aligned} P_{\mathrm{A}}^{Naka} = & \frac{1}{\overline{\gamma}_{\mathrm{SD}}} \left(1 - \left[\frac{\gamma\left(m_{\mathrm{SR}}, m_{\mathrm{SR}} \frac{1}{\overline{\gamma}_{\mathrm{SR}}} \right)}{\Gamma(m_{\mathrm{SR}})} \right] \right) \int_{\gamma_{\mathrm{SD}}=\Theta^{-1}(0)}^{\Theta^{-1}(1)} \exp\left(-\frac{\gamma_{\mathrm{SD}}}{\overline{\gamma}_{\mathrm{SD}}} \right) \\ & \cdot \left[\frac{\gamma\left(m_{\mathrm{RD}}, m_{\mathrm{RD}} \frac{\Theta^{-1}(1-\Theta(\gamma_{\mathrm{SD}}))}{\overline{\gamma}_{\mathrm{RD}}} \right)}{\Gamma(m_{\mathrm{RD}})} \right] d\gamma_{\mathrm{SD}}, \end{aligned} \tag{101}$$

$$\begin{aligned} P_{\mathrm{B}}^{Naka} = & \int_{\gamma_{\mathrm{SR}}=\Theta^{-1}(0)}^{\Theta^{-1}(1)} \frac{m_{\mathrm{SR}}^{m_{\mathrm{SR}}} (\gamma_{\mathrm{SR}})^{m_{\mathrm{SR}}-1}}{(\overline{\gamma}_{\mathrm{SR}})^{m_{\mathrm{SR}}} \Gamma(m_{\mathrm{SR}})} \exp\left(-\frac{m_{\mathrm{SR}} \gamma_{\mathrm{SR}}}{\overline{\gamma}_{\mathrm{SR}}} \right) \\ & \cdot \left[1 - \exp\left(-\frac{\Theta^{-1}(1-\Theta(\gamma_{\mathrm{SR}}))}{\overline{\gamma}_{\mathrm{SD}}} \right) \right] d\gamma_{\mathrm{SR}}, \end{aligned} \tag{102}$$

and

$$\begin{aligned} P_{\mathrm{C}}^{Naka} = & \frac{1}{\overline{\gamma}_{\mathrm{SD}}} \int_{\gamma_{\mathrm{SR}}=\Theta^{-1}(0)}^{\Theta^{-1}(1)} \int_{\gamma_{\mathrm{SD}}=\Theta^{-1}(1-\Theta(\gamma_{\mathrm{SR}}))}^{\Theta^{-1}(1)} \exp\left(\frac{-\gamma_{\mathrm{SD}}}{\overline{\gamma}_{\mathrm{SD}}} \right) \frac{m_{\mathrm{SR}}^{m_{\mathrm{SR}}} (\gamma_{\mathrm{SR}})^{m_{\mathrm{SR}}-1}}{(\overline{\gamma}_{\mathrm{SR}})^{m_{\mathrm{SR}}} \Gamma(m_{\mathrm{SR}})} \\ & \cdot \exp\left(-\frac{m_{\mathrm{SR}} \gamma_{\mathrm{SR}}}{\overline{\gamma}_{\mathrm{SR}}} \right) \left[\frac{\gamma\left(m_{\mathrm{RD}}, m_{\mathrm{RD}} \frac{\xi(\gamma_{\mathrm{SD}}, \gamma_{\mathrm{SR}})}{\overline{\gamma}_{\mathrm{RD}}} \right)}{\Gamma(m_{\mathrm{RD}})} \right] d\gamma_{\mathrm{SD}} d\gamma_{\mathrm{SR}}, \end{aligned} \tag{103}$$

where $\gamma(\cdot,\cdot)$ is the lower incomplete gamma function. Note that since the factor K of Rician fading is connected to the factor m of Nakagami-m fading by (97), the impact of the difference in the statistical characteristics with a fair parameter setting between Rician and Nakagami-m fading on the outage performance can be evaluated by adjusting the factor K in Rician fading and the factor m in Nakagami-m fading.

2.3.3 Kullback-Leibler divergence and Jensen-Shannon divergence

The Kullback-Leibler divergence (KLD) is used to measure the difference between probability distributions. Based on Nakagami-m pdf, (5) in section 2.1.1, and Rician pdf, (96) in section 2.3.1, the KLD of Rician relative to Nakagami-m distribution is given as [82]

$$d_{\mathrm{KL}}(p^{\mathrm{Rici}}(\gamma)\,||p^{\mathrm{Naka}}(\gamma)) = \int_{\gamma} p^{\mathrm{Rici}}(\gamma) \ln \frac{p^{\mathrm{Rici}}(\gamma)}{p^{\mathrm{Naka}}(\gamma)} d\gamma. \tag{104}$$

The KLD of Nakagami-m relative to Rician distribution is defined as

$$d_{\mathrm{KL}}(p^{\mathrm{Naka}}(\gamma)\,||p^{\mathrm{Rici}}(\gamma)) = \int_{\gamma} p^{\mathrm{Naka}}(\gamma) \ln \frac{p^{\mathrm{Naka}}(\gamma)}{p^{\mathrm{Rici}}(\gamma)} d\gamma. \tag{105}$$

Obviously, since (104) and (105) have different value, and hence KLD does not satisfy the definition of "distance". Nevertheless, it is used to measure the information distance between Rician and Nakagami-m distributions [82]. When $K = 0$ and $m = 1$, $d_{\mathrm{KL}}(p^{\mathrm{Rici}}(\gamma)\,||p^{\mathrm{Naka}}(\gamma)) = 0$ and $d_{\mathrm{KL}}(p^{\mathrm{Naka}}(\gamma)\,||p^{\mathrm{Rici}}(\gamma)) = 0$, which indicates that the Rician and Nakagami-m distributions converge to the identical Rayleigh distribution.

Jensen-Shannon divergence (JSD) is another method of measuring how similar/different two probability distributions are. The JSD is defined by

$$\begin{aligned} d_{\mathrm{JD}}(p^{\mathrm{Rici}}(\gamma)\,||p^{\mathrm{Naka}}(\gamma)) =& \frac{1}{2}\left\{ d_{\mathrm{KL}}\left[p^{\mathrm{Rici}}(\gamma)\,||\frac{1}{2}\left(p^{\mathrm{Rici}}(\gamma) + p^{\mathrm{Naka}}(\gamma)\right)\right]\right\} \\ &+ \frac{1}{2}\left\{ d_{\mathrm{KL}}\left[p^{\mathrm{Naka}}(\gamma)\,||\frac{1}{2}\left(p^{\mathrm{Naka}}(\gamma) + p^{\mathrm{Rici}}(\gamma)\right)\right]\right\}. \end{aligned} \tag{106}$$

Fig. 23 shows the KLD and JSD curves, $d_{\mathrm{KL}}\left(p^{\mathrm{Rici}}(\gamma)\,||p^{\mathrm{Naka}}(\gamma)\right)$, $d_{\mathrm{KL}}(p^{\mathrm{Naka}}(\gamma)\,||p^{\mathrm{Rici}}(\gamma))$ and $d_{\mathrm{JD}}\left(p^{\mathrm{Rici}}(\gamma)\,||p^{\mathrm{Naka}}(\gamma)\right)$, all as a function of the factor K (or its corresponding m value by (97)). We can easily find that $d_{\mathrm{KL}}\left(p^{\mathrm{Rici}}(\gamma)\,||p^{\mathrm{Naka}}(\gamma)\right)$ and $d_{\mathrm{KL}}(p^{\mathrm{Naka}}(\gamma)\,||p^{\mathrm{Rici}}(\gamma))$ are not identical to each other, because of the asymmetricity of KLD. We can also see from Fig. 23 that the values of KLD and JSD first increase and then gradually decrease as K (and hence m) becomes large. This observation is used to verify the outage difference of LF relaying over Rician and Nakagami-m fading channels in the next subsection.

2.3.4 Numerical Results

The theoretical outage probabilities of LF relaying with the S-R and R-D links suffering from Rician fading, which is denoted as $P_{\mathrm{out}}^{\mathrm{Rici}}$, and that suffering from Nakagami-m fading, which is denoted as $P_{\mathrm{out}}^{\mathrm{Naka}}$, are presented in Fig. 24. The relay is located on a line parallel to the line connecting S and D with the distant between the relay and the line connecting S and D is set at $\frac{1}{2}$ of the length of the S-D link. The value of K_{SR} and

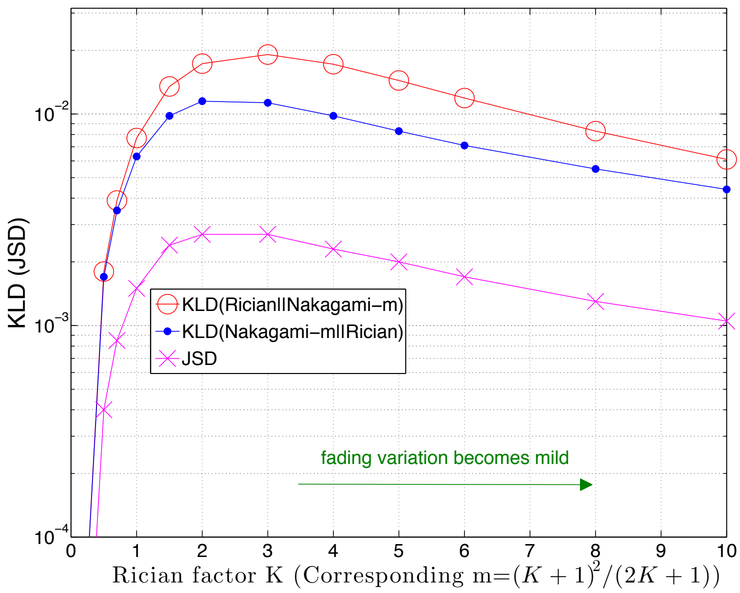

Fig. 23. KLD and JSD between Rician and Nakagami-m distributions.

m_{SR} is set at $K_{\mathrm{SR}} = 0$ and $m_{\mathrm{SR}} = 1$, respectively, which indicates that the S-R link also suffering from Rayleigh fading. It is found from Fig. 24 that the $P_{\mathrm{out}}^{\mathrm{Rici}}$ and $P_{\mathrm{out}}^{\mathrm{Naka}}$ curves show the same tendency: the larger the K_{RD} (or m_{RD}) value is, the smaller the outage probability, for a given average SNR value. This indicates that as the channel variation of the R-D link becomes mild, low outage probability can be achieved. However, the decay in outage curves keeps the same when K_{RD} (or m_{RD}) value increases. This is because that, even the LOS component power in the R-D link increases, the equivalent diversity order (decay of the outage curve) of the LF relying system does not change. The equivalent diversity order of the system is determined by either the S-R link or the R-D link which achieves small equivalent diversity order.

Fig. 25 shows the theoretical outage probabilities $P_{\mathrm{out}}^{\mathrm{Rici}}$ and $P_{\mathrm{out}}^{\mathrm{Naka}}$ versus the average SNR of the S-D link, where $K_{\mathrm{SR}} = K_{\mathrm{RD}}$ ($m_{\mathrm{SR}} = m_{\mathrm{RD}}$). It is found that the outage curves can achieve sharper decay than that with 2nd order diversity, when the values of K (m) of both the S-R and R-D links increase simultaneously. This is because the increased LOS component power in the S-R and R-D links increase the equivalent diversity order of the LF relaying system.

From Fig. 25 we also found that, when $K_{\mathrm{SR}} = K_{\mathrm{RD}} = 0$ ($m_{\mathrm{SR}} = m_{\mathrm{RD}} = 1$), $P_{\mathrm{out}}^{\mathrm{Rici}}$ and $P_{\mathrm{out}}^{\mathrm{Naka}}$ show the same outage probability. This is because obviously, the S-R and

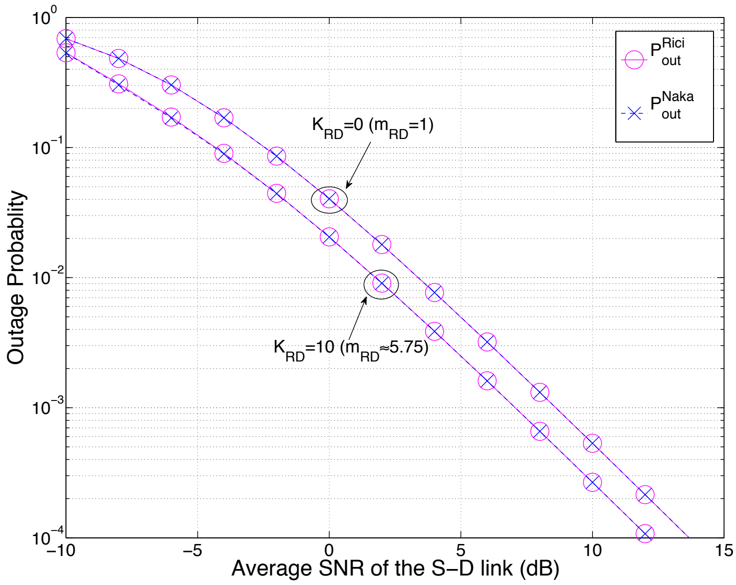

Fig. 24. Comparison of the outage probability of LF relaying and in Rician and Nakagami-m fading. $K_{SR} = 0$ **(**$m_{SR} = 1$**).**

R-D links reduce to Rayleigh fading. However, when the K_{SR} and K_{RD} (m_{RD} and m_{RD}) value increase, the outage curves in Rician and Nakagami-m fading exhibit different outage performances. Again, the difference diminishes when K_{SR} and K_{RD} (m_{SR} and m_{RD}) become large, which is consistent to the KLD and JSD analyses provided in the previous subsection. This observation indicates that even with a specific parameter setting yielding the same LOS ratio, Rician is not equivalent to Nakagami-m model for representing the shape of the entire portion of distribution.

2.4 Summary

In this chapter, the outage probability of three-node one-way relaying has been analyzed over fading channels on each link having different statistical properties.

First of all, for LF relaying over Nakagami-m fading channels, the exact outage probability expressions for arbitrary values of the shape factor m were derived in (20), (21), and (22) in section [2.1.2 Outage Probability Analysis]-[Outage Event of LF relaying]. The equivalent diversity order and coding gain of LF relaying were defined and derived in (33) and (34) in section [2.1.3 Equivalent Diversity Order and Coding

Gain] through yet accurate enough approximation of the outage expressions (23), (24), and (25). It is found from (33) as well as from Fig. 9 that, with the increased LOS component power, the lower outage probability can be achieved. However, the outage curve decay is dominated by the less reliable channel of either the S-R or R-D link. It can be concluded from the numerical results provided in section [2.1.2 Outage Probability Analysis] and from Fig. 7 that LF relaying achieve better performance than conventional DF relaying. Since the relay in LF always forwards the decoder output to the destination, where re-interleaving performed for the decoded sequence, the whole system can be regarded as a distributed turbo code. It is also found from Figs.10, 11, and 12 that LF relaying not only reduces the outage probability, but also expands the search area for a relay (helper) while keeping the outage probability the same as that with DF or even lower.

Then, in the outage analysis of LF, DF, and ADF relaying over Rayleigh fading channels, the diversity order and coding gain was derived in section [2.2.3 Outage Analysis in Independent Fading], with yet accurate approximations (45), (46), and (47), in independent fading. It is proven by Theorems 2 and 3 that the coding gain of LF is larger than DF but smaller ADF since ADF utilize the error-free feedback from the relay which results in the situation that errors are not included in the encoders of both the source and the relay. The diversity orders for LF, DF, and ADF relaying were also obtained in (68), (69), and (70) in correlated fading in section [2.2.4 Outage Analysis in Correlated Fading]-[Diversity Order]. It is found from (68), (69), and (70) that the full diversity order can be achieved by LF, DF, and ADF relaying as long as the channels are not spatially or temporary fully correlated. The observations from numerical results provided in sections [2.2.5 Optimal Relay Locations for Minimizing the Outage Probability] and [2.2.6 Optimal Power Allocation for Minimizing the Outage Probability] suggest that compared to the independent fading case, the relay should be located close to the destination, or more transmit power should be allocated to the relay to reduce the diversity gain loss caused by the fading correlation, and hence can achieve the lowest outage probabilities, in correlated fading.

Finally, we analyzed the impact of different statistical properties of LOS component, i.e., Rician and Nakagami-m distributions, on outage performance. It is found from section [2.3.3 Kullback-Leibler divergence and Jensen-Shannon divergence] that the KLD and JSD between Nakagami-m and Rician distributions does not change monotonically as K or m becomes large. Instead, it first increases and then decreases. The KLD and JSD analyses, and the numerical results in Figs. 24 and 25 indicate

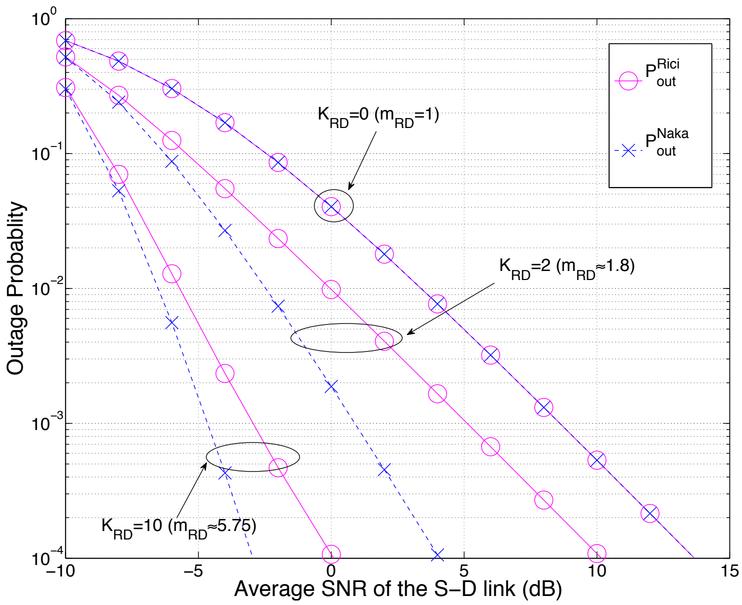

Fig. 25. Comparison of the outage probability of LF relaying and in Rician and Nakagami-m fading. $K_{SR} = K_{RD}$, $m_{SR} = m_{RD}$.

that even with a specific parameter setting yielding the same LOS ratio, Rician is not equivalent to Nakagami-m model for representing the shape of the entire portion of the distribution.

3 Performance Analysis for Two-Way Lossy-Forward Relaying with Random Rician K-factor

In this chapter, we derive the outage probability upper bound for a two-way LF relay system over Rician fading channels with random K-factor. The K-factor is assumed to follow empirical distributions, logistic and normal, derived from measurement data. It is found that two-way relaying with LF is superior to that with DF in terms of outage performance, regardless of either logistic or normal distribution is used to represent the variation of K-factor.

3.1 System Model

The system model is shown in Fig. 26, where two sources, A and B, exchange their i.i.d. binary information with the help of a relay R. All nodes are equipped with a single antenna. For achieving high spectral efficiency, we consider non-orthogonal two-way relaying in this Chapter. The entire transmission cycle is divided into two time slots, hence compared to three time slots systems in the orthogonal two-way relaying, $\frac{3}{2}$ times the spectrum efficiency gain is expected. In the first time slot, A and B encode their own information sequence $\mathrm{u_A}$ and $\mathrm{u_B}$ separately, and send them to R simultaneously over a MAC. $\mathrm{u_A}$ and $\mathrm{u_B}$ are also broadcast to B and A, respectively. Since the relay is not interested in the original information sequence sent from the sources, in the second time slot, the relay first decodes the information from A and B and then conducts the exclusive-or (XOR) based on the estimated binary information sequences $\hat{\mathrm{u}}_\mathrm{A}$ and $\hat{\mathrm{u}}_\mathrm{B}$. Then, regardless of whether the estimates are correct or not, the relay re-encodes, modulates the XOR-ed version of the estimates, and broadcasts the resulting sequence to A and B over a broadcast channel.[11]

The channel coefficient $h_{i,j}$ between two nodes, i and j, follows the Rician distribution with the K-factor $K_{i,j}$ $(i,j \in (\mathrm{A,B,R}), i \neq j)$. In this section, we set

[11] The self-interference due to the full duplex setting in sources A and B may not be perfectly cancelated in practical, however, in our theoretical analysis, we ignore the impact of self-interference and assumed that full-duplex wireless communication is feasible.

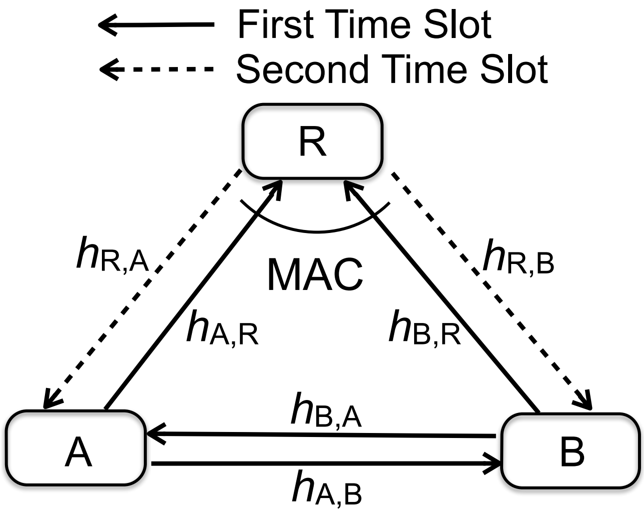

Fig. 26. Two-way relaying transmission.

$K_{\mathrm{A,B}} = K_{\mathrm{B,A}} = 0$[12]. The joint pdf of the instantaneous SNR $\gamma_{i,j}$ and the random K-factor with the Rician distribution is denoted as $p_{\gamma_{i,j}}(\gamma_{i,j}, K_{i,j}) = p_{\gamma_{i,j}}(\gamma_{i,j}|K_{i,j})\, p_{K_{i,j}}(K_{i,j})$. The channel coefficient $h_{i,j}$ and K-factor vary independently block-by-block and stay the same over one block duration due to the block fading assumption.

After the integration over the instantaneous SNR, the cumulative distribution function (cdf) of instantaneous SNR with Rician distribution is obtained and represented by $F_{\gamma_{i,j}}(\gamma_{i,j}, K_{i,j})$[13]. The geometric gains between every two nodes are assumed to be the same.

The distribution of K-factor is represented by either logistic distribution $p_{\log}(K) = \frac{\exp\left(-\frac{K-\mu}{\sigma}\right)}{\sigma\left[1+\exp\left(-\frac{K-\mu}{\sigma}\right)\right]^2}$ or normal distribution $p_{\mathrm{nor}}(K) = \frac{1}{\sigma\sqrt{2\pi}}\exp\left(\frac{-(K-\mu)^2}{2\sigma^2}\right)$, which are found to be well-fit models in [52]; μ and σ^2 denote mean and variance of the distributions, respectively.

[12]In cooperative networks, a reasonable assumption is that since the A-B (B-A) channel suffers from severe fading, B (A) needs the help of a relay via the R-B (R-A) channel suffering from moderate fading. Hence, it is reasonable that we set the K-factor of the A-B (B-A) channel at $K_{\mathrm{A,B}} = K_{\mathrm{B,A}} = 0$, which corresponds to Rayleigh fading.

[13]Refer to [21, Section 2.3.2] for the pdf and cdf expressions of Rician fading.

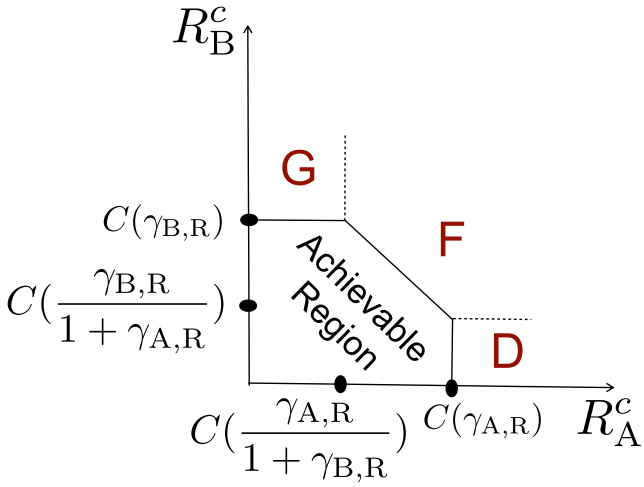

Fig. 27. Rate region for A-R and B-R transmissions.

3.2 Outage Probability

Two-way LF relaying fails in achieving reliable communication if at least one of destination nodes (A or B) is in outage. The outage event $\mathscr{E}_{\mathrm{O}}$ of the two-way LF relaying system is, therefore, defined as $\mathscr{E}_{\mathrm{O}} = \mathscr{E}_{\mathrm{OA}} \bigcup \mathscr{E}_{\mathrm{OB}}$, where $\mathscr{E}_{\mathrm{OA}}$ and $\mathscr{E}_{\mathrm{OB}}$ represents the outage event for A and B, respectively. Without loss of generality, we only focus on the derivation of $\mathscr{E}_{\mathrm{OA}}$, since, even though parameters that determine $p_{\gamma_{i,j}}(\gamma_{i,j}, K_{i,j})$ may be different for A and B, the mathematical outage expressions for A and B are the same.

First of all, we calculate the outage probability of $\mathrm{u_A}$ and $\mathrm{u_B}$ occurring in the first MAC time slot. It is obvious that for the first time slot transmission, the achievable region for $\{$A, B$\}$-to-R transmission is determined by the MAC rate region as shown in Fig. 27. The rate region outside the MAC achievable region can be divided into three sub-regions, D, G, and F, with P_{D}, P_{G}, and P_{F} denoting the probability that the rate pair $\left(R_{\mathrm{A}}^{c}, R_{\mathrm{B}}^{c}\right)$ falls into D, G, and F in Fig. 27, respectively. R_{A}^{c} and R_{B}^{c} denote the spectrum efficiency of A-R and B-R channel, respectively, including the channel coding rate and the modulation multiplicity. When the rate pair $(R_{\mathrm{A}}^{c}, R_{\mathrm{B}}^{c})$, falls in the achievable region, two sources can be recovered with arbitrarily small error probability at the relay. Neither of the information sequence from the two sources can be successfully recovered when the rate pair falls in the region F. When $(R_{\mathrm{A}}^{c}, R_{\mathrm{B}}^{c})$ falls into the regions D or G, only one of the information sequence can be perfectly recovered while the other probabilistically fails.

The probabilities that the rate pair (R^c_{A},R^c_{B}) falls into regions D, G, and F can be expressed as [43, 83]

$$P_{\mathrm{D}} =\Pr[R^c_{\mathrm{A}} > C(\gamma_{\mathrm{A,R}}), R^c_{\mathrm{B}} \leq C(\frac{\gamma_{\mathrm{B,R}}}{1+\gamma_{\mathrm{A,R}}})], \tag{107}$$

$$P_{\mathrm{G}} =\Pr[R^c_{B} > C(\gamma_{B,R}), R^c_{A} \leq C(\frac{\gamma_{A,R}}{1+\gamma_{B,R}})], \tag{108}$$

$$P_{\mathrm{F}} =\Pr[R^c_{\mathrm{A}} > C(\frac{\gamma_{\mathrm{A,R}}}{1+\gamma_{\mathrm{B,R}}}), R^c_{\mathrm{B}} > C(\frac{\gamma_{\mathrm{B,R}}}{1+\gamma_{\mathrm{A,R}}}), R^c_{\mathrm{A}}+R^c_{\mathrm{B}} > \log_2(1+\gamma_{\mathrm{A,R}}+\gamma_{\mathrm{B,R}})], \tag{109}$$

respectively.

With the random Rician K-factor, P_{D} and P_{F} are expressed as a set of integrals with respect to the pdfs of the instantaneous SNRs and K, as,

$$\begin{aligned}
P_D =& \int_{K_{\mathrm{A,R}}}\int_{K_{\mathrm{B,R}}}\int_{\gamma_{\mathrm{A,R}}=0}^{2^{R^c_{\mathrm{A}}}-1}\int_{\gamma_{\mathrm{B,R}}=\left(2^{2R^c_{\mathrm{B}}}-1\right)\left(1+\gamma_{\mathrm{A,R}}\right)}^{\infty} p_{\gamma_{\mathrm{A,R}}}(\gamma_{\mathrm{A,R}}|K_{\mathrm{A,R}})\\
&\cdot p_{\gamma_{\mathrm{B,R}}}(\gamma_{\mathrm{B,R}}|K_{\mathrm{B,R}}) p_{\log}(K_{\mathrm{A,R}}) p_{\log}(K_{\mathrm{B,R}}) d\gamma_{\mathrm{A,R}} d\gamma_{\mathrm{B,R}} d_{K_{\mathrm{A,R}}} d_{K_{\mathrm{B,R}}}\\
=& \int_{K_{\mathrm{A,R}}}\int_{K_{\mathrm{B,R}}}\int_{\gamma_{\mathrm{A,R}}=0}^{2^{R^c_{\mathrm{A}}}-1} p_{\gamma_{\mathrm{A,R}}}(\gamma_{\mathrm{A,R}}|K_{\mathrm{A,R}}) p_{\log}(K_{\mathrm{A,R}}) p_{\log}(K_{\mathrm{B,R}})\\
&\cdot \left(1-F_{\gamma_{\mathrm{B,R}}}\left[(2^{2R^c_{\mathrm{B}}}-1)(1+\gamma_{\mathrm{A,R}})|K_{\mathrm{B,R}}\right]\right) d\gamma_{\mathrm{A,R}} d_{K_{\mathrm{A,R}}} d_{K_{\mathrm{B,R}}}
\end{aligned} \tag{110}$$

and

$$\begin{aligned}
P_F =& \int_{K_{\mathrm{A,R}}}\int_{K_{\mathrm{B,R}}}\int_{\gamma_{\mathrm{A,R}}=0}^{2^{R^c_{\mathrm{A}}}-1} p_{\gamma_{\mathrm{A,R}}}(\gamma_{\mathrm{A,R}}|K_{\mathrm{A,R}}) p_{\log}(K_{\mathrm{A,R}}) p_{\log}(K_{\mathrm{B,R}})\\
&\cdot F_{\gamma_{\mathrm{B,R}}}\left[(2^{2R^c_{\mathrm{B}}}-1)(1+\gamma_{\mathrm{A,R}})|K_{\mathrm{B,R}}\right] d\gamma_{\mathrm{A,R}} d_{K_{\mathrm{A,R}}} d_{K_{\mathrm{B,R}}}\\
&+\int_{K_{\mathrm{A,R}}}\int_{K_{\mathrm{B,R}}}\int_{\gamma_{\mathrm{A,R}}=2^{R^c_{\mathrm{A}}}-1}^{2^{R^c_{\mathrm{B}}}\left(2^{R^c_{\mathrm{A}}}-1\right)} p_{\gamma_{\mathrm{A,R}}}(\gamma_{\mathrm{A,R}}|K_{\mathrm{A,R}}) p_{\log}(K_{\mathrm{A,R}})\\
&\cdot p_{\log}(K_{\mathrm{B,R}})\left\{F_{\gamma_{\mathrm{B,R}}}\left[(2^{R^c_{\mathrm{A}}+R^c_{\mathrm{B}}}-1-\gamma_{\mathrm{A,R}})|K_{\mathrm{B,R}}\right]\right.\\
&\left.-F_{\gamma_{\mathrm{B,R}}}\left[\frac{\gamma_{\mathrm{A,R}}}{2^{R^c_{\mathrm{A}}}-1}|K_{\mathrm{B,R}}\right]\right\} d\gamma_{\mathrm{A,R}} d_{K_{\mathrm{A,R}}} d_{K_{\mathrm{B,R}}}
\end{aligned} \tag{111}$$

for the logistic-distributed K-factor. With the normal-distributed K-factor, the expressions of P_D and P_F can be straightforwardly obtained by replacing $p_{\log}(K)$ with $p_{\mathrm{nor}}(K)$ in (110) and (111). P_G can be calculated similarly as P_D in (110).

Based on the decoding results for $\mathrm{u_A}$ and $\mathrm{u_B}$ at R, the calculation of the outage probability of $\mathscr{E}_\mathrm{OA}$, $\Pr(\mathscr{E}_\mathrm{OA})$, can be further classified into three cases as: Case 1: ($\hat{\mathrm{u}}_\mathrm{A} \neq \mathrm{u_A}$ and $\hat{\mathrm{u}}_\mathrm{B} = \mathrm{u_B}$) or ($\hat{\mathrm{u}}_\mathrm{A} = \mathrm{u_A}$ and $\hat{\mathrm{u}}_\mathrm{B} \neq \mathrm{u_B}$) with which Pr(Case 1) $= P_\mathrm{D} + P_\mathrm{G}$; Case 2: $\hat{\mathrm{u}}_\mathrm{A} \neq \mathrm{u_A}$ and $\hat{\mathrm{u}}_\mathrm{B} \neq \mathrm{u_B}$, Pr(Case 2) $= P_\mathrm{F}$; Case 3: $\hat{\mathrm{u}}_\mathrm{A} = \mathrm{u_A}$ and $\hat{\mathrm{u}}_\mathrm{B} = \mathrm{u_B}$, Pr(Case 3) $= 1 - P_\mathrm{D} - P_\mathrm{G} - P_\mathrm{F}$.

3.2.1 $\Pr(\mathscr{E}_\mathrm{OA}|\text{Case } 1)$

In Case 1, R can decode either $\mathrm{u_A}$ or $\mathrm{u_B}$ correctly. However, the XOR-ed sequence is correlated with the original information of A and B. Therefore, the problem can be regarded as source coding with a helper where the information sequence transmitted from the relay is regarded as a helper.

After canceling the successfully decoded information sequence, the calculation of the Hamming distortion of the other information sequence becomes the same as that in a point-to-point (P2P) transmission. The relationship between the XOR-ed version of the estimates $\hat{\mathrm{u}}_{\mathrm{A}\oplus\mathrm{B}} = \hat{\mathrm{u}}_\mathrm{A} \oplus \hat{\mathrm{u}}_\mathrm{B}$ and its original one (denoted by $\mathrm{u}_{\mathrm{A}\oplus\mathrm{B}} = \mathrm{u_A} \oplus \mathrm{u_B}$) can be modeled by bit-flipping model with bit-flipping probability p_f, $\hat{\mathrm{u}}_{\mathrm{A}\oplus\mathrm{B}} = \mathrm{u}_{\mathrm{A}\oplus\mathrm{B}} \oplus E$ where $\Pr(E = 1) = p_f$. Therefore, the Hamming distortion can be obtained by using the Shannon's lossy source-channel separation theorem as in section 2.1.2.

The admissible rate region in this case is illustrated in Fig. 28. The outage probability becomes $\Pr(\mathscr{E}_\mathrm{OA}|\text{Case } 1) = P_M + P_L$, where P_M and P_L are the probabilities that the source rate pair of A and R (R^s_A, R^s_R) falls into regions M and L in Fig. 28, respectively. With the relay-destination correlation also being represented by a bit-flipping model with probability p'_f, P_M and P_L can then be written as[14]

[14]Details of the relationship between the source rate and instantaneous SNR can be found in section 2.1.2.

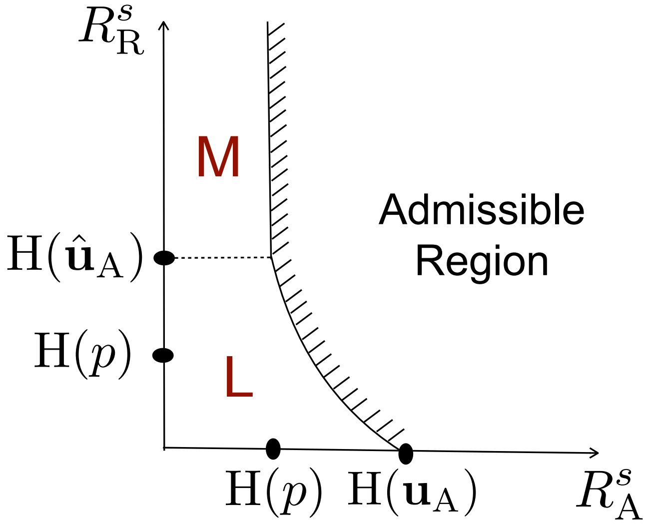

Fig. 28. Rate region for Case 1 according to the source coding with a helper theorem.

$$
\begin{aligned}
P_M = & \int_{K_{\mathrm{A,R}}} \int_{K_{\mathrm{R,B}}} \int_{\gamma_{\mathrm{A,R}}=0}^{1} \int_{\gamma_{\mathrm{R,B}}=1}^{\infty} \int_{\gamma_{\mathrm{A,B}}=0}^{2^{H(p_f)}-1} p_{\gamma_{\mathrm{A,B}}}(\gamma_{\mathrm{A,B}}|K_{\mathrm{A,B}}) \\
& \cdot p_{\gamma_{\mathrm{R,B}}}(\gamma_{\mathrm{R,B}}|K_{\mathrm{R,B}}) p_{\gamma_{\mathrm{A,R}}}(\gamma_{\mathrm{A,R}}|K_{\mathrm{A,R}}) p_{\log}(K_{\mathrm{R,B}}) p_{\log}(K_{\mathrm{A,R}}) \\
& d\gamma_{\mathrm{A,B}} d\gamma_{\mathrm{R,B}} d\gamma_{\mathrm{A,R}} d_{K_{\mathrm{R,B}}} d_{K_{\mathrm{A,R}}} \\
= & \int_{K_{\mathrm{A,R}}} \int_{K_{\mathrm{R,B}}} \int_{\gamma_{\mathrm{A,R}}=0}^{1} F_{\gamma_{\mathrm{A,B}}}\left(2^{H(p_f)}-1\right)\left[1-F_{\gamma_{\mathrm{R,B}}}(1,K_{\mathrm{R,B}})\right] \\
& \cdot p_{\gamma_{\mathrm{A,R}}}(\gamma_{\mathrm{A,R}}|K_{\mathrm{A,R}}) p_{\log}(K_{\mathrm{A,R}}) p_{\log}(K_{\mathrm{R,B}}) d\gamma_{\mathrm{A,R}} d_{K_{\mathrm{R,B}}} d_{K_{\mathrm{A,R}}}
\end{aligned} \tag{112}
$$

and

$$
\begin{aligned}
P_L = & \int_{K_{\mathrm{A,R}}} \int_{K_{\mathrm{R,B}}} \int_{\gamma_{\mathrm{A,R}}=0}^{1} \int_{\gamma_{\mathrm{R,B}}=0}^{1} \int_{\gamma_{\mathrm{A,B}}=0}^{2^{H(p_f * p'_f)}-1} p_{\gamma_{\mathrm{A,B}}}(\gamma_{\mathrm{A,B}}|K_{\mathrm{A,B}}) \\
& \cdot p_{\gamma_{\mathrm{R,B}}}(\gamma_{\mathrm{R,B}}|K_{\mathrm{R,B}}) p_{\log}(K_{\mathrm{R,B}}) d\gamma_{\mathrm{A,B}} d\gamma_{\mathrm{R,B}} d\gamma_{\mathrm{A,R}} d_{K_{\mathrm{R,B}}} d_{K_{\mathrm{A,R}}}, \\
= & \int_{K_{\mathrm{A,R}}} \int_{K_{\mathrm{R,B}}} \int_{\gamma_{\mathrm{A,R}}=0}^{1} \int_{\gamma_{\mathrm{R,B}}=0}^{1} F_{\gamma_{\mathrm{A,B}}}\left(2^{H(p_f * p'_f)}-1\right) \\
& \cdot p_{\gamma_{\mathrm{R,B}}}(\gamma_{\mathrm{R,B}}|K_{\mathrm{R,B}}) p_{\log}(K_{\mathrm{R,B}}) d\gamma_{\mathrm{R,B}} d\gamma_{\mathrm{A,R}} d_{K_{\mathrm{R,B}}} d_{K_{\mathrm{A,R}}}.
\end{aligned} \tag{113}
$$

3.2.2 $\Pr\left(\mathscr{E}_{\mathrm{OA}}|\mathrm{Case}\ 2\right)$

In Case 2, neither $\mathrm{u_A}$ nor $\mathrm{u_B}$ can be decoded without error at R. Therefore, we ignore the influence of the helper. Then, outage probability only depends on the direct A-B link transmission, as

$$\Pr\left(\mathscr{E}_{\mathrm{OA}}|\mathrm{Case}\ 2\right) = \int_{\gamma_{\mathrm{A,B}}=0}^{2^{R^c_{\mathrm{A}}}-1} p_{\gamma_{\mathrm{A,B}}}(\gamma_{\mathrm{A,B}}|K_{\mathrm{A,B}})d\gamma_{\mathrm{A,B}}. \tag{114}$$

Since in Case 2, we ignore the signal from the relay, resulting that the obtained outage probability is an upper bound.

3.2.3 $\Pr\left(\mathscr{E}_{\mathrm{OA}}|\mathrm{Case}\ 3\right)$

In Case 3, R can fully recover $\mathrm{u_A}$ and $\mathrm{u_B}$. The admissible rate region of R^s_{A} and R^s_{R} is shown in Fig. 29.

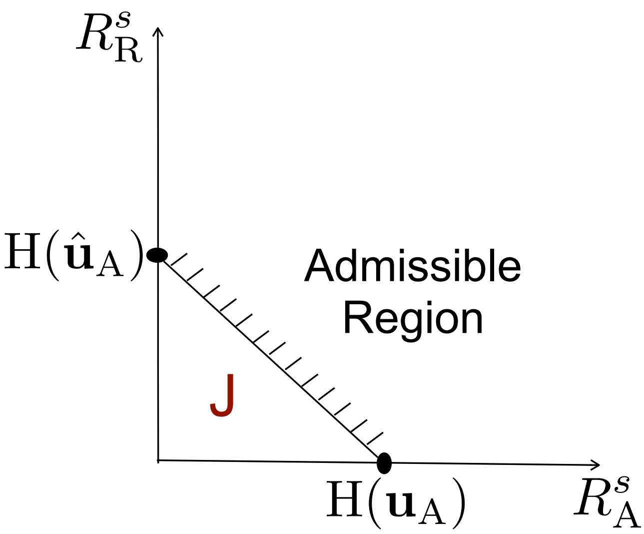

Fig. 29. Rate region for R^s_{A} and R^s_{R} in Case 2.

The outage occurs when $(R_{\text{A}}^{s}, R_{\text{R}}^{s})$ falls into the inadmissible rate region J in Fig. 29, with probability $\Pr(\mathscr{E}_{\text{OA}}|\text{Case 3}) = P_J$. Therefore, we have

$$\begin{aligned}
P_J =& \int_{K_{\text{A,R}}} \int_{K_{\text{R,B}}} \int_{\gamma_{\text{R,B}}=0}^{1} \int_{\gamma_{\text{A,B}}=0}^{2^{1-C(\gamma_{\text{R,B}})}-1} \int_{\gamma_{\text{A,R}}=1}^{\infty} p_{\gamma_{\text{A,B}}}(\gamma_{\text{A,B}}|K_{\text{A,B}}) \\
& \cdot p_{\gamma_{\text{A,R}}}(\gamma_{\text{A,R}}|K_{\text{A,R}}) p_{\gamma_{\text{R,B}}}(\gamma_{\text{R,B}}|K_{\text{R,B}}) p_{\log}(K_{\text{A,R}}) p_{\log}(K_{\text{R,B}}) \\
& d\gamma_{\text{A,R}} d\gamma_{\text{A,B}} d\gamma_{\text{R,B}} d_{K_{\text{R,B}}} d_{K_{\text{A,R}}} \\
=& \int_{K_{\text{A,R}}} \int_{K_{\text{R,B}}} \int_{\gamma_{\text{R,B}}=0}^{1} F_{\gamma_{\text{A,B}}}\left(2^{1-C(\gamma_{\text{R,B}})}-1\right)\left[1-F_{\gamma_{\text{A,R}}}(1, K_{\text{A,R}})\right] \\
& \cdot p_{\gamma_{\text{R,B}}}(\gamma_{\text{R,B}}|K_{\text{R,B}}) p_{\log}(K_{\text{A,R}}) p_{\log}(K_{\text{R,B}}) d\gamma_{\text{R,B}} d_{K_{\text{R,B}}} d_{K_{\text{A,R}}}.
\end{aligned} \tag{115}$$

The outage probability of $\mathscr{E}_{\text{OA}}$ is given as $\Pr(\mathscr{E}_{\text{OA}}) \leq \Pr(\mathscr{E}_{\text{OA}}|\text{Case 1})\Pr(\text{Case 1}) + \Pr(\mathscr{E}_{\text{OA}}|\text{Case 2})\Pr(\text{Case 2}) + \Pr(\mathscr{E}_{\text{OA}}|\text{Case 3})\Pr(\text{Case 3})$. Then, the outage probability of the two-way LF system can be expressed as $\Pr(\mathscr{E}_{\text{O}}) \leq 1 - [1-\Pr(\mathscr{E}_{\text{OA}})][1-\Pr(\mathscr{E}_{\text{OB}})]$, where $\Pr(\mathscr{E}_{\text{OB}})$ can be obtained by following the similar calculations as those for $\Pr(\mathscr{E}_{\text{OA}})$. It should be noted here that the sequences both A and B receive from the relay are correlated. Nevertheless, we calculate the outage probability by $1 - [1-\Pr(\mathscr{E}_{\text{OA}})][1-\Pr(\mathscr{E}_{\text{OB}})]$, assuming that they the outage probabilities occurred for A and B are independent.

3.3 Numerical Results

In this subsection, we present the outage probabilities of two-way LF relaying with the random Rician K-factor following the normal and logistic distributions. The outage probabilities of two-way DF relaying are also provided as the references. With two-way DF relaying, the relay keeps silent if error is detected after decoding in the information sequence sent from either A or B. The mean μ and variance σ^2 of the normal and logistic distributions follow the measurement data from urban, suburban, and rural areas, respectively [52], as shown in Table 7.

Fig. 30 compares the outage performance of two-way LF and two-way DF relaying. Since the outage probabilities of two-way DF in urban, suburban, and rural areas are almost the same, we only plot the outage curves of two-way DF relaying in rural area with Rican K-factor following the normal and logistic distributions, respectively. It is

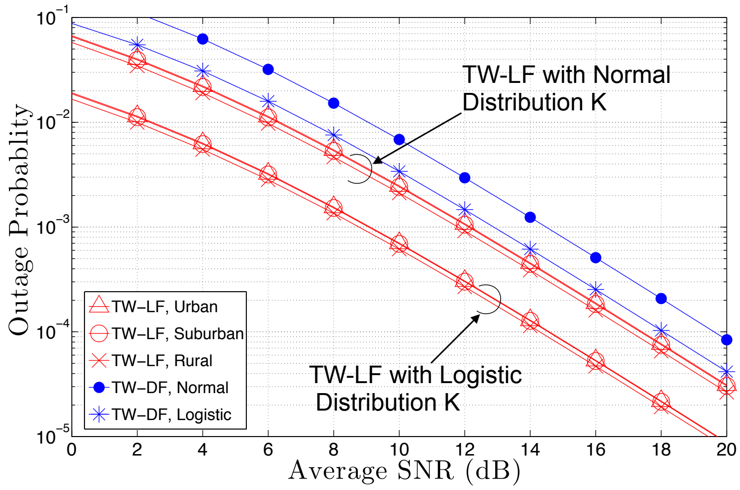

Fig. 30. Comparison of the outage probability of the two-way LF and two-way DF relaying, where $R_x^c = 1$ (bits/s/Hz) ($x \in$ (A,B)).

Table 7. Measurement data of mean μ and variance σ^2.

	Urban Area		Suburban Area		Rural Area	
	μ (dB)	σ^2 (dB)	μ (dB)	σ^2 (dB)	μ (dB)	σ^2 (dB)
$p_{\mathrm{nor}}(K)$	1.88	4.13	2.41	3.84	2.63	3.82
$p_{\log}(K)$	1.85	4.15	2.6	3.88	3	3.88

found that the outage probability of two-way LF relaying is superior to that of two-way DF with either normal-distributed or logistic-distributed K-factor.

3.4 Summary

We theoretically analyzed the outage probability of a two-way LF transmission system over Rician fading channels with the K-factor of the Rician fading being a random variable. The variation of K-factor follows either logistic or normal distribution estimated from measurement data. It is found that, compared to two-way DF relaying, two-way LF relaying achieves lower outage probability, regardless of either logistic or normal distribution is used to represent the variation of K-factor, as shown in Fig. 30. This is because with two-way LF relaying, the relay always broadcast the decoder output regardless of whether error is detected after decoding in the information part or not, and joint decoding is performed at the destination that compensate the decoding errors at the relay.

4 Performance Analysis for Two-Source Two-Relay Transmission over κ-μ Fading Channels

In this chapter, we derive the outage probability of a two-source two-relay transmission system, where all the links experience κ-μ fading variations. The source-relay links are assumed to be non-orthogonal MACs. Two transmission schemes are considered for relay-destination transmission, i.e., non-orthogonal maximum ratio transmission and orthogonal transmission with joint-decoding at the destination. It is found that, regardless of whether the LOS component exists in the channel or not, the outage performance of the system with orthogonal transmission with joint-decoding is superior to that with maximum ratio transmission.

4.1 System Model

In this chapter, we consider two sources S_1 and S_2 communicate with one common destination D with the help of two relays R_1 and R_2, as illustrated in Fig. 31, which has a symmetric topology, i.e., S_1 and S_2 as well as R_1 and R_2 are symmetric along the horizontal line through D. The relays are shared to both sources and no direct link exists between the sources and the destination. All nodes are equipped with a single antenna and operate in a half-duplex mode. The transmission is divided into two hops. In the first hop, S_1 and S_2 broadcast binary i.i.d. information sequence to R_1 and R_2 simultaneously over MACs. In the second hop, the relays decode the information sequences from both sources, re-encode, and forward them to the destination. We consider two schemes for the second hop transmission: 1) Non-orthogonal maximum ratio transmission scheme; 2) Orthogonal transmission with joint-decoding at D.

With the index $\{1,2,...,6\}$ representing the corresponding links shown in Fig. 31, the signal received at R_i ($i \in \{1,2\}$) can be written as

$$y_{\mathrm{R}_1} = \sqrt{G_1}h_1 s_1 + \sqrt{G_2}h_2 s_2 + n_{\mathrm{R}_1}, \tag{116}$$

$$y_{\mathrm{R}_2} = \sqrt{G_3}h_3 s_1 + \sqrt{G_4}h_4 s_2 + n_{\mathrm{R}_2}, \tag{117}$$

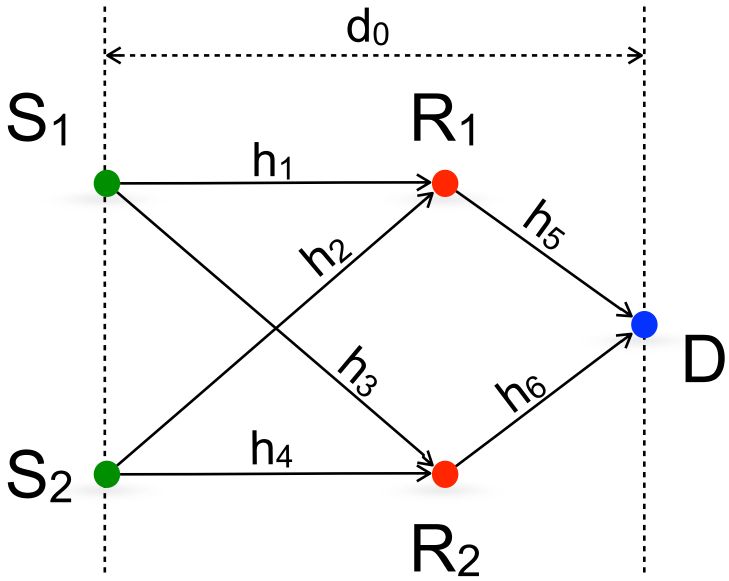

Fig. 31. Two-source two-relay transmission system.

respectively, where G_i is the geometric gain due to the distance of each link, h_i is the complex channel gain, and $n_{\mathrm{R}i}$ is the zero-mean AWGN with the variance $N_0/2$ per dimension. The modulated symbols of S_1 and S_2 are denoted by s_1 and s_2, respectively.

With the non-orthogonal transmission in the relay-destination link, the signal received at D in one time slot can be written as

$$y_{\mathrm{D}} = \sqrt{G_5} h_5 s_{\mathrm{R1}} + \sqrt{G_6} h_6 s_{\mathrm{R2}} + n_{\mathrm{D}}, \tag{118}$$

where s_{R1} and s_{R2} denote the modulated symbols transmitted from R_1 and R_2, respectively.

With the orthogonal transmission in the relay-destination link, the signal received at D in two time slots can be written as

$$y_{\mathrm{D}_1} = \sqrt{G_5} h_5 s_{\mathrm{R1}} + n_{\mathrm{D}_1}, \tag{119}$$
$$y_{\mathrm{D}_2} = \sqrt{G_6} h_6 s_{\mathrm{R2}} + n_{\mathrm{D}_2}, \tag{120}$$

respectively, where n_{D_1} and n_{D_2} denote the AWGN noise in two time slots with identical distributions.

All the links are assumed to suffer from block κ-μ fading. The pdf of instantaneous SNR of link i, γ_i, is given by [25]

$$f_{\kappa\mu}(\gamma_i) = \frac{\mu(1+\kappa)^{\frac{\mu+1}{2}} \cdot \gamma_i^{\frac{\mu-1}{2}}}{\kappa^{\frac{\mu-1}{2}} \exp(\mu\kappa)\overline{\gamma}_i^{\frac{\mu+1}{2}}} \cdot \exp(-\frac{\mu(1+\kappa)\gamma_i}{\overline{\gamma}_i})$$
$$\cdot I_{\mu-1}\left[2\mu \cdot \sqrt{\frac{\kappa(1+\kappa)\mu}{\overline{\gamma}_i}}\right], (i \in \{1,2,...,6\}), \tag{121}$$

where $\overline{\gamma}_i$ represents the average SNR of the link i. The parameter κ is related to the ratio of the total power of the dominant components to the total power of the scattered waves. The parameter μ represents the number of multipath clusters[15], and $I_{\mu-1}$ is the $(\mu-1)$th order modified Bessel function of the first kind. All the links are assumed mutually i.i.d. The cdf of κ-μ distribution is given by [25],

$$F_{\kappa\mu}(\gamma_i) = 1 - Q_1\left(\sqrt{2\kappa\mu}, \frac{\sqrt{2\kappa(1+\kappa)\gamma_i}}{\overline{\gamma}_i}\right). \tag{122}$$

We set the horizontal distance between the sources and the destination to d_0, the distance between S_1 and S_2 as well as the distance between R_1 and R_2 to $d_0/2$. With the geometric gain of the horizontal distance between the sources and the destination, G_0, being normalized to one, the geometric gains of the link i with length d_i can be defined as $G_i = (d_0/d_i)^\alpha$ [84], where α is the path loss factor.

4.2 Outage Probability

In this section, we provide the definition and derivation of the outage probability for the two-source two-relay system. The outage probabilities for S_1 and S_2 are the same due to the symmetry of the system topology. Therefore, we only focus on the derivation of the outage probability for S_1.

Since the transmission includes two hops, the overall outage probability of S_1 is calculated based on the law of Bayes' rule as,

$$\begin{aligned}\mathrm{P_{out}} = &\Pr(\text{outage}|\text{Case I})\Pr(\text{Case I})\\ &+\Pr(\text{outage}|\text{Case II})\Pr(\text{Case II})\\ &+\Pr(\text{outage}|\text{Case III})\Pr(\text{Case III}),\end{aligned} \tag{123}$$

[15] Signal arrives at a receiver clustered in time and in direction, and there may be several clusters.

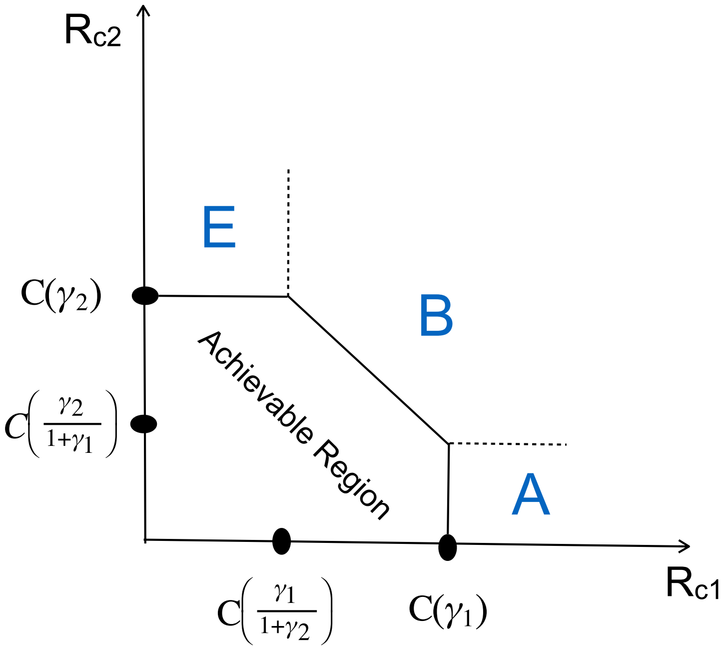

Fig. 32. MAC rate region for source-relay transmission.

where Case I, II, and III indicate that: In Case I, the information of S_1 cannot be decoded error-freely at both the relays; In Case II, information of S_1 can be recovered at both the relays without error; In Case III, only one of the relays can decode the information of S_1 with an arbitrary low error probability.

4.2.1 Outage Probability Calculation in Case I

For the source-relay transmission hop, the MAC rate region for (S_1-R_1, S_2-R_1) links is shown in Fig. 32. If the rate pair (R_{c1}, R_{c2})[16] falls into the region A or B shown in Fig. 32, error-free transmission for S_1 cannot be guaranteed. Therefore,

$$\Pr(\text{Case I}) = (\mathrm{P_A} + \mathrm{P_B})(\mathrm{P'_A} + \mathrm{P'_B}), \tag{124}$$

where $\mathrm{P_A}$ and $\mathrm{P_B}$ denotes the probability that $(\mathrm{R_{c1}}, \mathrm{R_{c2}})$ falls into the regions A and B, respectively. $\mathrm{P'_A}$ and $\mathrm{P'_B}$ denotes the probability that rate pair for (S_1-R_2, S_2-R_2) links falls into their corresponding MAC rate regions, respectively.

[16] R_{ci} denotes the spectrum efficiency of link i including the channel coding rate and the modulation multiplicity.

$\mathrm{P_A}$ and $\mathrm{P_B}$ can be expressed as [83]

$$\mathrm{P_A} = \Pr[R_{c1} > \log(1+\gamma_1), R_{c2} \le \log(1+\frac{\gamma_2}{1+\gamma_1})], \tag{125}$$

$$\begin{aligned}\mathrm{P_B} = \Pr[&R_{c1} > \log(1+\frac{\gamma_1}{1+\gamma_2}), R_{c2} > \log(1+\frac{\gamma_2}{1+\gamma_1}),\\ &R_{c1}+R_{c2} > \log(1+\gamma_1+\gamma_2)].\end{aligned} \tag{126}$$

With the assumption that all links suffer from statistically independent block κ-μ fading, $\mathrm{P_A}$ and $\mathrm{P_B}$ can be calculated by integral with respect to the pdf of the instantaneous SNRs of the corresponding links, as,

$$\begin{aligned}\mathrm{P_A} &= \int_{\gamma_1=0}^{2^{R_{c1}}-1} f_{\kappa\mu}(\gamma_1)d\gamma_1 \int_{\gamma_2=(2^{R_{c2}}-1)(1+\gamma_1)}^{\infty} f_{\kappa\mu}(\gamma_2)d\gamma_2\\ &= \int_{\gamma_1=0}^{2^{R_{c1}}-1} f_{\kappa\mu}(\gamma_1)\cdot\left(1-F_{\kappa\mu}\left[(2^{R_{c2}}-1)(1+\gamma_1)\right]\right)d\gamma_1\end{aligned} \tag{127}$$

and

$$\begin{aligned}\mathrm{P_B} &= \int_{\gamma_1=0}^{2^{R_{c1}}-1} f_{\kappa\mu}(\gamma_1)d\gamma_1 \int_{\gamma_2=0}^{(2^{R_{c2}}-1)(1+\gamma_1)} f_{\kappa\mu}(\gamma_2)d\gamma_2\\ &\quad+\int_{\gamma_1=2^{R_{c1}}-1}^{2^{R_{c2}}(2^{R_{c1}}-1)} f_{\kappa\mu}(\gamma_1)d\gamma_1 \int_{\gamma_2=\frac{\gamma_1}{2^{R_{c1}}-1}-1}^{2^{(R_{c1}+R_{c2})}-1-\gamma_1} f_{\kappa\mu}(\gamma_2)d\gamma_2\\ &= \int_{\gamma_1=0}^{2^{R_{c1}}-1} f_{\kappa\mu}(\gamma_1)\cdot F_{\kappa\mu}\left[(2^{R_{c2}}-1)(1+\gamma_1)\right]\\ &\quad+\int_{\gamma_1=2^{R_{c1}}-1}^{2^{R_{c2}}(2^{R_{c1}}-1)} f_{\kappa\mu}(\gamma_1)\left\{F_{\kappa\mu}\left(\frac{\gamma_1}{2^{R_{c1}}-1}-1\right)\right.\\ &\quad\left.-F_{\kappa\mu}\left(2^{(R_{c1}+R_{c2})}-1-\gamma_1\right)\right\}d\gamma_1.\end{aligned} \tag{128}$$

$\mathrm{P'_A}$ and $\mathrm{P'_B}$ can be calculated by following the similar technique based on their corresponding MAC rate region.

Since in Case I, neither $\mathrm{R_1}$ nor $\mathrm{R_2}$ can fully decode the information of $\mathrm{S_1}$. Therefore, the decoded information sequences of $\mathrm{S_1}$ at the two relays can be regarded as noisy versions of the original ones. In this case, the outage analysis falls into the chief executive officer (CEO) problem [85] in the relay-destination hop. For the purpose of simplicity, we set $\Pr(\text{outage}|\text{Case I}) = 1$, and therefore, the calculate outage curve represents theoretical upper bound.

4.2.2 Outage Probability Calculation in Case II

For Case II where the information of the source S_1 is fully recovered at R_1 and R_2, it is easy to have

$$\Pr(\text{Case II}) = (1 - P_A - P_B)(1 - P'_A - P'_B). \tag{129}$$

We consider two transmit schemes for the second hop (relay-destination) in Case II, i.e, non-orthogonal maximum ratio transmission and orthogonal transmission with joint-decoding.

Maximum Ratio Transmission Scheme

With maximum ratio transmission, the outage probability is given by

$$\begin{aligned}\Pr(\text{outage}|\text{Case II}) =& \Pr[R_c > \log(1+\gamma_5+\gamma_6)]\\ =& \int_{\gamma_5=0}^{2^{R_{c5}}-1} f_{\kappa\mu}(\gamma_5)d\gamma_5 \int_{\gamma_6=0}^{(2^{R_{c6}}-1-\gamma_5)} f_{\kappa\mu}(\gamma_6)d\gamma_6\\ =& \int_{\gamma_5=0}^{2^{R_{c5}}-1} f_{\kappa\mu}(\gamma_5)F_{\kappa\mu}\left(2^{R_{c6}}-1-\gamma_5\right)d\gamma_5. \end{aligned} \tag{130}$$

Orthogonal Transmission with Joint-decoding Scheme

Let b_{R1} and b_{R2} denotes the successfully recovered information sequences of S_1 at the R_1 and R_2, respectively. The admissible rate region of the R_1-D and R_2-D links are shown in Fig. 33.

The outage happens when the information coding rate pair of R_1 and R_2 (R_{R1}, R_{R2}) falls into the inadmissible area F shown in Fig. 33, with probability P_F. Therefore, we have

$$\begin{aligned}&\Pr(\text{outage}|\text{Case II}) = P_F\\ &= \int_{\gamma_5=0}^{2^{R_{c5}}-1} f_{\kappa\mu}(\gamma_5)\left(1-F_{\kappa\mu}(1)\right)\cdot F_{\kappa\mu}\left(2^{\left(1-\frac{\log(1+\gamma_5)}{R_{c5}}\right)R_{c6}}-1\right)d\gamma_5. \end{aligned} \tag{131}$$

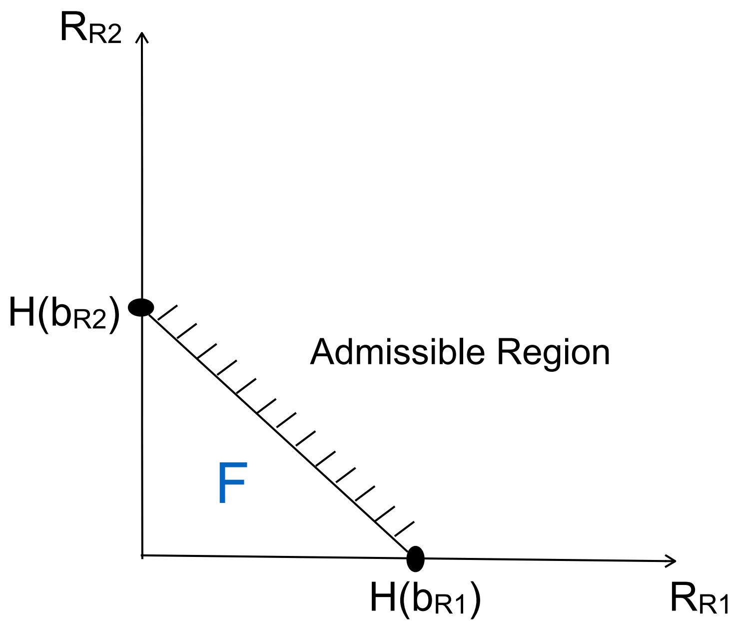

Fig. 33. Rate region for R_{R1} and R_{R2} in Case II for orthogonal transmission with joint-decoding scheme.

4.2.3 Outage Probability Calculation in Case III

In Case III, only one of the relays, either R_1 or R_2 can successfully decode the information sent from S_1. Therefore, the possibility of Case III is given as

$$\begin{aligned}\Pr(\text{Case III}) =& (1-P_A-P_B)(P'_A+P'_B)\\ &+(1-P'_A-P'_B)(P_A+P_B).\end{aligned} \tag{132}$$

The fully decoded information sequence at one relay is exactly the same as the original one. Even though decoding error is detected at the other relay, the erroneously decoded information sequence is correlated with the source sequence. Therefore, the decoded sequences at the two relays are correlated. Hence, the problem falls into the category of source coding with a helper. The outage probability is defined as the probability that (R_{R1}, R_{R2}) falls into the inadmissible areas J and K in Fig. 34, denoted as P_J and P_K, respectively. p_f represents the bit flipping probability between the information sequences obtained after decoding at R_1 and R_2.

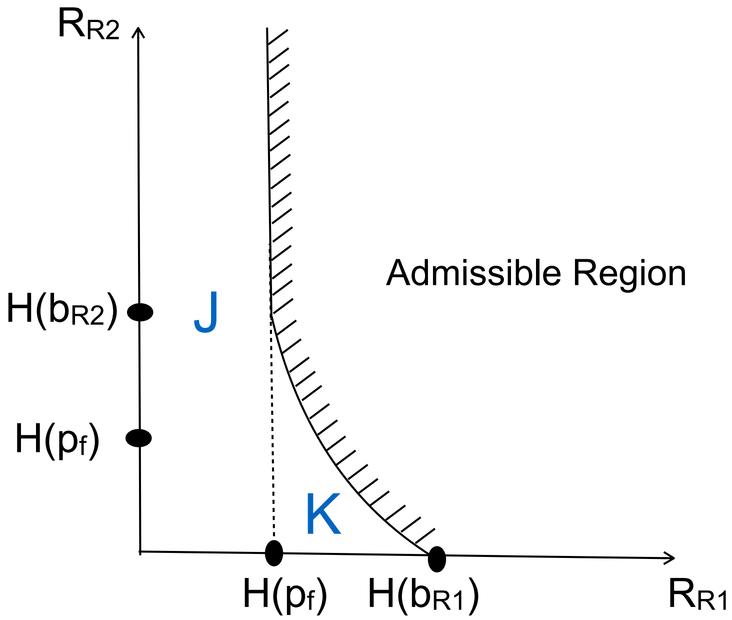

Fig. 34. Rate region for R_{R1} and R_{R2} in Case III.

We assume the recovered information of S_1 at R_2 is erroneous and the message are fully recovered at R_1. According to Shannon's lossless source channel separation theorem [73], the relationship between γ_5 and R_{R1} is established as $\gamma_5 \geq \left(2^{R_{\mathrm{R1}} R_{c5}} - 1\right)$.

Following the similar techniques in section 2.1.2, with the Hamming distortion measure for binary sources, the relationship between p_f and γ_3 can be established as $p_f = H^{-1}\left(1 - \log_2\left(1+\gamma_3\right)\right)$, according to Shannon's lossy source channel separation theorem [86].

Then, the outage probability in Case III can be written as

$$\begin{aligned}
&\Pr(\text{outage}|\text{Case III}) = \mathrm{P_J} + \mathrm{P_K} = \int_{\gamma_3=0}^{2^{R_{c3}}-1} f_{\kappa\mu}(\gamma_3) \\
&\cdot F_{\kappa\mu}\left(2^{\left(1-\frac{\log(1+\gamma_3)}{R_{c5}}\right)R_{c5}} - 1\right) d\gamma_3 \\
&+ \int_{\gamma_3=0}^{1} \int_{\gamma_5=2^{\left[1-H_2^{-1}\left(1-\log(1+\gamma_3)\right)\right]}-1}^{1} f_{\kappa\mu}(\gamma_3) f_{\kappa\mu}(\gamma_5) \\
&\cdot F_{\kappa\mu}\left(2^{\xi(\gamma_3,\gamma_5)} - 1\right) d\gamma_3 d\gamma_5.
\end{aligned} \tag{133}$$

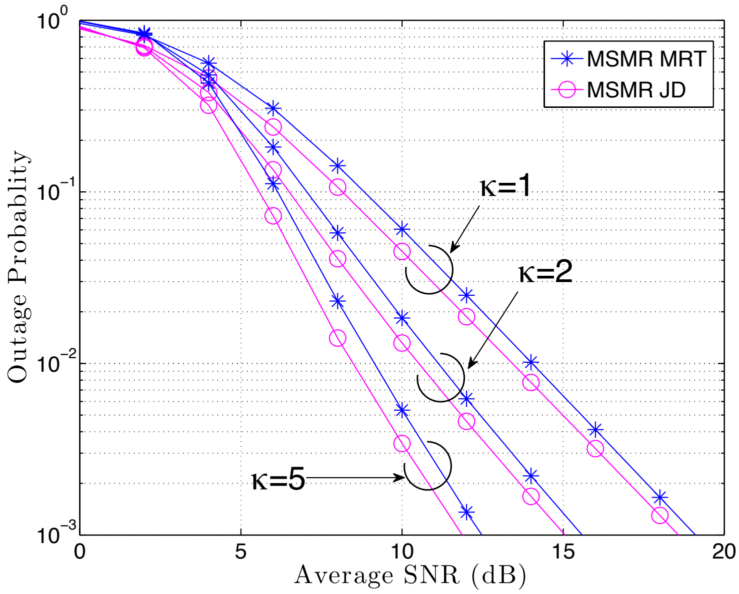

Fig. 35. Outage probabilities of the two-source two-relay system with maximum ratio transmission and orthogonal transmission with joint-decoding schemes; $\mu = 1$.

4.3 Numerical Results

The outage performance of the two-source two-relay system is illustrated in this section. The path loss factor is set at $\alpha = 3.52$ [84]. We assume the κ and μ values in each link are identical and represented by generic symbols κ and μ.

Fig. 35 shows the theoretical outage probabilities of the two-source two-relay system for S_1, the same results can be obtained for S_2 due to the symmetric topology. The outage probabilities are calculated with maximum ratio transmission and orthogonal transmission with joint-decoding schemes in the relay-destination hop, denoted as "MSMR MRT" and "MSMR JD" in Fig. 35, respectively. It can be found that the outage probability curves exhibit the tendency that the larger the κ values, the smaller the outage probability. With $\mu = 1$, the κ-μ fading becomes Rician fading, where κ equals to Rician factor K [87, Chapter 19]. Therefore, as the channel LOS component power increases (large κ), low outage probability can be achieved. It is also found that the outage probability with orthogonal transmission with joint-decoding is superior to that with maximum ratio transmission scheme, with ($\kappa > 1$) or without ($\kappa = 1$) the LOS component in the channels. This is because maximum ratio transmission performs signal

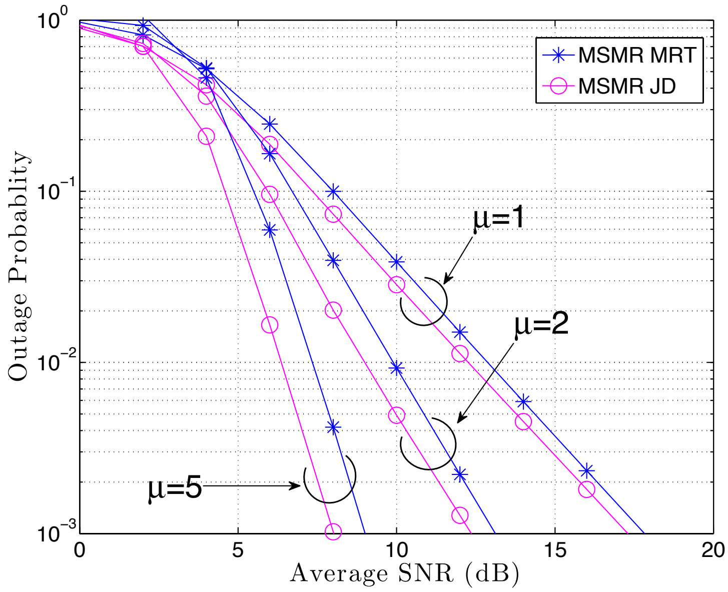

Fig. 36. Outage probabilities of the two-source two-relay system with maximum ratio transmission , and with joint-decoding; $\kappa = 1$**.**

level combining before decoding, whereas orthogonal transmission with joint-decoding is information level combining after decoding.[17]

Fig. 36 also compares the outage performance of the two-source two-relay system with orthogonal transmission with joint-decoding and maximum ratio transmission schemes with different μ (number of multipath clusters). It can be observed from Fig. 36 that, the higher the μ value, the lower the outage probability for a given SNR. However, the outage performance of the two-source two-relay system with orthogonal transmission with joint-decoding always outperforms that with maximum ratio transmission.

4.4 Summary

We derived the outage probability for a two-source two-relay cooperative communications system over κ-μ fading channels, of which result is shown in (123) in section [4.2

[17] Since cooperative communication is a diversity technique seeking for coverage extension and degrees of freedom enhancement, the spectrum efficiency loss is not taken into account in the performance comparison between maximum ratio transmission and orthogonal transmission with joint-decoding schemes in this section. Note that, CSI is not needed for orthogonal transmission with joint-decoding scheme at the transmitter side, however, maximum ratio transmission requires full CSI at the transmitter side for implementation.

Outage Probability]. Both non-orthogonal maximum ratio transmission and orthogonal transmission with joint-decoding are considered for the relay-destination transmission. The theoretical results, demonstrated in Fig. 35 and Fig. 36, show that the two-source two-relay system with orthogonal transmission with joint-decoding scheme outperforms maximum ratio transmission scheme in terms of outage probability.

5 Conclusions and Further Work

5.1 Conclusions

We have investigated cooperative wireless communications by focusing on exploiting the statistical nature of channel variations. The major contributions of this dissertation are summarized as follows.

First of all, we analyzed the outage performance for a three-node one-way LF relaying system. Based on the source coding with a helper theorem, the outage probability of LF relaying over independent block Nakagami-m fading channels with arbitrary values of the shape factor m was derived. The equivalent diversity order (defined as the decay of the outage curve) and coding gain of LF relaying was identified. It is shown that LF relaying is superior to conventional DF relaying in terms of the outage probability. Moreover, with LF, while keeping the outage probability the same or even lower, the search area for a relay (helper) can be increased over conventional DF relaying. Diversity orders were also derived for LF, DF, and ADF relaying assuming each link suffers from statistically independent or correlated Rayleigh fading. It is found that compared to independent fading, in correlated fading, to achieve the lowest outage probability, the relay should be located closer to the destination, or more transmit power should be allocated to the relay, both to recover the gain loss caused by the fading correlation. Furthermore, Rician is found not equivalent to Nakagami-m model for representing the entire shape of the distributions, even with a specific parameter setting yielding the same LOS components power ratio.

Then, we evaluated the outage performance of a two-way LF relaying system over Rician fading channels with random K-factor. The K-factor is assumed to follow empirical distributions, i.e., logistic or normal, derived from measurement data. It is found that two-way relaying with LF is superior to that with DF in terms of outage performance, regardless of either logistic or normal distribution is used to represent the variation of K-factor.

Finally, the work was extended to a two-source two-relay transmission system, where all the links experience κ-μ fading variations. It is found that, with or without the LOS component in channels, the outage probability of the two-source two-relay transmission system with orthogonal transmission with joint-decoding is lower than with non-orthogonal maximum ratio transmission.

5.2 Future Work

There are several interesting and challenging issues left as future work, which are listed below:

- In the impact analysis of the spatial and temporal correlations of the fading variations on the outage performance in Chapter 2, only the simple three-node relay system was considered. The work can be extended to more complex network topologies, such as multi-relay systems. However, in many cases of the structures, exact information theoretic bounds are still unknown. For example, one-source, one-destination, and multi-relay case falls into the source coding with multiple helper problem, which is one of the open problems in the network information theory and the rate region has not yet been known.
- Also in the impact analysis of the spatial and temporal correlations of the fading variations on the outage performance in Chapter 2, the Rayleigh fading is assumed for performance analyses. More generic channel models, such as Nakagami-m, κ-μ, or η-μ fading should be considered. However, for more generic channel models, the joint pdf for even two realizations following correlated distributions need to be obtained first.
- In the outage analysis for two-way LF relaying in Chapter 3, the errors in the two source-to-relay links are ignored in the case when the information of neither of the source can be decoded at the relay without errors. Hence, the outage probability in this case only depends on the direct source-destination link transmission, which results in the calculated outage probability being an upper bound. However, even though neither of the source information can be decoded without error at the relay, there is still a possibility that the errors can be corrected at the destination by joint decoding the two information sequences, one received via the source-destination link, and the other via the relay-destination link. A tighter bound of the theoretical outage probability can be derived, if the relationship between the error probabilities and the SNRs of two source-to-relay links can be explicitly defined.
- Also in Chapter 3, perfect self-interference cancellation due to the full duplex setting is assumed in the two-way LF transmission. In practice, self-interference may not be canceled completely, and it causes inter-symbol interference. Therefore, the work can be extended to the rate region analysis, as well as the outage probability calculation with inter-symbol interference being taken into consideration, which is also left as future work.

- Even though the source coding theory, e.g. the source coding with a helper theorem, is utilized for outage calculation. However, practical source coding is not considered in the performance analysis. Combining source coding, e.g., the Huffman coding, and channel coding is left as a important future study.
- So far, we focused on frequency flat fading only. The system performance in frequency selective fading is not yet known and therefore, needs to be analyzed with channel estimation and equalization.
- This dissertation considered the Rayleigh fading model for NLOS scenario. However, in vehicle-to-vehicle communications, the amplitude distribution of the received signal will be a product of two Rayleigh random processes if both the source and destination nodes in the network are moving, hence giving rise to the double-Rayleigh amplitude distribution [88]. This is also left as future work.

References

1. Gupta A & Jha RK (2015) A survey of 5G network: Architecture and emerging technologies. IEEE Access 3: 1206–1232.
2. Meulen ECVD (1971) Three-terminal communication channels. Advanced Appl. Prob. 3(1): 120–154.
3. Cover T & Gamal AE (1979) Capacity theorems for the relay channel. IEEE Trans. Inform. Theory 25(5): 572–584.
4. Nosratinia A, Hunter T & Hedayat A (2004) Cooperative communication in wireless networks. IEEE Commun. Mag. 42(10): 74–80.
5. Li Q, Hu R, Qian Y & Wu G (2012) Cooperative communications for wireless networks: techniques and applications in LTE-advanced systems. IEEE Wireless Commun. Mag. 19(2): 22–29.
6. Kramer G, Gastpar M & Gupta P (2005) Cooperative strategies and capacity theorems for relay networks. IEEE Trans. Inform. Theory 51(9): 3037–3063.
7. Laneman JN (2012) Cooperative diversity in wireless networks: Algorithms and architectures. Ph.D. dissertation, MIT, MA.
8. Laneman JN & Wornell GW (2003) Distributed space-time-coded protocols for exploiting cooperative diversity in wireless networks. IEEE Trans. Inform. Theory 49(10): 2415–2425.
9. Nazer B & Gastpar M (2011) Compute-and-forward: Harnessing interference through structured codes. IEEE Trans. Inform. Theory 57(10): 6463–6486.
10. Karmakar S & Varanasi MK (2011) The diversity-multiplexing tradeoff of the dynamic decode-and-forward protocol on a MIMO half-duplex relay channel. IEEE Trans. Inform. Theory 57(10): 6569–6590.
11. Torbatian M & Damen MO (2014) Diversity-multiplexing tradeoff of asynchronous decode-and-forward cooperative networks. IEEE Trans. Commun. 62(7): 2340–2352.
12. Cheng Z, Devroye N & Liu T (2016) The degrees of freedom of full-duplex bidirectional interference networks with and without a MIMO relay. IEEE Trans. Wireless Commun. 15(4): 2912–2924.
13. Zhao B & Valenti MC (2003) Distributed turbo coded diversity for relay channel. Electron. Lett. 39(10): 786–787.
14. Razaghi P & Yu W (2007) Bilayer low-density parity-check codes for decode-and-forward in relay channels. IEEE Trans. Inform. Theory 53(10): 3723–3739.
15. Stefanov A & Erkip E (2004) Cooperative coding for wireless networks. IEEE Trans. Commun. 52(9): 1470–1476.
16. Sharma GVV, Ganwani V, Desai UB & Merchant SN (2010) Performance analysis of maximum likelihood detection for decode and forward MIMO relay channels in rayleigh fading. IEEE Trans. Wireless Commun. 9(9): 2880–2889.
17. Sneessens HH, Vandendorpe L & Laneman JN (2009) Adaptive compress-and-forward relaying in fading environments with or without Wyner-Ziv coding. In: Proc. IEEE Int. Conf. Commun., pp. 1–5.
18. Wyner A & Ziv J (1976) The rate-distortion function for source coding with side information at the decoder. IEEE Trans. Inform. Theory 22(1): 1–10.

19. Laneman J, Tse D & Wornell GW (2004) Cooperative diversity in wireless networks: Efficient protocols and outage behavior. IEEE Trans. Inform. Theory 50(12): 3062–3080.
20. Goldsmith A (2005) Wireless Communications. Cambridge University, USA.
21. Dohler M & Li Y (2010) Cooperative Communications: Hardware, Channel and PHY. Wiley Publishing.
22. Nakagami M (1960) The m-distribution, a general formula of intensity distribution of rapid fading. Stat. Method of Radio Propagat. in W. C. Hoffman (ed.): 3–36.
23. Hasna MO & Alouini MS (2004) Harmonic mean and end-to-end performance of transmission systems with relays. IEEE Trans. Commun. 52(1): 130–135.
24. Dersch U & Braun W (1991) A physical mobile radio channel model. In: Proc. IEEE Veh. Technol. Conf., pp. 289–294.
25. Yacoub MD (2007) The κ-μ distribution and the η-μ distribution. IEEE Antennas Propagat. Mag. 49(1): 68–81.
26. Garcia-Frias J & Zhao Y (2005) Near-Shannon/Slepian-Wolf performance for unknown correlated sources over AWGN channels. IEEE Trans. Commun. 53(4): 555–559.
27. Anwar K & Matsumoto T (2012) Accumulator-assisted distributed turbo codes for relay systems exploiting source-relay correlation. IEEE Commun. Lett. 16(7): 1114–1117.
28. Zhou X, Cheng M, He X & Matsumoto T (2014) Exact and approximated outage probability analyses for decode-and-forward relaying system allowing intra-link errors. IEEE Trans. Wireless Commun. 13(12): 7062–7071.
29. Li Y (2009) Distributed coding for cooperative wireless networks: An overview and recent advances. IEEE Commun. Mag. 47(8): 71–77.
30. Gamal AE & Kim YH (2011) Network Information Theory. Cambridge University, New York.
31. Zhou X, Cheng M, Anwar K & Matsumoto T (2012) Distributed joint source-channel coding for relay systems exploiting source-relay correlation and source memory. EURASIP J. Wireless Comm. and Netw. 2012(1): 260. URI: https://doi.org/10.1186/1687-1499-2012-260.
32. Aaron A & Girod B (2002) Compression with side information using turbo codes. In: Proc. Data Compr. Conf., pp. 252–261.
33. Garcia-Frias J, Zhao Y & Zhong W (2007) Turbo-like codes for transmission of correlated sources over noisy channels. IEEE Signal Processing Mag. 24(5): 58–66.
34. Varodayan D, Lin YC & Girod B (2012) Adaptive distributed source coding. IEEE Trans. Image Processing 21(5): 2630–2640.
35. Shahid I & Yahampath P (2013) Distributed joint source-channel coding using unequal error protection LDPC codes. IEEE Trans. Commun. 61(8): 3472–3482.
36. Aljohani AJ, Ng SX & Hanzo L (2016) Distributed source coding and its applications in relaying-based transmission. IEEE Access 4: 1940–1970.
37. Hu R & Li J (2005) Exploiting Slepian-Wolf codes in wireless user cooperation. In: Proc. IEEE Works. on Sign. Proc. Adv. in Wirel. Comms., pp. 275–279.
38. Zhao B & Valenti MC (2003) Distributed turbo coded diversity for relay channel. Electron. Lett. 39(10): 786–787.
39. Sneessens HH, Louveaux J & Vandendorpe L (2008) Turbo-coded decode-and-forward strategy resilient to relay errors. In: Proc. IEEE Int. Conf. Acoust., Speech, Signal Processing, pp. 3213–3216.

40. Cheng M, Anwar K & Matsumoto T (2013) Outage probability of a relay strategy allowing intra-link errors utilizing Slepian-Wolf theorem. EURASIP J. Advances Signal Processing 2013(1): 34.
41. Slepian D & Wolf J (1973) Noiseless coding of correlated information sources. IEEE Trans. Inform. Theory 19(4): 471–480.
42. Lu PS, Zhou X & Matsumoto T (2015) Outage probabilities of orthogonal multiple-access relaying techniques with imperfect source-relay links. IEEE Trans. Wireless Commun. 14(4): 2269–2280.
43. He J, Hussain I, Juntti M & Matsumotov T (2016) End-to-end outage probability analysis for multi-source multi-relay systems. In: Proc. IEEE Int. Conf. Commun., pp. 1–6.
44. Wolf A, Matthé M, Festag A & Fettweis G (2015) Outage based power allocation for a lossy forwarding two-relaying system. pp. 267–272.
45. Wolf A, González DC, Filho JCSS & Fettweis G (2016) Asymptotically optimal power allocation for WSNs with mutually correlated sensing data. IEEE Commun. Lett. 20(7): 1317–1320.
46. Shiu DS, Foschini GJ, Gans MJ & Kahn JM (2000) Fading correlation and its effect on the capacity of multielement antenna systems. IEEE Trans. Commun. 48(3): 502–513.
47. Chuah CN, Tse DNC, Kahn JM & Valenzuela RA (2002) Capacity scaling in MIMO wireless systems under correlated fading. IEEE Trans. Inform. Theory 48(3): 637–650.
48. Mesleh RY, Haas H, Sinanovic S, Ahn CW & Yun S (2008) Spatial modulation. IEEE Trans. Veh. Technol. 57(4): 2228–2241.
49. Chuah CN, Tse DNC, Kahn JM & Valenzuela RA (2002) Capacity scaling in MIMO wireless systems under correlated fading. IEEE Trans. Inform. Theory 48(3): 637–650.
50. Wang Z & Giannakis GB (2003) A simple and general parameterization quantifying performance in fading channels. IEEE Trans. Commun. 51(8): 1389–1398.
51. Kang M & Alouini MS (2006) Capacity of mimo rician channels. IEEE Trans. Wireless Commun. 5(1): 112–122.
52. Zhu S, Ghazaany TS, Jones SMR, Abd-Alhameed RA, Noras JM, Buren TV, Wilson J, Suggett T & Marker S (2014) Probability distribution of Rician K-factor in urban, suburban and rural areas using real-world captured data. IEEE Trans. Antennas Propagat. 62(7): 3835–3839.
53. Qian S, He J, Juntti M & Matsumoto T (accepted) Fading correlations for wireless cooperative communications: Diversity and coding gains. IEEE Access .
54. Qian S, Zhou X, He X, He J, Juntti M & Matsumoto T (accepted) Performance analysis for lossy-forward relaying over Nakagami-m fading channels. IEEE Trans. Veh. Technol. .
55. Qian S, He J, Juntti M & Matsumoto T (accepted) Outage performance analysis for two-way relaying with random line-of-sight components. IEICE Commun. Express .
56. Qian S, He J, Juntti M & Matsumoto T (2016) Performance analysis for multi-source multi-relay transmission over κ-μ fading channels. In: Proc. Annual Asilomar Conf. Signals, Syst., Comp., pp. 1308–1312.
57. Qian S, He J, He X, Jiang W, Juntti M & Matsumoto T (2016) Line-of-sight component impact analyses for lossy forward relaying over fading channels having different statistical properties. In: Proc. Asia Pacific Wireless Commun. Symp., pp. 1–5.
58. Qian S, Juntti M & Matsumoto T (2016) Joint optimization of power allocation and relay position for lossy-forwarding relaying. In: Proc. IEEE Wireless Commun. and Networking Conf., pp. 1–6.

59. Qian S, Tervo V, He J, Juntti M & Matsumoto T (2016) A comparative study of different relaying strategies over one-way relay networks. In: Proc. European Wireless Conf., pp. 1–6.
60. Qian S, Cheng M & Matsumoto T (2015) Outage based power allocation for a lossy-forwarding relaying system. In: Proc. IEEE Int. Conf. Commun. (Workshop), pp. 2139–2144.
61. Qian S, Juntti M & Matsumoto T (2015) A comparative study on outage probabilities of decode-and-forward and lossy-forward relay techniques. pp. 278–282.
62. He J, Tervo V, Qian S, Xue Q, Juntti M & Matsumoto T (submitted) Performance analysis of lossy decode-and-forward for non-orthogonal MARCs. IEEE Trans. Wireless Commun. .
63. He J, Li Y, Wu G, Qian S, Xue Q, & Matsumoto T (2017) Performance improvement of joint source-channel coding with unequal power allocation. IEEE Wireless Commun. Lett. PP(99): 1–1.
64. He J, Tervo V, Qian S, , Juntti M & Matsumoto T (2017) Performance analysis of OSTBC transmission in lossy forward MIMO relay networks. IEEE Commun. Lett. 21(8): 1791–1794.
65. He J, Hussain I, Qian S, Juntti M & Matsumoto T (2016) On the performance of dynamic multi-source multi-antenna multi-relay wireless networks. In: Proc. European Wireless Conf., pp. 1–6.
66. Jiang W, He X, Qian S, Juntti M & Matsumoto T (2015) Finite-SNR diversity-multiplexing tradeoff for decode-and-forward relaying system allowing intra-link errors. In: Proc. Int. Conf. on Inform. Commun. and Sign. Proc., pp. 1–5.
67. He J, Yi N, Hou J, He X, Qian S, Matsumoto T & Wolf A (2016) ICT-619555-RESCUE Theoretical Results Update of Assessment on Feasibility, Achievability, and Limits. Deliverable D1.2.2.
68. Wolf A, Qian S, Padmanabhan A, Tervo V, Yi N & Hou J (2016) ICT-619555-RESCUE Final Report of Detailed Optimisation Algorithm and Performance Comparisons. Deliverable D2.2.2.
69. He J, He X, Hou J, Jiang W, Kühlmorgen S, Matsumoto T, Paatelma A, Qian S, Tervo V, Wolf A & Yi N (2016) ICT-619555-RESCUE Final Report of The Coding/Decoding Algorithms and Performance Comparison. Deliverable D2.1.2.
70. Sośnik S, Tervo V, Wszolek J, Xin He SQ, Hou J, Sikora M, Łoziak K, Gozdecki J, Matthe M, Bułat J, Schneider C, Trzeciakowski L, Szott S, Khalife H & Pach A (2015) ICT-619555-RESCUE Feasibility Assessment in Model Based Environments. Deliverable D2.3.
71. Hou J, Matsumoto T, Qian S, Yi N, Matthé M, Wolf A, Tervo V & Zhou X (2015) ICT-619555-RESCUE Detailed Optimisation Algorithm and Performance Comparisons. Deliverable D2.2.1.
72. Woldegebreal DH & Karl H (2007) Multiple-access relay channel with network coding and non-ideal source-relay channels. In: Proc. Int. Symp. Wireless Commun. Systems, pp. 732–736.
73. Shannon CE (1948) A mathematical theory of communication. Bell Syst. Tech. J. 27: 397–423.
74. Shannon CE (1959) Coding theorems for a discrete source with a fidelity criterion. Institute of Radio Engineers, International Convention Record 7: 325–350.
75. Zhu GC & Alajaji F (2006) Joint source-channel turbo coding for binary Markov sources. IEEE Trans. Wireless Commun. 5(5): 1065–1075.

76. Gradshteyn IS & Ryzhik IM (2007) Table of Integrals, Series, and Products. Elsevier/Academic Press, Burlington, MA, USA, seventh edition.
77. Gander W & Gautschi W (2000) Adaptive quadrature-revisited. BIT Numer. Math., Springer 40: 84–101.
78. Mischa Schwartz WRB & Stein S (1995) Communication Systems and Techniques. John Wiley & Sons, first edition.
79. Abramowitz M & Stegun IA (1964) Handbook of Mathematical Functions with Formulas, Graphs, and Mathematical Tables. Dover, New York, Tenth Printing edition.
80. Press WH, Teukolsky SA, Vetterling WT & Flannery BP (2007) Numerical Recipes: The Art of Scientific Computing. Cambridge University Press, New York, Third edition.
81. Simon MK & Alouini MS (2005) Digital Communications over Fading Channels. Wiley.
82. Cover TM & Thomas JA (2006) Elements of Information Theory. John Wiley & Sons, Inc., USA, 2nd edition.
83. Narasimhan R (2007) Individual outage rate regions for fading multiple access channels. In: Proc. IEEE Int. Symp. Inform. Theory, pp. 1571–1575.
84. Liang D, Ng SX & Hanzo L (2010) Relay-induced error propagation reduction for decode-and-forward cooperative communications. In: Proc. IEEE Global Telecommun. Conf., pp. 1–5.
85. Berger T, Zhang Z & Viswanathan H (1996) The CEO problem. IEEE Trans. Inform. Theory 42(3): 887–902.
86. Shannon CE (1959) Coding theorems for a discrete source with a fidelity criterion 4(142-163): 1.
87. Mirza Milišić MH & Hadžialić M (2011) Outage Performance and Symbol Error Rate Analysis of L-Branch Maximal-Ratio Combiner for κ-μ and η-μ Fading, Vehicular Technologies: Increasing Connectivity, Dr. Miguel Almeida (Ed.). InTech, Rijeka, Croatia.
88. Salo J, El-Sallabi HM & Vainikainen P (2006) Impact of double-Rayleigh fading on system performance. In: Wireless Pers. Commun., Kluwer, pp. 1–5.
89. Ahlswede R, Cai N, Li SYR & Yeung RW (2000) Network information flow. IEEE Trans. Inform. Theory 46(4): 1204–1216.
90. Shampine L (2008) Matlab program for quadrature in 2D. J. Comput. Appl. Math. 202(1): 266 – 274.
91. Rubio L, Reig J & Cardona N (2007) Evaluation of Nakagami fading behaviour based on measurements in urban scenarios. AEÜ Int. J. Electron. and Commun. 61(2): 135.
92. Hu Z, Yuan C, Zhu F & Gao F (2016) Weighted sum transmit power minimization for full-duplex system with SWIPT and self-energy recycling. IEEE Access 4: 4874–4881.
93. Zhu GC & Alajaji F (2006) Joint source-channel turbo coding for binary Markov sources. IEEE Trans. Wireless Commun. 5(5): 1065–1075.
94. Vazquez-Araujo FJ, Fresnedo O, Castedo L & Garcia-Frias J (2014) Analog joint source-channel coding over MIMO channels. EURASIP J. Wireless Comm. and Netw. 2014(1): 25.
95. Etkin RH & Tse DNC (2006) Degrees of freedom in some underspread MIMO fading channels. IEEE Trans. Inform. Theory 52(4): 1576–1608.
96. Goldsmith A, Jafar SA, Jindal N & Vishwanath S (2003) Capacity limits of MIMO channels. IEEE J. Select. Areas Commun. 21(5): 684–702.
97. Shin H & Lee JH (2003) Capacity of multiple-antenna fading channels: spatial fading correlation, double scattering, and keyhole. IEEE Trans. Inform. Theory 49(10): 2636–2647.

98. Liu Q, Zhang W, Ma X & Zhou GT (2012) Designing peak power constrained amplify-and-forward relay networks with cooperative diversity. IEEE Trans. Wireless Commun. 11(5): 1733–1743.
99. Rubio L, Reig J & Cardona N (2007) Evaluation of nakagami fading behaviour based on measurements in urban scenarios. AEÜ Int. J. Electron. and Commun. 61(2): 135 – 138.
100. Kumar P & Dhaka K (2015) Performance analysis of a decode-and-forward relay system in κ-μ and η-μ fading channels. IEEE Trans. Veh. Technol. PP(99): 1–1.
101. Moraes AC, Costa DB & Yacoub MD (2012) An outage analysis of multibranch diversity receivers with cochannel interference in α-μ, κ-μ, and η-μ fading scenarios 64(1): 3–19.
102. Ungerboeck G (1982) Channel coding with multilevel/phase signals. IEEE Trans. Inform. Theory 28(1): 55–67.
103. Adinoyi A & Yanikomeroglu H (2007) Cooperative relaying in multi-antenna fixed relay networks. IEEE Trans. Wireless Commun. 6(2): 533–544.
104. Benjillali M & Alouini MS (2013) Partner cooperation with decode-and-forward: Closed-form outage analysis and comparison. IEEE Trans. Veh. Technol. 62(1): 127–139.
105. Ozarow LH, Shamai S & Wyner AD (1994) Information theoretic considerations for cellular mobile radio. IEEE Trans. Veh. Technol. 43(2): 359–378.
106. Caire G, Taricco G & Biglieri E (1999) Optimum power control over fading channels. IEEE Trans. Inform. Theory 45(5): 1468–1489.
107. Anwar K & Matsumoto T (2012) Spatially concatenated codes with turbo equalization for correlated sources. IEEE Trans. Signal Processing 60(10): 5572–5577.
108. Liu P, Tao Z, Lin Z, Erkip E & Panwar S (2006) Cooperative wireless communications: a cross-layer approach. IEEE Wireless Commun. Mag. 13(4): 84–92.
109. Garcia-Frias J & Zhao Y (2005) Near-Shannon/Slepian-Wolf performance for unknown correlated sources over AWGN channels. IEEE Trans. Commun. 53(4): 555–559.
110. Ungerboeck G (1982) Channel coding with multilevel/phase signals. IEEE Trans. Inform. Theory 28(1): 55–67.
111. Youssef R & Graell i Amat A (2011) Distributed serially concatenated codes for multi-source cooperative relay networks. IEEE Trans. Wireless Commun. 10(1): 253 –263.
112. Cover T & Gamal A (1979) Capacity theorems for the relay channel. IEEE Trans. Inform. Theory 25(5): 572–584.
113. Morales-Jimenez D & Paris JF (2010) Outage probability analysis for η-μ fading channels. IEEE Commun. Lett. 14(6): 521–523.
114. Beaulieu NC & Hu J (2006) A closed-form expression for the outage probability of decode-and-forward relaying in dissimilar Rayleigh fading channels. IEEE Commun. Lett. 10(12): 813–815.
115. Wang Y, Xu Y, Li N, Xie W, Xu K & Xia X (2016) Relay selection of full-duplex decode-and-forward relaying over Nakagami-m fading channels. Electron. Lett. 10(2): 170–179.
116. Lu T, Ge J, Yang Y & Gao Y (2013) Outage probability analysis of signal space cooperative communications over Nakagami-m fading channels. Electron. Lett. 49(18): 1186–1188.
117. Ikki S & Ahmed M (2010) Performance analysis of adaptive decode-and-forward cooperative diversity networks with best-relay selection. IEEE Trans. Commun. 58(1): 68–72.
118. Rao M, Lopez-Martinez FJ & Goldsmith A (2014) Statistics and system performance metrics for the two wave with diffuse power fading model. In: Proc. Conf. Inform. Sciences Syst. (CISS), pp. 1–6.

119. He J, Hussain I, Juntti M & Matsumoto T (2016) End-to-end outage probability analysis for multi-source multi-relay systems. In: Proc. IEEE Int. Conf. Commun., pp. 1–6.
120. Duarte M & Sabharwal A (2010) Full-duplex wireless communications using off-the-shelf radios: Feasibility and first results. In: Proc. Annual Asilomar Conf. Signals, Syst., Comp., pp. 1558–1562.
121. Kosek-Szott K, Natkaniec M, Prasnal L & Szott S (2016) CLF-MAC: A coordinated MAC protocol supporting lossy forwarding in WLANs. In: Proc. Int. Symp. Wireless Commun. Systems, pp. 434–438.
122. Qian S, Cheng M & Matsumoto T (2015) Outage based power allocation for a lossy-forwarding relaying system. In: Proc. IEEE Int. Conf. Commun., pp. 2139–2144.
123. Simoens S, Vidal J & Munoz O (2006) Compress-and-forward cooperative relaying in mimo-ofdm systems. In: 2006 IEEE 7th Workshop on Signal Processing Advances in Wireless Communications, pp. 1–5.
124. Brulatout M, Khalifé H, Conan V, Szott S, Natkaniec M, Kosek-Szott K & Prasnal L (2016) A cooperative MAC protocol for lossy forwarding networks. In: Proc. Wireless Days Conf., pp. 1–3.
125. Luo J, Blum RS, Cimini LJ, Greenstein LJ & Haimovich AM (2005) Link-failure probabilities for practical cooperative relay networks. In: Proc. IEEE Veh. Technol. Conf., volume 3, pp. 1489–1493 Vol. 3.
126. Luo K, Gohary R & Yanikomeroglu H (2011) On the generalization of decode-and-forward and compress-and-forward for Gaussian relay channels. In: IEEE ITW, pp. 623–627.
127. Huang SQ, Chen HH & Lee MY (2011) On performance bounds of mixed amplify-and-forward and decode-and-forward cooperative relay systems. In: 6th International ICST Conference on CHINACOM, pp. 521–527.
128. Ikki S & Ahmed M (2009) Performance analysis of decode-and-forward incremental Relaying cooperative-diversity networks over Rayleigh fading channels. In: IEEE 69th VTC Spring, pp. 1–6.
129. Yi Z & Kim IM (2007) Decode-and-forward cooperative networks with relay selection. In: Proc. IEEE Veh. Technol. Conf., pp. 1167–1171.
130. Qian S, Cheng M, Anwar K & Matsumoto T (2013) Outage probability analysis for correlated sources transmission over Rician fading channels. In: Proc. IEEE Int. Symp. Pers., Indoor, Mobile Radio Commun., pp. 1087–1091.
131. Liu Z, Stankovic V & Xiong Z (2005) Wyner-Ziv coding for the half-duplex relay channel. In: Proc. IEEE Int. Conf. Acoust., Speech, Signal Processing, volume 5, pp. 1113–1116.
132. Ochiai H, Mitran P & Tarokh V (2004) Design and analysis of collaborative diversity protocols for wireless sensor networks. In: IEEE 60th VTC Fall, volume 7, pp. 4645–4649 Vol. 7.
133. Souryal M & Vojcic B (2006) Performance of amplify-and-forward and decode-and-forward relaying in Rayleigh fading with turbo codes. In: Proc. IEEE Int. Conf. Acoust., Speech, Signal Processing, volume 4, pp. 5–5.
134. Majhi S, Qian H, Xiang W, Addepalli S & Gao Z (2011) Analysis of outage probability for opportunistic decode-and-forward relaying network over asymmetric fading channels. In: 3rd International Conference on ICUFN, pp. 135–139.
135. Sneessens H, Vandendorpe L & Laneman J (2009) Adaptive compress-and-forward relaying in fading environments with or without Wyner-Ziv coding. In: IEEE ICC ’09, pp. 1–5.

136. Dabora R & Servetto S (2007) Estimate-and-forward relaying for the Gaussian relay channel with coded modulation. In: IEEE ISIT, pp. 1046–1050.
137. Luo K, Gohary R & Yanikomeroglu H (2011) On the generalization of decode-and-forward and compress-and-forward for Gaussian relay channels. In: IEEE ITW, pp. 623–627.
138. Tse D & Viswanath P (2005) Fundamentals of Wireless Communication. Cambridge University Press, New York, NY, USA.
139. McEliece RJ (2002) The Theory of Information and Coding. Cambridge University, UK, 2nd edition.
140. Lu PS (2015) Decoding and Lossy Forwarding based Multiple Access Relaying. Ph.D. dissertation, Japan Advanced Institute of Science and Technology, School of Information Science, Nomi, Japan.

Appendix 1 Proof of Convexity of (71), (72), and (73)

By taking second-order partial derivative of $P_{\text{out}}^{\text{LF, Ind}}$, $P_{\text{out}}^{\text{DF, Ind}}$, and $P_{\text{out}}^{\text{ADF, Ind}}$ in (71), (72), and (73) with respect to d, respectively, we have

$$\frac{\partial^2 P_{\text{out}}^{\text{LF, Ind}}}{\partial d^2} = \frac{9\alpha d^{\alpha}(\alpha+1)}{4\overline{\gamma}_{\text{SD}} d^{(\alpha+2)}\left(\overline{\gamma}_{\text{SD}} + 10\lg\left(\frac{1}{d^{\alpha}}\right)\right)^3} + \frac{90\alpha^2 d^{2\alpha}}{\overline{\gamma}_{\text{SD}} d^{(2\alpha+2)}\left(\overline{\gamma}_{\text{SD}} + 10\lg\left(\frac{1}{d^{\alpha}}\right)\right)^4}, \tag{134}$$

$$\frac{\partial^2 P_{\text{out}}^{\text{DF, Ind}}}{\partial d^2} = \frac{20\alpha^2 d^{2\alpha}}{\overline{\gamma}_{\text{SD}} d^{(2\alpha+2)}\left(\overline{\gamma}_{\text{SD}} + 10\lg\left(\frac{1}{d^{\alpha}}\right)\right)^3} + \frac{10\alpha^2 d^{(\alpha-1)}}{\overline{\gamma}_{\text{SD}} d^{(\alpha+1)}\left(\overline{\gamma}_{\text{SD}} + 10\lg\left(\frac{1}{d^{\alpha}}\right)\right)^2}, \tag{135}$$

and

$$\frac{\partial^2 P_{\text{out}}^{\text{ADF, Ind}}}{\partial d^2} = \frac{20\alpha^2\left(\frac{1}{\overline{\gamma}_{\text{SD}} + 10\lg\left(\frac{1}{d^{\alpha}}\right)} - 1\right)(1-d)^{2\alpha}}{\overline{\gamma}_{\text{SD}}\left(\overline{\gamma}_{\text{SD}} + 10\lg\left(\frac{1}{d^{\alpha}}\right)\right)^3 (1-d)^{(2\alpha+2)}} + \frac{\alpha^2 d^{(\alpha-1)}}{\overline{\gamma}_{\text{SD}}\left(\overline{\gamma}_{\text{SD}} + 10\lg\left(\frac{1}{d^{\alpha}}\right)\right)^2 d^{(\alpha+1)}}. \tag{136}$$

Obviously, (134), (135), and (136) are positive in the range $0 < d < 1$ which indicates that the objective functions are convex with respect to $0 < d < 1$.

Appendix 2 Proof of Convexity of (85), (86), and (87)

Taking the second-order derivative of $P_{\text{out}}^{\text{LF, Cor}}$, $P_{\text{out}}^{\text{DF, Cor}}$, and $P_{\text{out}}^{\text{ADF, Cor}}$ in (85), (86), and (87) with respect to k, respectively, we have

$$\begin{aligned}\frac{\partial^2 P_{\text{out}}^{\text{LF, Cor}}}{\partial k^2} &= \frac{\left(\frac{1}{P^T G_{\text{SR}} k}+1\right)}{5P_T^3 G_{\text{SD}}^2 G_{\text{RD}} k^3 (1-k)^2} + \frac{6\left(\frac{1}{10 P^T G_{\text{SR}} k}+\frac{19}{50}\right)}{P_T^2 G_{\text{SD}} G_{\text{RD}} k^4} \\ &+ \frac{17}{25 P_T^3 G_{\text{SD}} G_{\text{SR}}^2 k^5} + \frac{9\left(\frac{1}{P^T G_{\text{SR}} k}+1\right)}{20 P_T^3 G_{\text{SD}}^2 G_{\text{RD}} G_{\text{SR}} k^4 (1-k)},\end{aligned} \tag{137}$$

$$\begin{aligned}\frac{\partial^2 P_{\text{out}}^{\text{DF, Cor}}}{\partial k^2} &= \frac{9\left(\frac{1}{P^T G_{\text{SR}} k}+1\right)}{2P_T^3 G_{\text{SD}}^2 G_{\text{RD}} k^4 (1-k)} + \frac{5\left(\frac{1}{P^T G_{\text{SR}} k}+1\right)}{P_T^3 G_{\text{SD}}^2 G_{\text{RD}} k^3 (1-k)^2} \\ &+ \frac{6}{P_T^2 G_{\text{SD}} G_{\text{SR}} k^4} + \frac{5}{2 P_T^4 G_{\text{SD}}^2 G_{\text{RD}} G_{\text{SR}} k^5 (1-k)},\end{aligned} \tag{138}$$

and

$$\begin{aligned}\frac{\partial^2 P_{\text{out}}^{\text{ADF, Cor}}}{\partial k^2} &= \frac{\left(\frac{1}{P^T G_{\text{SR}} k}+1\right)}{5P_T^3 G_{\text{SD}}^2 G_{\text{RD}} k^3 (1-k)^2} + \frac{12\left(\frac{1}{10 P^T G_{\text{SR}} k}+\frac{19}{50}\right)}{P_T^3 G_{\text{SD}} G_{\text{RD}} k^5} \\ &+ \frac{9}{10 P_T^4 G_{\text{SD}}^2 G_{\text{SR}} k^6} + \frac{9\left(\frac{1}{P^T G_{\text{SR}} k}+1\right)}{20 P_T^3 G_{\text{SD}}^2 G_{\text{RD}} G_{\text{SR}} k^4 (1-k)}.\end{aligned} \tag{139}$$

It is not difficult to find that (138), (137), and (139) are positive in the range $0 < k < 1$ which indicates that the objective functions are convex with respect to $0 < k < 1$.